

Fatigue life assessment of welded bridge details using structural hot spot stress method

A numerical and experimental case study

Master's Thesis in the Master's Programme Structural Engineering and Building Performance Design

FARSHID ZAMIRI AKHLAGHI

Department of Civil and Environmental Engineering
Division of Structural Engineering
Steel and Timber Structures
CHALMERS UNIVERSITY OF TECHNOLOGY
Göteborg, Sweden 2009
Master's Thesis 2009:104

Fatigue life assessment of welded bridge details using structural hot spot stress method

A numerical and experimental case study

*Master's Thesis in the Master's Programme Structural Engineering and Building
Performance Design*

FARSHID ZAMIRI AKHLAGHI

Department of Civil and Environmental Engineering
*Division of Structural Engineering
Steel and Timber Structures*

CHALMERS UNIVERSITY OF TECHNOLOGY

Göteborg, Sweden 2009

Fatigue life assessment of welded bridge details using structural hot spot stress method

A numerical and experimental case study

Master's Thesis in the Master's Programme Structural Engineering and Building Performance Design

FARSHID ZAMIRI AKHLAGHI

© FARSHID ZAMIRI AKHLAGHI, 2009

Examensarbete 2009:104

Department of Civil and Environmental Engineering

Division of Structural Engineering

Steel and Timber Structures

Chalmers University of Technology

SE-412 96 Göteborg

Sweden

Telephone: + 46 (0)31-772 1000

Cover:

Results of finite element analysis (top left) are post-processed to calculate the structural hot spot stress (SHSS) at the weld toes (bottom left) these SHSS values are used in the fatigue strength S-N curves (bottom right) to determine the fatigue life of the part. SHSS values and their corresponding endurance are also calculated from the fatigue tests (top right).

Chalmers Reproservice / Department of Civil and Environmental Engineering
Göteborg, Sweden 2009

Fatigue life assessment of welded bridge details using structural hot spot stress method

A numerical and experimental case study

Master's Thesis in the Master's Programme Structural Engineering and Building Performance Design

FARSHID ZAMIRI AKHLAGHI

Department of Civil and Environmental Engineering

Division of Structural Engineering

Steel and Timber Structures

Chalmers University of Technology

ABSTRACT

Recent developments in numerical modelling methods and tools have led to the application of new and improved fatigue design and assessment methods. The structural hot spot stress (SHSS) approach is a relatively new approach for fatigue assessment of weldments. The method is advantageous compared to the traditional nominal stress method mainly because of its ability to assess more types and variations of the structural details. It incorporates the effect of structural geometry into the local stress ranges at the welds and predicts the fatigue life based on these local stress ranges. The method has been in use in other industries, but is less applied in the structural engineering field until recent years. Eurocode 3 accepts the structural hot spot stress method for fatigue design of welded steel structures. As Eurocode 3 will be the governing design code for steel structures in Sweden starting from 2010, this study can be of practical interest.

The aim of this project was to investigate the application of the SHSS method in the fatigue life assessment of details available in orthotropic steel bridge decks by experimental and numerical studies. The experimental part of the study was carried out at the Institute of Theoretical and Applied Mechanics (ITAM) in Prague. The numerical study included finite element modelling and analysis of the test specimens. Several finite element models with both shell and solid elements were made based on available guidelines. The FE results were then post-processed with a MATLAB code to determine the SHSS in different hot spot locations in the detail. The fatigue life predicted by the FE analysis was then compared to that of the experiments and also to the service life estimated by the nominal stress method.

The results show that SHSS values derived from fine-meshed solid element models are in good agreement with the experimental measurements. Noticeable difference in computed structural hot spot stress between the solid element models and shell element models was found. The models predict a shorter fatigue life for the specimens, which is on the safe side. However, the fatigue life estimated by nominal stress method is longer than the fatigue life of the tested specimens. Some recommendations for further studies are presented at the last part of this study.

Key words: fatigue assessment, local approaches, structural hot spot stress, geometric stress, orthotropic deck, steel bridges, welded joints, finite element method.

Utvärdering av utmattning livslängden hos svetsade brodetaljer med hot spot spänningsmetoden

En numerisk och experimentell fallstudie

Examensarbete inom Magisterprogrammet 'Structural Engineering and Building Performance Design'

FARSHID ZAMIRI AKHLAGHI

Institutionen för bygg- och miljöteknik

Avdelningen för Konstruktionsteknik

Stål- och Träbyggnad

Chalmers tekniska högskola

SAMMANFATTNING

Numeriska modelleringsmetoder och modelleringsprogram har blivit mer tillämpningsbara vid utmattningsdimensionering och utvärdering av svetsade stålkonstruktioner med de senaste utvecklingarna. Hot spot spänningsmetoden är en relativt ny metod vid utvärdering av utmattningshållfastheten hos svetsade detaljer. Den främsta fördelen med denna metod jämfört med den nominella metoden är metodens förmåga att utvärdera olika typer av konstruktionsdetaljer. Genom denna metod lägges de geometriska effekterna till den lokala spänningen vid svetstån och bestäms utmattning livslängden baserad på denna lokala spänning. Metoden har använts i andra branscher, men har mindre tillämpats inom byggtkniska området fram till de senaste åren. Enligt Eurokod 3 får hot spot metoden tillämpas för utmattningsdimensionering. Förutsatt att Eurokod 3 kommer att vara den ledande dimensioneringsnormen för stålkonstruktioner i Sverige från och med år 2010, kan denna studie vara av praktiskt intresse.

Syftet med detta arbete var att undersöka, genom experimentella och numeriska studier, tillämpningen av hot spot spänningsmetoden för utvärdering av utmattning livslängden hos ett svetsförband som finns i ortotrop brobaneplatta. Den experimentella delen av studien genomfördes vid ITAM i Prag. Den numeriska studien omfattade finita elementmodeller och analyser. Olika typer av FE modeller både med skal- och solidelement uppbyggdes på grundval av tillgängliga riktlinjer. FEA resultaten var då efterbehandlade med MATLAB-kod för att bestämma hot spot spänningen i olika hot spot punkterna i detaljerna. Den erhållna utmattning livslängden från FE Analysen jämfördes sedan med den i experimentet och även livslängden uppskattades enligt metoden med nominella spänningar. Resultaten visade att de hot spot spänningsvärden som erhållits från tätt solidelement modellerna överensstämde med dem från experimentet. En anmärkningsbar skillnad mellan de beräknade hot spot spänningsvärden från modeller med solidelement och skalelement hittades. FE modellerna förutsäger en kortare utmattning livslängd för provkroppar, dvs. det ligger på den säkra sidan. Men utmattning livslängden som uppskattas av nominell stress metod var längre än utmattning livslängden som erhållits från utmattningsprovet. Några rekommendationer för vidare studier har presenterats på den sista delen av denna studie.

Nyckelord: Utmattning dimensionering, lokal metoder, hot spot spänningsmetod, geometriska spänningar, ortotrop brobaneplatta, stålbroar, svetsförband.

Contents

ABSTRACT	I
SAMMANFATTNING	II
CONTENTS	III
PREFACE	V
NOTATIONS	VI
1 INTRODUCTION	1
1.1 Aim and scope	2
1.2 Limitations	3
1.3 Structure of the thesis	3
2 BACKGROUND	4
2.1 Classification of fatigue assessment methods for welded structures	4
2.1.1 Modelling of weld complexities in the local approaches	6
2.2 Nominal stress approach	7
2.3 Structural hot spot stress approach	9
2.3.1 Applications	14
2.3.2 Limitations	18
2.3.3 Types of hot spots	19
2.3.4 Multiaxial stress states	19
2.3.5 Experimental evaluation of SHSS	20
2.3.6 Calculation of structural hot spot stress using FEM	22
2.3.7 Hot spot S-N design curves	29
3 FATIGUE TESTS	32
3.1 Orthotropic bridge decks	32
3.2 The assessed detail	32
3.3 Test method	33
3.4 Measurements	36
3.5 Specimens	40
3.5.1 Specimen A2	40
3.5.2 Specimen A3	43
3.5.3 Specimen A4	50
3.6 Summary of test results	54
4 FINITE ELEMENT MODELLING AND ANALYSIS	55
4.1 Modelling	55
4.2 Description of the models	58

4.2.1	Model FR	58
4.2.2	Model SH10	60
4.2.3	Model SH04	63
4.2.4	Model BR10	65
4.2.5	Model BR04	67
4.2.6	Model OP04	69
4.2.7	Model SW04	73
4.2.8	Model TS02	75
4.2.9	Verification of the models	78
4.3	Analysis of the models	79
4.4	Post-processing of the results	80
5	FATIGUE LIFE ASSESSMENT OF SPECIMENS	82
5.1	Structural hot spot stress method	82
5.1.1	Calculation of SHSS from finite element analysis results	82
5.1.2	Comparison of SHSS values from finite element models to experimental measurements	82
5.1.3	Comparison of the SHSS values for all finite element models	84
5.1.4	Comparison of numerical and experimental results	89
5.2	Nominal stress method	91
6	CONCLUSION	94
7	REFERENCES	97
8	APPENDIX A: CALCULATIONS FOR NOMINAL STRESS METHOD	101
9	APPENDIX B: VERIFICATION OF THE FINITE ELEMENT MODELS	107
10	APPENDIX C: HS-FATIGUE PROGRAM SOURCE CODE	110
11	APPENDIX D: STUDY OF DIFFERENT TECHNIQUES FOR MODELLING OF SIMPLE AND NOTCHED JOINTS	115

Preface

This Master's thesis has been carried out at the Division of Structural Engineering of the Department of Civil and Environmental Engineering at Chalmers University of Technology. The research presented here focuses on the fatigue assessment of a detail available in the orthotropic decks in steel bridges. It is one of a series researches performed within the framework of BriFaG (Bridge Fatigue Guidance) project.

I express my deepest appreciation to Dr. Mohammad Al-Emrani, the supervisor and examiner of this thesis, for inspiring me with the idea of this research. I am greatly indebted to him for his insightful comments, critical discussions and illuminating guidelines.

My sincere thanks go to Mustafa Aygöl, PhD student at the Division of Structural Engineering, for his fruitful consultation and comments on the thesis.

Professor Ladislav Frýba and Dr. Shota Urushadze of the Institute of Theoretical and Applied Mechanics (ITAM), Prague, have provided the experimental results. I would like to thank them for their valuable contribution to this part of the research.

I send my appreciation to Professor Erkki Niemi (Lappeenranta University of Technology), Professor Lennart Josefson (Mechanical Engineering Department, Chalmers University of Technology), Dr. Claes Olsson (Techstrat AB), and Dr Inge Lotsberg (DNV Norway) for their insightful comments.

I would like to thank Dr. Hamid Movaffaghi of Mechanical Engineering Department for his guidance on solving some modelling issues in ABAQUS.

I would also like to thank my opponents Thomas Petersson and David Fall for their comments and proposals to improve the project.

My most sincere thanks is extended to my family, specially my parents whose continuous support and belief in higher education provided me valuable motivation.

Last, but not least, I send my love and gratitude to my wife, Toktam, for her invaluable support and patience throughout the whole task. Also, she kindly helped me in proofreading of the draft.

Göteborg, August 2009

Farshid Zamiri Akhlaghi

Notations

Roman upper case letters

D_{σ}	Damage caused by normal (direct) stress
D_{τ}	Damage caused by shear stress
D_{tot}	Total damage calculated from Palmgren-Miner's rule
E	Modulus of elasticity for steel

Roman lower case letters

da/dN	Crack propagation rate
k_m	Stress magnification factor due to misalignments
t	Plate thickness

Greek Upper case letters

$\Delta \varepsilon_k$	Elastic-plastic strain range
$\Delta \sigma_{eq}$	Equivalent stress range
$\Delta \sigma_k$	Elastic notch stress range
$\Delta \sigma_n$	Nominal stress range
$\Delta \sigma_s$	Structural stress range
ΔK	Stress intensity range

Greek lower Case letters

δ	Distance from the weld toe in the Dong method.
$\varepsilon_{0.4t}$	Measured strain in the reference point located $0.4t$ from the weld toe
$\varepsilon_{1.0t}$	Measured strain in the reference point located $1.0t$ from the weld toe
ε_{12mm}	Measured strain in the reference point located 12 mm from the weld toe
ε_{4mm}	Measured strain in the reference point located 4 mm from the weld toe
ε_{8mm}	Measured strain in the reference point located 8 mm from the weld toe
ε_{hs}	Structural strain at the weld toe (hot spot)
ε_x	Strain in the direction perpendicular to the weld toe (Longitudinal strain)
ε_y	Strain in the direction parallel to the weld toe (transverse strain)
$\sigma_{0.4t}$	Stress in the reference point located $0.4t$ from the hot spot.
$\sigma_{0.5t}$	Stress in the reference point located $0.5t$ from the hot spot.
$\sigma_{1.0t}$	Stress in the reference point located $1.0t$ from the hot spot.
$\sigma_{1.5t}$	Stress in the reference point located $1.5t$ from the hot spot.
σ_{12mm}	Stress in the reference point located 12 mm from the hot spot.
σ_{15mm}	Stress in the reference point located 15 mm from the hot spot.
σ_{4mm}	Stress in the reference point located 4 mm from the hot spot.
σ_{5mm}	Stress in the reference point located 5 mm from the hot spot.

σ_{8mm}	Stress in the reference point located 8 mm from the hot spot.
σ_{ben}	Shell bending stress calculated through the thickness of the plate
σ_{hs}	Structural hot spot stress (geometric stress)
σ_k	Notch stress
σ_{nlp}	Non-linear peak stress calculated through the thickness of the plate
σ_{nom}	Nominal stress
$\sigma_{nom,mod}$	Modified nominal stress
σ_{mem}	Membrane stress calculated through the thickness of the plate
ν	Poisson's ratio for the steel

1 Introduction

American Society for Testing and Materials (ASTM) defines the fatigue as: “The process of progressive localised permanent structural change occurring in a material subjected to conditions that produce fluctuating stresses and strains at some point or points and that may culminate in cracks or complete fracture after a sufficient number of fluctuations” (ESDEP,1993).

Fatigue of materials is a complex phenomenon. Fatigue of welds is even more complex. Material homogeneity is disturbed by weld metal itself and also by the change of the crystalline structure in the heat affected zone (HAZ) (Fricke 2003, Radaj 1996). Welding residual stresses and distortions due to these stresses also make the stress state in the welded specimen much more different than a similar un-welded specimen, as stated in Radaj (1996). Furthermore, an 'ideal' weld can rarely be found in reality. Weld defects such as inclusions, pores, cavities, undercuts, etc may occur. The weld profile and non-welded root gaps differ widely from the theoretical shape.

Therefore, the fatigue failure in welded structures usually forms at welds (or areas affected by weld) rather than in the base metal, according to Fricke (2003). This is reflected in Figure 1.1. The figure shows the dramatic decrease of fatigue strength of the welded component compared to the plain specimen and even specimen with a hole. It is noticeable that this decrease is resulted by adding the material to the component and not decreasing the cross sectional area of the component. This is in contrast to the general rule for statically loaded structures, in which adding the material to the cross section does not cause a decrease in the strength of the structure.

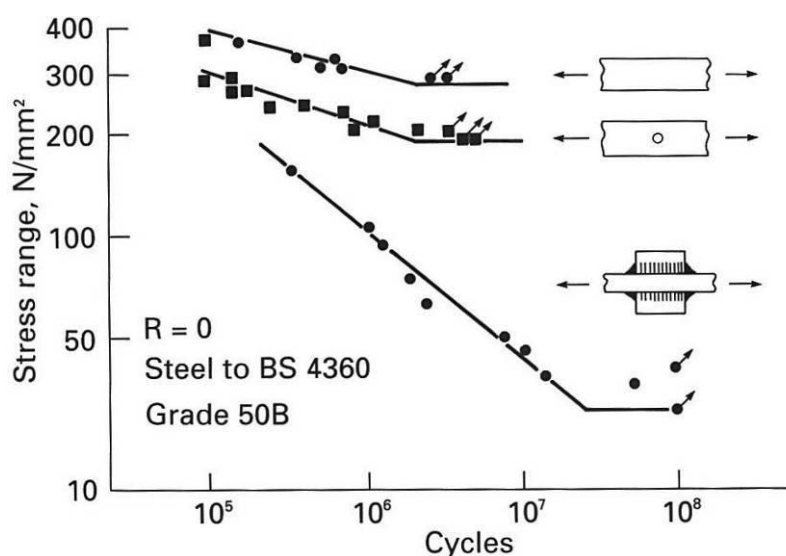


Figure 1.1 Comparison of fatigue strength of welded, holed and plain specimen, after Maddox (1991).

Considering wide use of welding process in several industries, a vast amount of research is conducted with reference to fatigue design of new structures and fatigue life assessment of existing ones. Several fatigue assessment methods have been proposed. These methods can be categorized as global (nominal stress) and local approaches.

The nominal stress approach has traditionally been used for fatigue life evaluation of steel structures. The nominal stress method uses the far-field stress away from the weld. On the other hand, fatigue failure of structural components, is a localised process. Local parameters of geometry, loading, and material influence the fatigue life of a structure. These are considered roughly in the nominal stress method by defining ‘detail classes’ or ‘fatigue classes (FATs)’. This method has some limitations in the fatigue assessment of complex structural details which will be discussed later. A more accurate approach to take local effects into account is fatigue assessment using ‘local methods’. These approaches generally use the finite element method for evaluating local stresses and use experimental strain measurements as a basis to verify the theoretical calculations (Radaj et al. 2006). These methods are discussed in more detail in Chapter 2.

1.1 Aim and scope

The structural hot spot stress (SHSS) method has been accepted widely in the offshore industry for many years as an efficient and reliable method to assess the fatigue strength of welded steel details. In recent years use of SHSS method in fatigue design has been accepted by Eurocode 3. It is expected that this method leads to more realistic fatigue life assessment of welded details.

In this study the application of a local method, namely hot spot method, for fatigue life assessment of stiffener to cross beam joint in orthotropic bridge decks is studied. This research is part of investigations on applying SHSS method in the design and assessment of welded details of steel bridges, determining some of the feasibilities and limitations of the method and solving the problems involved. More specifically, the influences of various modelling techniques on the predicted fatigue life are investigated based on the suggestions given by the previous researchers in the field. The predicted life is compared to the experimental results from the tests being done in the ITAM¹ in Prague. Also, the fatigue life is assessed using the nominal stress method based on Eurocode 3 and is compared to both the hot spot and experimental results. Fatigue life assessment using Eurocode 3 is of special practical interest since it will be the governing design code for design of steel structures in Sweden starting from 2010.

¹ Institute of Theoretical and Applied Mechanics

1.2 Limitations

In this research, fatigue life in the high cycle fatigue (i.e. fatigue that occurs at relatively large number of loading cycles) is investigated. The only weld type studied in both numerical and experimental investigations is fillet weld. Furthermore, cracking in the weld toe is considered as the governing mode of failure. This is confirmed by the experiments. It should be noted that root cracking is also a possible failure mode in the weldments that has to be avoided by choosing proper weld dimensions. Root cracking cannot be directly assessed by hot spot method².

The first cracks in the tested specimens were observed in the weld toes. Continuing the test procedure, some cracks appeared in the non-welded parts of the detail. Hot spot method cannot be used for these cracks. Hence, they were not considered in this study.

1.3 Structure of the thesis

The introduction to the method, previous work in the field, and literature review are presented in the Chapter 2. Since the method has not yet been used widely in the bridge engineering field, this chapter is intended to be in a more descriptive and pedagogical form. Fatigue tests and primary results from the tests are presented in Chapter 3. Numerical modelling and finite element analysis were another major part of this study. These steps are described in Chapter 4. Different finite element models together with Primary results of the finite element analysis are presented in this chapter. The results of the finite element analysis are post-processed to calculate the structural hot spot stresses at the critical (i.e. cracking) locations in the studied detail. These results, comparison of the results with experimental measurements, are presented in Chapter 5. The comparison of results Finally, Chapter 6 includes the concluding remarks and suggestions for further studies.

² Some researchers (Radaj et al. 2006 and Fricke & Doerk 2006) have proposed methods to consider root cracking in SHSS method. This is also introduced in the 2008 edition of IIW code.

2 Background

In this chapter, different categories of fatigue assessment methods are introduced. Structural hot spot stress method is investigated in more detail. Its applications and limitations are discussed and various SHSS evaluation methods are described. The IIW³ recommendations regarding building of FE models are also described. Finally, the fatigue S-N curves that should be used in the SHSS method are introduced based on IIW and Eurocode recommendations.

2.1 Classification of fatigue assessment methods for welded structures

According to Radaj (1996) and Radaj et al. (2009), the evaluation of fatigue strength and service life of welded components falls into two main categories: “Global approaches” and “local approaches”.

Global approach means that the fatigue strength assessment is directly based on the external force (and/or moment) ranges or from the nominal stress ranges in the critical cross-section by using e.g. simple beam theory (therefore, this latter method is called “nominal stress approach”). The nominal stress ranges then are compared to S-N diagrams pertaining to the investigated detail or component.

Strength assessments are named “local approaches” if they are based on local stress and strain parameters. The local aspects of fatigue damage (i.e. crack initiation, crack propagation and final fracture) can be considered in these approaches.

Different variants of the local approaches exist. They differ by the local stress or strain parameters chosen and type of failure criteria introduced. Various parameters together with characteristic diagrams are shown in Figure 2.1 for the global approach and variants of local approaches. Moving from variants in the left hand side of the figure to the variants in the right hand side, increasingly more detailed local conditions are taken into account. The multitude of available approaches can be assigned to the following categories:

- Nominal stress approach: uses the nominal stress range ($\Delta\sigma_n$) which is determined by simple calculations based on simple strength of materials theory.
- Structural hot spot stress method: takes into account change in structural stress range ($\Delta\sigma_s$) due to the part geometry. The approach is suitable for welded joints of hollow section members and for plated structures.
- Notch stress, notch stress intensity and notch strain approaches: these methods use the elastic notch stress range ($\Delta\sigma_k$) or stress intensity or elastic-plastic strain range ($\Delta\varepsilon_k$) at the weld toe or root to assess the fatigue strength and service life of the weldments.

³ International Institute of Welding

- Crack propagation approach: based on linear elastic fracture mechanics (LEFM) theory, assumes a crack is already available and uses special parameters such as J-integral or the range of the stress intensity (ΔK) to determine the increase in the crack length per cycle (or: crack propagation rate da/dN).

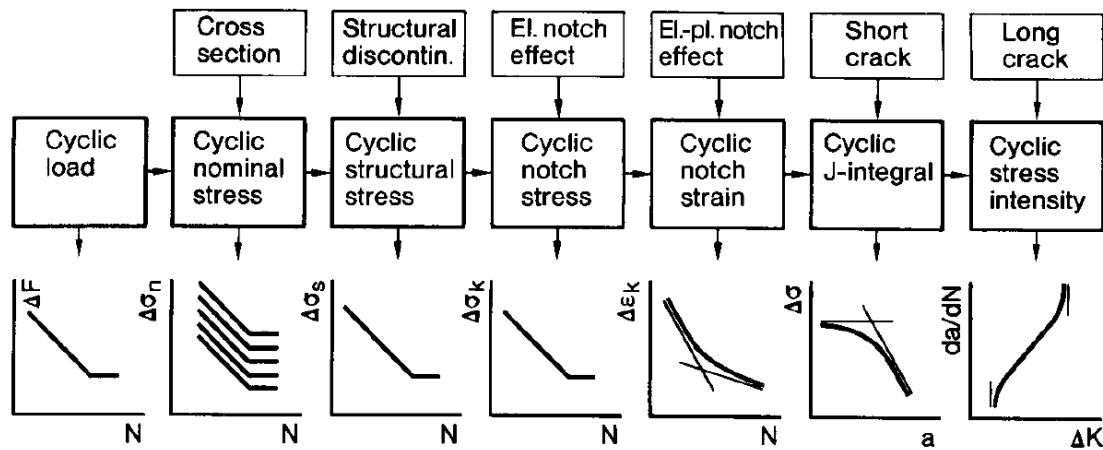


Figure 2.1 Parameters and design curves used in global and local approaches for determination of fatigue strength and service life, after Radaj et al. (2006). El. means 'elastic' and El-pl. meaning 'elastic-plastic'; ΔF is cyclic load range, $\Delta\sigma_n$ cyclic nominal stress range, $\Delta\sigma_s$ cyclic structural hot spot stress range, $\Delta\sigma_k$ cyclic notch stress, $\Delta\epsilon_k$ cyclic notch strain, $\Delta\sigma$ cyclic stress at crack tip, da/dN crack propagation rate, N number of cycles to failure, a crack length and ΔK cyclic stress intensity factor.

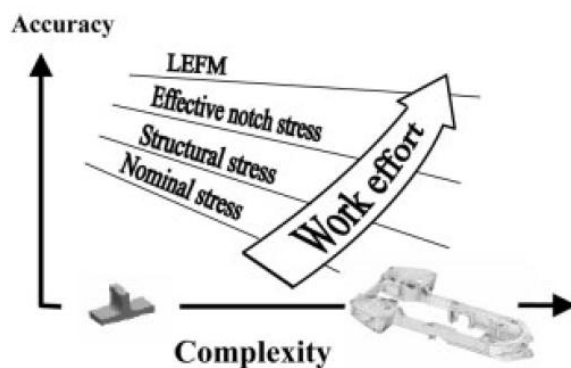


Figure 2.2 Comparison of accuracy and effort for fatigue assessment methods in weldments, after Marquis & Samuelsson (2005).

Marquis & Samuelsson (2005) provided a qualitative comparison of accuracy and work effort for the aforementioned fatigue assessment methods. This is shown in Figure 2.2. The nominal stress method has acceptable accuracy for simple structures

and requires less computational effort compared to the other methods, but its accuracy decreases for more complex structures. Structural hot spot stress method has better accuracy for the complex structures but it demands more work effort. The computational demand for effective notch stress method and LEFM methods are more than two other methods, but in turn, they provide more accurate results.

It should be noted that S-N curves do not state much about the progress of fatigue damage. Only, the total fatigue life is provided. But, local approaches based on notch stress method and fracture mechanics can describe and model whole fatigue life of the structure taking into account all significant parameters in the estimation. Notch stress and strain approach covers the crack initiation phase, while crack propagation and final fracture can be modelled by the crack propagation approach (i.e. fracture mechanics). Structural hot spot stress approach acts as a link between the global and local concepts (Radaj et al. 2006).

2.1.1 Modelling of weld complexities in the local approaches

The abnormalities and irregularities available in the weldments can be divided into 4 categories, as stated by Radaj et al. (2006):

1. **Inhomogeneous material:** This is the characteristic of welded joints. The filler material is similar to the base material but specially alloyed to attain a higher weld quality. The base metal micro-structure is being altered in the heat affected zone (HAZ) due to the high temperature during welding process.
2. **Welding defects and imperfections:** Such as cracks, porosity, inclusions and root failure, welding start-stop points, etc. In nominal stress approach, these are taken into account by the concept of quality classes (the permissible nominal stress is determined according to the quality class). In the local approaches (including structural hot spot stress method), defects should be considered and modelled individually.
3. **Welding residual stresses and distortions:** If the material is ductile enough, welding residual stresses will generally change in a favourable manner under cyclic loading with sufficient load amplitude.
4. **Geometry and dimensions of weld:** Some weld dimensions (such as radius of curvature in the weld toe) are not determined in the specifications. Even, the specified weld dimensions vary within a large scatter range due to the nature of welding process.

All of these peculiarities can affect the fatigue strength and service life of the joint. In general, taking into account all these factors is an intricate job and can make local approaches too complex. As a result, simplifying assumptions are introduced: The material characteristic values of the base material are used, the effect of residual stresses is only roughly taken into account and the worst case of geometric weld parameters is considered. Welding defects and imperfections can be introduced into local approaches in an Individual basis considering the worst case.

2.2 Nominal stress approach

Nominal stress approach is the basic and most widely used fatigue design method. Based on huge numbers of laboratory fatigue test results for different weld details with different geometries, a number of design S-N curves that represent a 97.7% survival probability for the details that are associated with each curve have been provided in the design codes. The fatigue strength S-N curves pertaining to the nominal stress method for welded structures include the influence of material, geometry and weld quality

The regulations for nominal stress method in chapter 9 of Eurocode 3 (2005) provide a set of 14 fatigue resistance S-N curves, equally spaced⁴. For each curve, a set of constructional details are associated. Figure 2.3 shows these design S-N curves for normal stress in the Eurocode 3. The design is carried out as the following procedure:

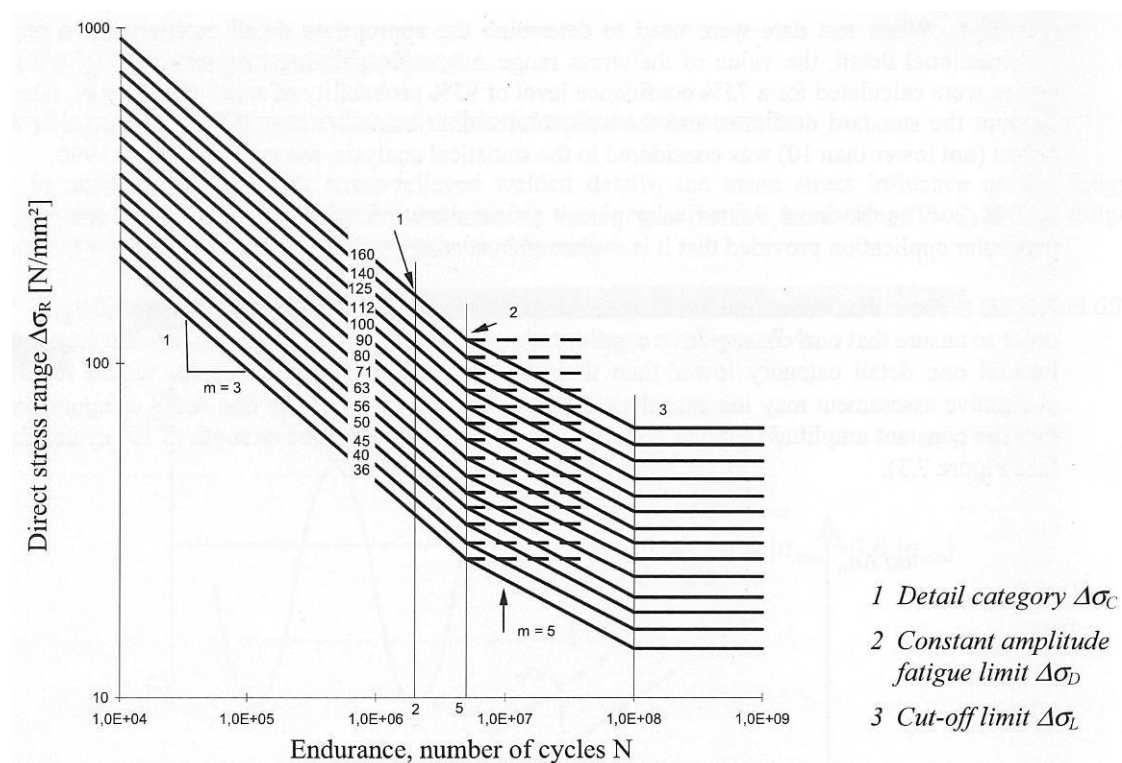


Figure 2.3 Eurocode 3 (2005) fatigue strength curves for direct (normal) stress range. The numbers on the curves indicate the detail category.

⁴ The same S-N curves are recommended by IIW for nominal stress approach

1. Direct (normal) or shear stress in the critical section of welded detail is calculated using simple basic elastic theories (such as Navier's formula for stresses in the beams). Relatively simple finite element models may also be used to determine the nominal stresses in more complex or statically indeterminate structures.
2. The detail category pertaining to that specific detail is determined by the tables from the design code and thus the proper S-N curve is established. The nominal stress in the detail is compared to the S-N curve to determine the fatigue strength and/or service life.

If both direct and shear stresses are present in the region prone to cracking (Multiaxial fatigue), then Eurocode 3 recommends the damage ratios due to each stress effect being calculated and then the two damage ratios summed up to calculate the total damage ratio. For design purposes, the damage ratio should be kept less than or equal to unity (This is analogous to Palmgren-Miner's theory in which it is assumed that total fatigue damage caused by combination of several sources is the summation of damages caused by each individual source).

$$D_{\sigma} + D_{\tau} \leq 1 \quad (2.1)$$

Where D_{σ} and D_{τ} are damage due to the normal stress and shear stress, respectively.

Damage ratio for each source is the number of cycles that detail is exposed to during its service life divided to the number of cycles to failure at that stress level (evaluated from the S-N curve):

$$D_{tot} = D_{\sigma} + D_{\tau} = \left(\frac{n}{N}\right)_{\sigma} + \left(\frac{n}{N}\right)_{\tau} \leq 1 \quad (2.2)^5$$

One obvious limitation of the nominal stress method is that if the studied detail is not available in the tables of standard details provided by the code, it cannot be designed unless laboratory fatigue tests are carried out and the data from test results are consolidated into a single S-N curve for that detail.

To come up with some limitations of the nominal stress method, a modified nominal stress method (also named local nominal stress) is introduced in Eurocode 3 (2005) and IIW recommendations (2003). According to IIW recommendations, modified nominal stress comprises nominal stress including macrogeometric effects (such as large openings, beam curvature, shear lag and eccentricity), concentrated load effects and misalignments but disregarding the stress raising effects of the welded joint itself. Figure 2.4 shows some examples of macrogeometric effects.

The stress raising effects due to these factors are presented by stress concentration factors (SCFs). So, the modified nominal stress can be stated as:

$$\sigma_{nom,mod} = SCF \cdot \sigma_{nom} \quad (2.3)$$

⁵ This equation holds for Constant Amplitude Fatigue Loading (CAFL) case.

Where $\sigma_{nom,mod}$ is the modified nominal stress and σ_{nom} is the nominal stress in the critical section to be designed. This modified nominal stress can be used in conjunction with S-N curves described earlier for fatigue design and assessment of some variants of the standard details.

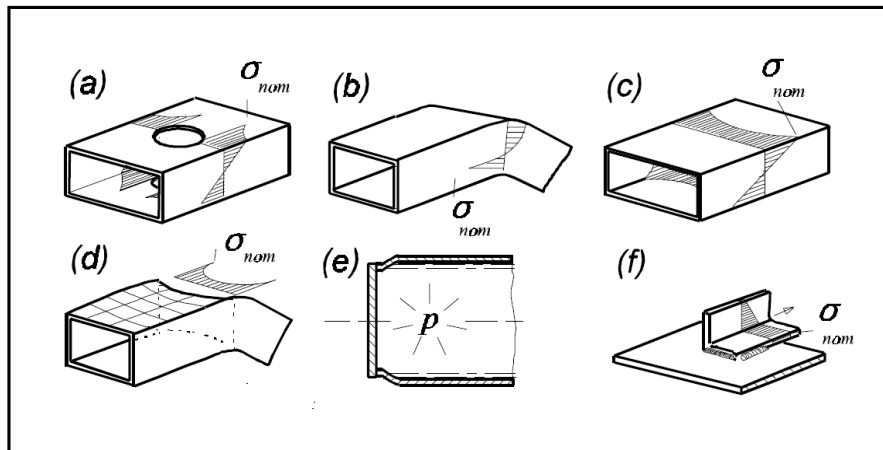


Figure 2.4 Examples of macrogeometric effects, after IIW (2003). σ_{nom} shown on the figure is actually $\sigma_{nom,mod}$, i.e. modified nominal stress.

2.3 Structural hot spot stress approach

The stress distribution through the plate thickness in vicinity of the weld toe is disturbed by notch effect of the weld. This is shown⁶ in Figure 2.5. The notch stresses are much higher than nominal stresses in the weld toe. As a result, they control the fatigue cracking in the plate. Due to the plastic deformations before crack initiation in this point, the temperature in this region rises, and that is why it is named ‘hotspot’ (Dieter Radaj et al. 2006).

Considering the non-linear stress distribution shown in Figure 2.5, three stress components can be distinguished:

- σ_{mem} membrane stress
- σ_{ben} shell bending stress
- σ_{nlp} non-linear stress peak

⁶ This distribution is for the cases where the stress profile does not change in the direction parallel to the weld toe, i.e. type ‘a’ hot spot (See Section 2.3.3)

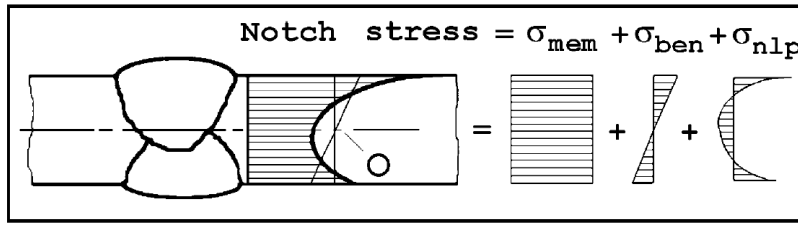


Figure 2.5 Typical stress distribution through the plate thickness at the weld toe, decomposed to three components: membrane stress, plate bending stress, and non-linear stress peak (Niemi et al. 2006).

The membrane stress (σ_{mem}) is constant through the thickness and is equal to the average stress through the plate thickness. The distribution of shell bending stress (σ_{ben}) is linear through the thickness and is zero in the mid-plane. The remaining part of the stresses is the non-linear stress peak (σ_{nlp}). This part is in self-equilibrium and depends on the size and form of the weld and weld toe geometry (Niemi et al. 2006). For a given stress distribution $\sigma(x)$, these three components can be calculated by the following equations (Hobbacher 2003):

$$\sigma_{\text{mem}} = \frac{1}{t} \int_{x=0}^{x=t} \sigma(x) \cdot dx \quad (2.4)$$

$$\sigma_{\text{ben}} = \frac{\sigma}{t^2} \int_{x=0}^{x=t} \sigma(x) \cdot \left(\frac{t}{2} - x\right) \cdot dx \quad (2.5)$$

$$\sigma_{\text{nlp}} = \sigma(x) - \sigma_{\text{mem}} - \left(1 - \frac{x}{2}\right) \cdot \sigma_{\text{ben}} \quad (2.6)$$

The idea of structural hot spot stress approach is to exclude this latter part (non-linear notch effect - σ_{nlp}) from the structural stress. This is reasonable because the exact and detailed geometry of the weld is not known accurately during design phase. The non-linear notch effect is indirectly included in the S-N curves (The variations in the local weld geometry are the main reason for scatter in the test results, see also Section 2.3.7). So, only the two linearly distributed stress components build up the structural hot spot stress:

$$\sigma_{\text{hs}} = \sigma_{\text{mem}} + \sigma_{\text{ben}} \quad (2.7)$$

Where σ_{hs} is the structural hot spot stress.

According to IIW recommendations (2003), the structural hot spot stress (also called geometric stress) includes all the stress raising effects due to the structural configuration (global geometry or macro-geometry). But it does not include the non-

linear notch effect due to the detailed geometry of the weld itself (e.g. weld profile and weld dimensions)⁷.

The concept can also be described in a different way. Figure 2.6 shows stress state near a weld toe prone to fatigue cracking. The figure shows increase of the stress at the plate surface near the weld toe (and perpendicular to it). We can assume that this increase is due to two different factors:

1. Change in structural configuration (macro-geometry) acts as a stress raiser in the vicinity of the weld toe.
2. Local geometry of the weld results in a notch effect. This notch effect causes a drastic increase in the stress in the region very close to the weld toe (if the notch radius at the weld toe is assumed to be zero, the elastic stress will be singular at that point).

The stress corresponding to the first factor above is hot spot stress. It should be emphasized that the hot spot stress is a fictitious value. We try to break down the stress in the weld toe to two separate parts (Eriksson et al. 2003): one part caused by the notch effect at the weld toe and the next part caused by other stress raiser (macrogeometric) factors. An easy way to do this separation is extrapolation of the surface stress towards weld toe from appropriate points which are located in a reasonable distance from the weld toe. The non-linear notch stress effects normally vanish within a distance $0.3t$ to $0.4t$ from the weld toe (t being the plate thickness). It is why IIW recommends that the extrapolation points being located $0.4t$ and $1.0t$ from the weld toe, for linear extrapolation. This concept is shown in Figure 2.7. The figure also shows the equivalence of the two definitions of structural hot spot stress; i.e.: through thickness stress linearization and surface stress extrapolation.

⁷ Eurocode 3 definition is slightly different in case of multiaxial stress state. See Section 2.3.4

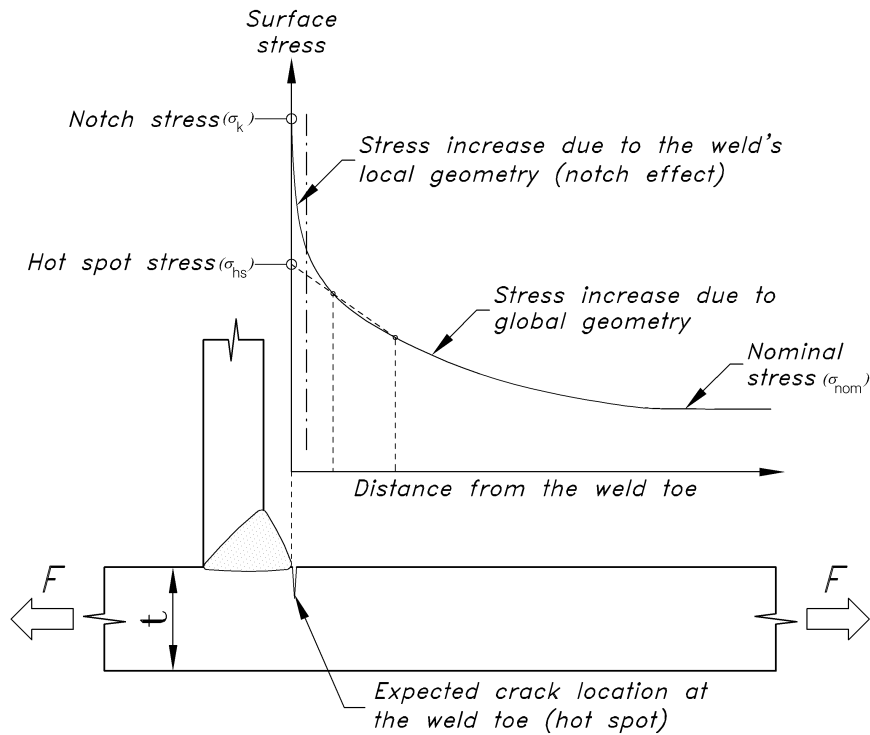


Figure 2.6 Variation of the stresses (perpendicular to weld toe) in the vicinity of the weld toe (note that the shown crack is not formed, but is expected to occur during fatigue process).

For the case of surface stress extrapolation, similar to the other definition of hot spot stress (i.e. through thickness linearization of stresses), the effects due to the global geometry are included in the structural stress. Therefore, the fatigue strength S-N curve does not need to include these effects. In fact, the hot spot S-N curves include only notch effect from the weld geometry at the crack initiation point. Thus, the S-N curves for a specific weld type can be used for any detail with arbitrary geometric configuration as long as the weld type and properties are similar to the original weld type associated with the S-N curve.

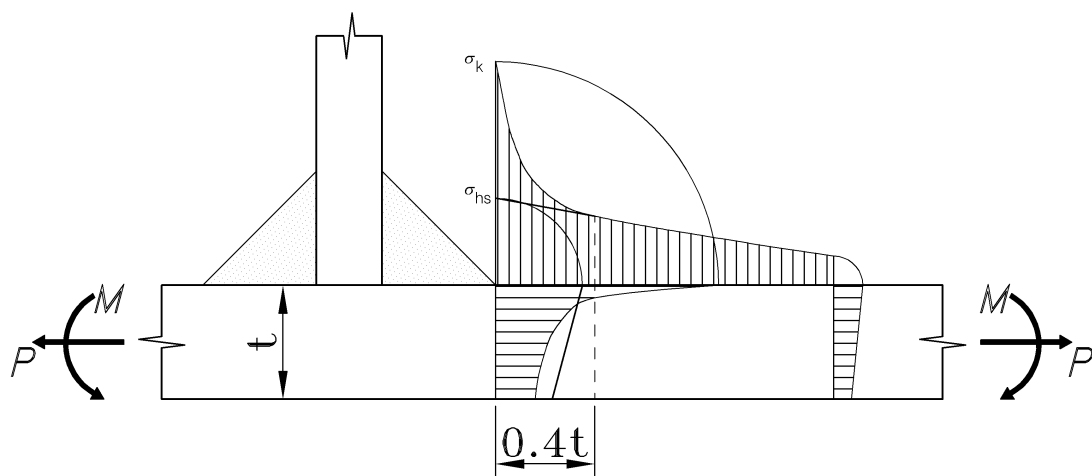


Figure 2.7 Relation between the two definitions of the hot spot stress.

As stated by Radaj et al. (2006), early investigations to exclude the stress concentration due to the weld toe, were carried out by Peterson, Manson and Haibach in 1960s. Their method was simply measuring stress or strain at a certain distance from the weld toe and relating it to the fatigue service life of the component. The idea was developed further in 70s and the fatigue assessment procedure evolved to evaluation of stresses at defined reference points in a certain distance from the weld toe (usually two or three points) and then extrapolating the stresses to estimate the structural stress in the weld toe.

The method was originally developed for welded joints of circular and rectangular hollow sections and has been in use for more than 30 years in offshore industry, where the fatigue assessment of such details is of special interest. The method has been later applied successfully to welded plate structures (Fricke (2003); Niemi & Marquis (2002); Maddox (2002); Eriksson et al. (2003)). This has led to extension of the method to other industries like shipbuilding, automotive industry and last but not least, bridge engineering.

For the case of plated structures, three alternative procedures for evaluation of hot spot structural stress from the finite element analysis exist (Radaj et al. (2006)):

- a. surface stress extrapolation (SSE)
- b. through thickness stress linearization (TT)
- c. Linearized equilibrium stresses from normal and shear stresses in a distance δ from the weld toe (Dong method)

Methods (a) and (b) are already introduced and method (c) will be briefly introduced later in this chapter. It is emphasized again that all of this three methods are attempting to compute the same stress value and so they theoretically give the same results Poutiainen et al. (2004). Figure 2.8 shows a summary of the three methods.

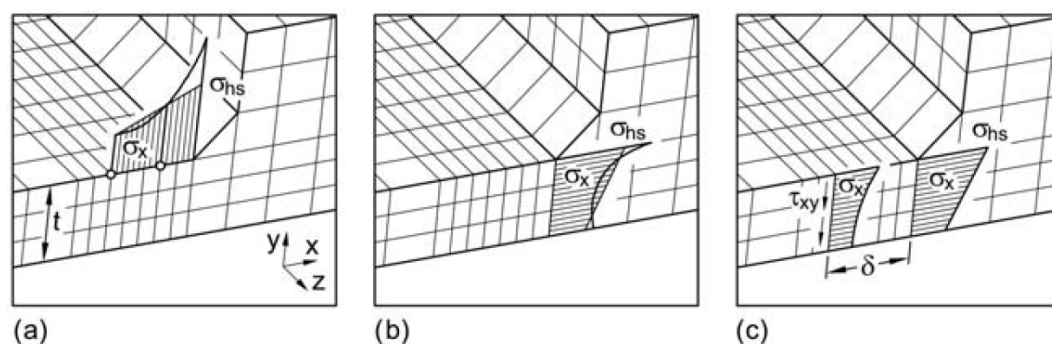


Figure 2.8 Poutiainen et al. (2004) Alternative methods for calculation of structural hot spot stress: surface stress extrapolation (a); Linearization of stresses through thickness (b); Linearized equilibrium stresses at distance d from the weld toe proposed by Dong (c).

As reported by Hobbacher (2009), currently, there is a considerable amount of ongoing research towards improving the structural hot spot stress method and reducing its limitations. As a measure for the amount of research work and resulted improvements, comparison of the 1996 version of IIW recommendations with the recent 2006 revision, reveals that the section dedicated to structural hot spot stress has been substantially revised. This is also the case for the new 2009 draft of the code.

The European pre-standard ENV 1993-1-1 (Eurocode 3) was the first *general* design code to include the structural hot spot stress approach (Eurocode uses the term ‘geometric stress’ approach). But, its instructions are insufficient and there is no clear guidance regarding the finite element modelling and hot spot (or geometric) stress calculation. In contrast, the IIW recommendations (specially its recent 2006 version) has comprehensive guidelines and recommendations in this regard.

2.3.1 Applications

The structural hot spot stress (SHSS) method is still a new method. It has not been used as wide as nominal stress method. It is suited to use in the following situations:

1. When fatigue design of a new welded detail or fatigue assessment of an existing detail is required, but the detail is not a “standard detail” that can be found in the tables provided by the design code. This means either the detail is not available in the code at all or some of its features -such as construction tolerances or misalignments- do not match with the code requirements.
2. In complex details which a clear definition for the nominal stress cannot be made.
3. When modelling a component with a detailed finite element model, calculation of the nominal stress is not trivial and at least needs some post-processing. Besides, if one wants to utilize the accuracy and power of finite element method to better estimation of the fatigue life of the components, then the use of a local approach such as structural hot spot stress method is the choice.

It should be mentioned that although structural hot spot stress method requires a relatively fine mesh in the weld region, it is not as demanding as other local approaches (namely notch stress method and LEFM) that require a *very* fine mesh in the weld region. In addition, the LEFM methods are very sensitive to the chosen initial crack size and as a result, they are mainly used for welded details with known flaws (Niemi & Marquis 2002). Thus, the SHSS method is advantageous, compared to other local approaches in terms of computational cost. The method also provides a valuable tool for choosing the locations of strain gauges when verifying the design by field or laboratory tests, according to Niemi & Marquis (2002).

As an example for comparison of the SHSS method with nominal stress method, the investigation conducted by Eriksson et al. (2003) is explained here. The fatigue life of a plate with fillet-welded longitudinal attachments on both sides with different

attachment lengths was evaluated using the hot spot method. The detail is shown in the upper right corner of Figure 2.9. The height of the gussets is 100 mm and the thickness of the plate is 10 mm. The joint is loaded with an axial force in the direction shown in Figure 2.9. The resulted nominal stress in the plate is 80 MPa. Table 2.1 shows the recommended fatigue categories⁸ for the studied detail in the IIW recommendations. These values should be used in the nominal stress approach. It is obvious that the fatigue strength (FAT), and consequently fatigue life, are a continuous function of the gusset length (L); but for the sake of simplicity, this continuous function is substituted by a step function in the code; like the one shown by a dashed line in Figure 2.9.

⁸ 'Fatigue category' (FAT) concept in IIW code is the same as 'detail category' in the Eurocode

Table 2.1 Fatigue categories for the plate with longitudinal gusset (nominal stress approach).

Gusset Length (L), [mm]	Fatigue category (FAT)
$L < 50\text{mm}$	80
$50\text{mm} < L < 150\text{mm}$	71
$150\text{mm} < L < 300\text{mm}$	63
$L > 300\text{mm}$	50

However, this limitation does not exist for the hot spot method. Based on the weld type, the hot spot stress fatigue category is FAT 100 for the details with arbitrary gusset length (see Table 2.4). The structural hot spot stress is calculated for gusset lengths of 40, 75, 150, 200 and 300 millimetres by constructing one finite element model for each gusset length and then calculating the stress profile at the weld toe and finally extrapolating the stresses at reference points into the weld toe (hot spot). One of the FE models used for the hot spot stress evaluation is shown in Figure 2.10. The detail has three planes of symmetry (both in loading and geometry). So, only one quarter of the detail is modelled. The gap between the plates is not modelled.

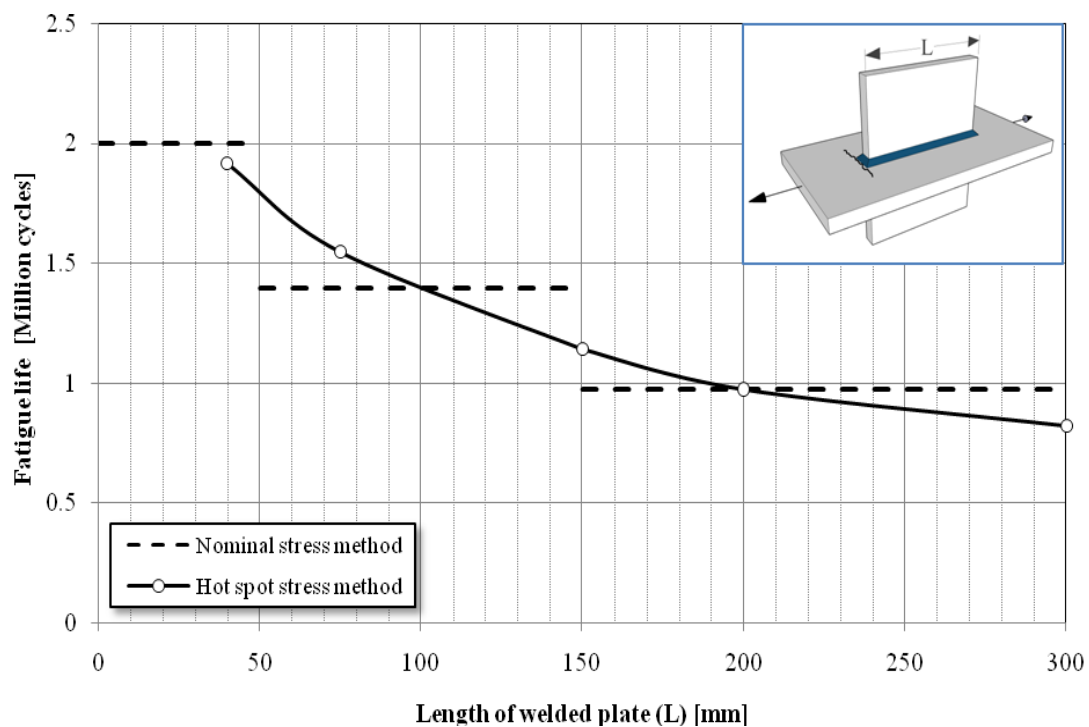


Figure 2.9 Fatigue life predictions of plate with a longitudinal attachment with various lengths, Data from Eriksson et al. (2003).

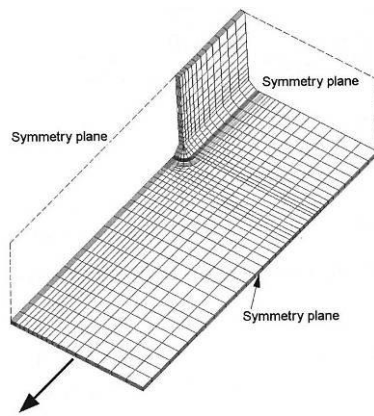


Figure 2.10 Computational model for the investigation conducted by Eriksson et al. (2003).

The hot spot stresses are then used to evaluate the fatigue life of the details and the results are shown in Figure 2.9 together with the results from the nominal stress method. The figure shows that the ‘continuous’ relation between the fatigue life of the detail and the gusset length is maintained in the SHSS method. This rationally leads to more realistic fatigue life estimation. On the other hand, the stepped shape of the fatigue life curve for the nominal stress approach will lead to either some non-conservative results or results which are much on the safe side. It should be added that the authors did not provide the actual fatigue life from the laboratory tests to determine which method better models the real behaviour, or if one method is conservative or non-conservative.

SHSS method can be applied to welded joints where the principal cyclic stress is predominantly exerted perpendicular to the weld toe or the end points of a longitudinal weld. These are the locations prone to fatigue cracking. Figure 2.11-(a) to (e) show some examples in which cracking initiation can be predicted by SHSS method. However, cases (f) to (j) in the figure cannot be dealt with by SHSS method. This is discussed further in the Section 2.3.2.

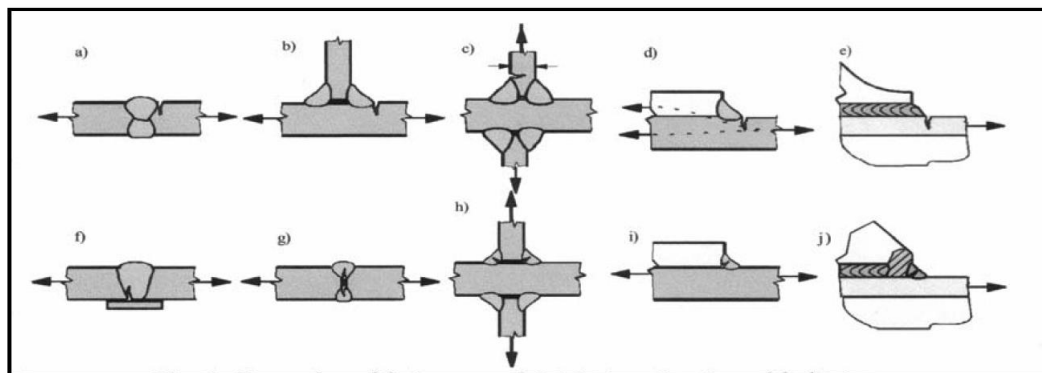


Figure 2.11 Examples of fatigue crack initiation points in welded plate joints, after Niemi et al. (2006).

Fricke (2002) showed the wide variety of applications of the hot spot method together with a summary of modelling aspects. He presented some successful applications of the method from different engineering disciplines. However, in a case study of a complex structural detail with various competing hot spots, he showed that the hot spot stress approach could lead to incorrect conclusions if used alone. He mentioned that some influencing factors, such as favourable residual stresses, exist which are neglected in the geometric stress approach.

Several researchers have contributed to investigation of applicability of SHSS method into fatigue life assessment of weldments. This is done mainly by comparing the finite element analysis followed by SHSS evaluation based on the S-N curves and compare this estimated service life with the actual service life from the small scale or full scale fatigue tests. To name a few, Biot et al. (2001) and Lindemark et al. (2009) followed this procedure to evaluate the applicability of the SHSS method in the field of marine structures. Both groups conducted full scale tests. Biot et al. (2001) reported that the results were consistent between numerical approach and experiment. Lindemark et al. (2009) proposed some modifications in the definition of hot spot stress and fatigue failure criteria for gaining more consistent results. Fatigue failure criterion for the welded plate connections is usually considered the formation of a through thickness crack. These authors believed that for a full scale test specimen, a critical crack length along the weld line is more relevant to define the failure.

In the field of bridge engineering, Miki & Tateishi (1997) proposed parametric geometric stress concentration factors for cope hole details in steel bridge girders. Chan et al. (2003) conducted a large study for finite element modelling of a large suspension bridge located in Hong Kong. As part of their study, they used local FE models in conjunction with structural hot spot stress method to evaluate the fatigue life of certain welded details. Schumacher & Nussbaumer (2006) investigated the fatigue service life of some welded K-joints of circular hollow sections by experimental measurement of structural hot spot stress in their test specimens. They showed the influence of size effect (wall thickness of welded sections) on fatigue life in their study.

2.3.2 Limitations

The crack locations in the part or detail under investigation should be known prior to hot spot analysis. This can be made by examining several different possible cracking points by structural analysis, preliminary finite element study, laboratory testing of similar details, or observation of similar details that have been cracked during their service life.

As stated earlier, the method is limited to surface cracks (toe cracking). For the root cracking failure mode, other methods (e.g. nominal stress method) can be used. This failure mode should be avoided in good design practice, because the crack cannot be detected until it is propagated through the weld. Some examples of root cracking are presented in Figure 2.11-(f) to (j). It should be added that according to Radaj et al. (2006), assessment of weld root fatigue cracking using the hot spot method is investigated by some researchers, but the topic is not yet mature enough to be involved in the design codes.

As Radaj et al. (2006) report, previous investigations have shown that the extrapolated hot spot stress is not independent of the location of the points selected as reference points. The element type and mesh size of the finite element model also affect the results. To overcome this limitation and make SHSS approach a practical and reliable method, extensive research has been conducted. This research has lead to prescription of some provisions in the design codes to limit the variability of the results. These rules are described in more detail in the following sections in this chapter.

Another alternative way to reduce the uncertainties in the extrapolation procedure has come into focus in recent years, according to Niemi et al. (2006). That is, calculation of the hot spot stress from the through-thickness stress distributions provided by finite element analysis. These methods such as the method introduced by Dong (2001) eliminate the need for the extrapolation and claim to be mesh-independent. This means that structural hot spot stress results are not affected by reasonable changes in the mesh size.

2.3.3 Types of hot spots

According to the designer's guide to the structural hot spot stress approach published by IIW (Niemi et al. 2006), two types of hot spots can be distinguished in the welded details:

Type 'a' the hot spot is placed on the plate surface

Type 'b' the hot spot is located on a plate edge

These two types can be seen in Figure 2.12.

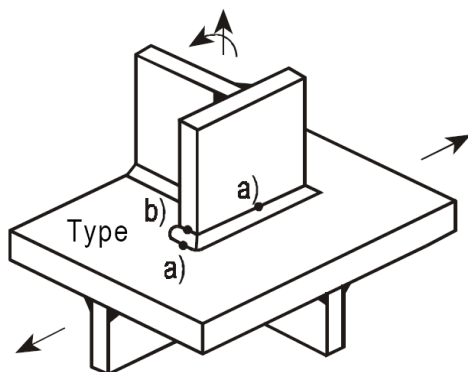


Figure 2.12 Different types of hot spots in a typical detail, after Niemi et al. (2006).

2.3.4 Multiaxial stress states

According to IIW recommendations, in a biaxial stress state, the larger of the two following extrapolated stresses should be taken as hot spot stress:

- a) The principal stress which is acting within $\pm 45^\circ$ of the normal to the weld toe (i.e. the principal stress more close to the normal to the weld toe)
- b) The direct (normal) stress component perpendicular to the weld toe.

Niemi et al. (2006) state that the accurate way to calculate the first of the two above stresses, is to extrapolate each stress component (direct and shear stresses) to the weld toe and then calculate the principal stress at the weld toe. But, they also consider it sufficient in practical cases that just the principal stresses being estimated in the reference points and then extrapolated into the weld toe.

Eurocode recommends a different method for calculation of hot spot stress in the case of biaxial stresses. It recommends using the maximum *principal* stress in the parent material adjacent to the weld toe as the SHSS.

In type ‘a’ hot spots, the size effect (dependency of stress distribution on the size of the components) affects the stress values. So, to take into account this geometric size effect, the locations of the reference points are a (linear) function of the plate thickness (typically chosen as $0.4t$ and $1.0t$). However, this is not the case for type ‘b’ hot spots. That is, the stress profile approaching the weld toe is not affected by the change in plate thickness (Niemi et al. (2006)). Hence, the placement of the extrapolation points is not determined as proportional to the plate thickness and their distance from the weld toe is determined as absolute distances, namely 4, 8 and 12 mm. Because of the existence of higher stress gradients in vicinity of the weld toe in type ‘b’ hot spots, a quadratic extrapolation is preferable in this case. That is why three reference points are mentioned for type ‘b’ hot spots by IIW.

2.3.5 Experimental evaluation of SHSS

Regularly, the only available measurement points in the experimental stress analysis are the points on the plate surface. So, the SHSS is derived from the surface stress profile in the vicinity of the weld toe. This is done by extrapolation of the surface stresses from the reference points into weld toe.

Type ‘a’ hot spots

As mentioned earlier in this section, at a distance of $0.4t$ from the weld toe, the non-linear notch peak stress is vanished and the stress profile shape is almost linear for type ‘a’ hot spots. Figure 2.13 shows this situation together with the reference points for the extrapolation recommended by IIW. For linear extrapolation, this points are located $0.4t$ and $1.0t$ from the weld toe. Hence, the extrapolation will yield the structural hot spot strain as:

$$\varepsilon_{hs} = 1.67\varepsilon_{0.4t} - 0.67\varepsilon_{1.0t} \quad (2.8)$$

Where ε_{hs} is the structural strain at the weld toe and $\varepsilon_{0.4t}$ and $\varepsilon_{1.0t}$ are the measured strains in the reference points located at the distances $0.4t$ and $1.0t$ from the weld toe, respectively. In some cases where the plate is resting on a stiff elastic support (like a beam flange supported by the web) the linear extrapolation may underestimate the hot

spot stress. IIW recommends using a quadratic extrapolation scheme for these situations.

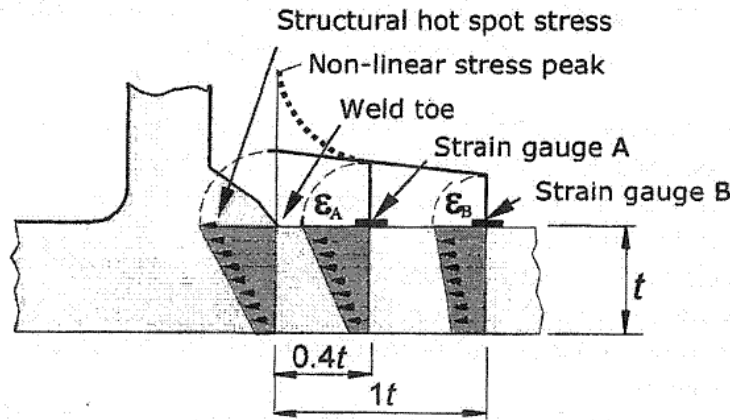


Figure 2.13 Linear extrapolation of strains into the weld toe to evaluate SHSS stress in type 'a' hotspots, after Niemi et al. (2006).

Type 'b' hot spots

As mentioned before, a quadratic extrapolation from the reference points placed at the absolute distances of 4, 8 and 12 mm is recommended by IIW in the case of type 'b' hot spots. The following equation is given for estimation of the structural hot spot strain:

$$\varepsilon_{hs} = 3\varepsilon_{4mm} - 3\varepsilon_{8mm} + \varepsilon_{12mm} \quad (2.9)$$

If the stress state is uni-axial, SHSS for both type 'a' and type 'b' can be estimated from the Hooke's law:

$$\sigma_{hs} = E \cdot \varepsilon_{hs} \quad (2.10)$$

Where σ_{hs} is the structural hot spot stress and E is the modulus of elasticity for the steel.

According to IIW, for the case of bi-axial stress state the hot spot stresses may be up to 10% larger than the value given by the above equation. In this case IIW recommends that the ratio of the longitudinal and transverse strains ($\varepsilon_y/\varepsilon_x$) being estimated from the FEA results or rosette strain gauge measurements. Consequently, the structural hot spot stress can be evaluated from the following equation:

$$\sigma_{hs} = E \cdot \varepsilon_x \frac{1 + \nu \frac{\varepsilon_y}{\varepsilon_x}}{1 - \nu^2} \quad (2.11)$$

Where ν is the Poisson's ratio of the steel. In the derivation of the above relation, it is assumed that the principal stress is approximately perpendicular to the weld toe.

2.3.6 Calculation of structural hot spot stress using FEM

Except for some simplified cases, the analytical determination of structural hot spot stresses in structural details is not generally possible. As a result, finite element method is used to determine SHSS in the structural details. A good understanding of the FEM principles and the concept of the hot spot method are required to gain reliable results. The results are within the accuracy range of $\pm 10\%$, according to Niemi & Marquis (2003).

The finite element model usually is made based on the idealized geometry, neglecting the possible misalignments. On the other hand, manufacturing misalignments can generally have a considerable stress raising effect and hence, reduce the fatigue service life of the detail (Eriksson et al. (2003)). The effects of misalignments can be taken into account by using the appropriate stress magnification factors (k_m) given by the IIW recommendations for different categories of misalignments.

To determine the SHSS, linear elastic analysis is used. The mechanical properties of the material are selected same as the parent metal. Both shell and solid element models can be used. The elements' type and mesh size should be such that the model can capture the formation of abrupt stress gradients at the weld toe. But at the same time only the linear stress distribution in the plate thickness is needed to be determined. This is obviously a requirement put by the definition of the structural hot spot stress. To satisfy these two requirements, some rules and guidelines should be followed in the numerical modelling of the structure. These provisions are presented here according to IIW recommendations.

In shell element models (Figure 2.14, left part) the elements are placed in the mid-plane of the real structural parts. Use of 8-node isoparametric elements is recommended. Usually the welds are not introduced into the model in simplified models. But, if there is an offset between plates (such as cover plates), or there is a small distance between two adjacent welds, then the welds should be modelled. The welds can be modelled in several ways. A few methods to model the welds are as follows:

- Increasing the thickness of shell elements in the weld region to compensate for the increase stiffness in that region.
- Modelling the weld with oblique shell elements.
- Using rigid links between the corresponding nodes on the two joined plates.
- Using solid elements to model the weld and shell elements to model the plates.

Eriksson et al. (2003) have investigated various modelling techniques and their advantages and limitations. They have given comprehensive guidelines based on these investigations. They also point out the issue of using shell elements with dimensions

that are much smaller than the plate thickness. This can be troublesome in some commercial FEM software. Hence, the software manuals should be consulted to avoid any problems in this regard.

If the weld geometry is not modelled in the FE model, special care should be taken in selection of the extrapolation points. In this case several authors advise that extrapolation should be performed into a point on the intersection of the two plates, rather than the point on the weld toe (Niemi et al. (2006); Radaj et al. (2006)). This is to compensate for stress reduction due to omitted weld stiffness in the model.

Solid elements (Figure 2.14, right part) also may be used and they are recommended in modelling complex structures. Usually prismatic solid elements with quadratic shape functions and reduced integration are used. Another less selected choice is tetrahedral elements. These elements are desirable because of easy and automatic mesh generation technique (free meshing). In this case, a sufficiently fine mesh of second order tetrahedral elements should be used and the user should verify the results in proper ways. When using solid elements, modelling of the weld is always recommended. The gap between the two joined plates does not need to be modelled, according to Eriksson et al. (2003), since it has little effect on the results. This is also confirmed in the research conducted by Notaro et al. (2007).

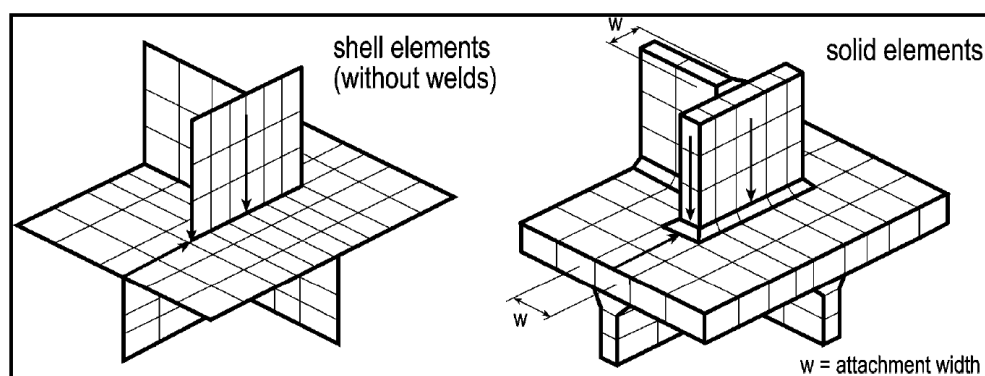


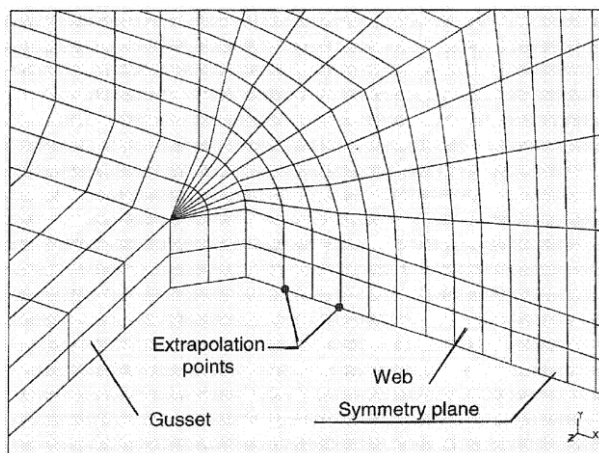
Figure 2.14 Two types of FE models for evaluation of SHSS. Left: shell elements model; Right: Solid elements model. From Niemi et al. (2006).

Below, some rules that should be followed for both types of the elements are presented, according to Hobbacher (2003):

- The chosen element types should allow for a linear stress distribution through the thickness. This is because the non-linear stress is to be omitted. This can be achieved by eight-node shell elements or 20-node solid elements with reduced integration. A single layer of solid elements through the thickness is sufficient. But if more layers of solid elements through the plate thickness are used, then the stress results should be linearized through the thickness to omit the nonlinear peak stress contribution.
- The sizes of the elements in the vicinity of the hot spot should be chosen such that the extrapolation points coincide with the elements' integration points or

nodal points. This way, the achievement of the highest possible accuracy is insured.

- When the computation of SHSS is based on nodal stress values, care should be taken that no stress averaging across the element boundaries for intersecting shell or solid elements are conducted. For example, at an intersection between two shell elements when one shell element is highly stressed and the other is not stressed, the nodal average values for the stresses have no practical usefulness.
- The largest allowed aspect ratio for the elements is limited to 3.
- The transition from fine mesh at the weld region into coarser mesh in other parts of the model should be gradual.
- When loading causes bending in the plate, the weld should be modeled curved around the ends of the gusset, like the one shown in Figure 2.12 (this is the case when modelling with solid elements).



2.12 *Modelling of the weld near the end of the gusset plate, according to Niemi et al. (2006).*

It is worth mentioning the study conducted by Doerk et al. (2003) here. They compared geometric stress results from different meshes and calculation techniques with the experimental measurements. Their conclusions mainly supported the IIW guidelines which are presented in this section. In addition, they emphasized that the SHSS results are mesh-sensitive and even the mesh *outside* the stress evaluation area in front of the weld toe can affect the results. They recommended that the designer should always remind the limitations due to FE model, and due to the hot spot method.

Recently, Fricke et al. (2008) conducted a round robin study of two structural details of ship structures using various FEM software and different meshing techniques. Some scatter in the analysis results was observed. The scatter was higher in the case of the second detail which was more complex. They showed that the scatter was due

to several factors. Namely, different types and properties of the finite elements, changes in mesh size, and various stress extrapolation techniques (linear or quadratic extrapolation) were main factors that produced this scatter in the results.

In the following sections, Section 2.3.6.1 to Section 2.3.6.3, different methods for ‘post-processing’ the finite element analysis results and calculation of SHSS are described. A comparison of the methods is presented in Section 2.3.6.4 based on the previous research in the field.

2.3.6.1 Through thickness integration

As shown earlier in this chapter, the structural hot spot stress can be assumed as the sum of membrane stress (σ_{mem}) and shell bending stress (σ_{ben}). Some FEM programs (including ABAQUS) have the ‘stress linearization’ capability in their post-processing section that calculated this so called ‘linearized’ stress. This feature can be used in type ‘a’ hot spots to linearize the stresses directly at the weld toe through the plate thickness and hence, calculate the hot spot stress. In order to compute the structural stress with the through thickness stress linearization at the weld toe (TTWT), at least three elements through the plate thickness are needed (Poutiainen et al. 2004).

2.3.6.2 Surface stress extrapolation methods

Extrapolation of the surface stresses in FEM model is quite similar to the extrapolations discussed in the section 2.3.5 (Experimental evaluation of SHSS). IIW document (2003) proposes two meshing options: a coarse mesh and a fine mesh which gives more accurate results. These two methods are presented in Table 2.2 and Table 2.3. These two meshing methods are described more in the following:

Fine mesh: for evaluation of type ‘a’ hot spots, first element length should not exceed $0.4t$. Stress evaluation points should be on nodal points $0.4t$ and $1.0t$ away from the hot spot and linear extrapolations is used⁹:

$$\sigma_{hs} = 1.67 \cdot \sigma_{0.4t} - 0.67 \cdot \sigma_{1.0t} \quad (2.13)$$

For type ‘b’ hot spots, lengths of the first three elements along the edge should be equal to, or less than 4 mm at the hot spot. Reference points should be coincident with the nodal points at the 4 mm, 8 mm, and 12 mm from the hot spot. Quadratic extrapolation is used in this case:

$$\sigma_{hs} = 3 \cdot \sigma_{4mm} - 3 \cdot \sigma_{8mm} + \sigma_{12mm} \quad (2.14)$$

‘Designer’s guide to the structural hot spot method’ (Niemi et al. (2006)) recommends use of fine mesh in the following situations:

- High stress gradients are available in the joint;

⁹ In cases where the plate is resting on a stiff elastic support IIW recommends using a quadratic extrapolation scheme.

- Discontinuities exist adjacent to the weld;
- Comparing finite element results and measured stresses are required.

Table 2.2 IIW (2006) guidelines for meshing and stress evaluation using surface stress extrapolation (See also Table 2.3).

Types of model and hot spot		Relatively coarse mesh		Relatively fine mesh	
		Type a	Type b	Type a	Type b
Element size	Shell	$t \times t$, max $t \times w/2$	10mm×10mm	$\leq 0.4t \times t$ or $0.4t \times w/2$	$\leq 4\text{mm} \times 4\text{mm}$
	Solid	$t \times t$, max $t \times w$	10mm×10mm	$\leq 0.4t \times t$ or $0.4t \times w/2$	$\leq 4\text{mm} \times 4\text{mm}$
Extrapolation points	Shell	0.5t / 1.5t (mid-side points)	5mm / 15mm (mid-side points)	0.4t / 1.0t (nodal points)	4mm / 8mm / 12mm (nodal points)
	Solid	0.5t / 1.5t (surface centre)	5mm / 15mm (surface centre)	0.4t / 1.0t (nodal points)	4mm / 8mm / 12mm (nodal points)

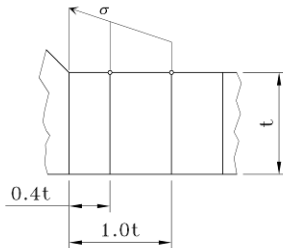
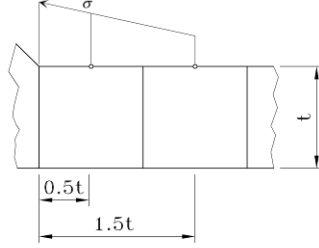
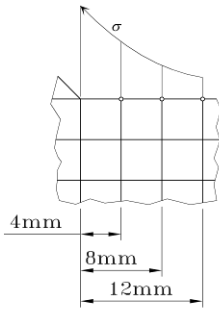
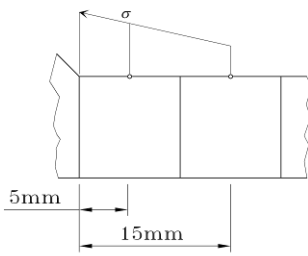
Note: w=attachment width, define as attachment thickness plus twice the weld leg length (See Figure 2.14).

Coarse mesh: this meshing option can be used if no other severe discontinuities exist close to the weld and the stress gradient close to the hot spot is not extremely high. Second order elements should be used. The lengths of elements at the hot spot region should be equal to the plate thickness (i.e. $1.0t$, for type ‘a’ hot spots) or 10 mm (for type ‘b’ hot spots). The element widths (in the direction parallel to the weld) can also affect the results. Too wide elements may lead to non-conservative results. Thus, some recommended values for the element widths are also given in the Table 2.2 and Table 2.3. Reference points for the stress extrapolation will be placed at the mid-side points of the first two elements. Linear extrapolation should be used:

$$\text{Type 'a': } \sigma_{hs} = 1.50 \cdot \sigma_{0.5t} - 0.50 \cdot \sigma_{1.5t} \quad (2.15)$$

$$\text{Type 'b': } \sigma_{hs} = 1.50 \cdot \sigma_{5mm} - 0.50 \cdot \sigma_{15mm} \quad (2.16)$$

Table 2.3 IIW (2006) illustrated guidelines on meshing and stress evaluation using surface stress extrapolation

	Relatively fine mesh (as shown or finer)	Relatively coarse mesh (fixed element sizes)
Hot spot Type 'a'	 <p>(i)</p>	 <p>(ii)</p>
Hot spot Type 'b'	 <p>(iii)</p>	 <p>(iv)</p>

2.3.6.3 Alternative methods

In recent years, some researchers have proposed other evaluation methods for structural hot spot stress. Among them, Dong (2001) and Xiao & Yamada (2004) have gained more interest. Dong method investigates the equilibrium conditions at an arbitrary (small) distance from the weld toe to assess the structural stress. This method is claimed to be mesh-insensitive (see next section). Xiao and Yamada suggest evaluation of the stress at 1 mm depth from the plate surface at the weld toe and taking this value as the structural hot spot stress.

2.3.6.4 Comparison of SHSS evaluation methods

Several groups of researchers have investigated different evaluation methods of geometric stress in structural details and have compared the fatigue life based on the analytical methods to the real specimens' fatigue lives. The number of comparison studies has increased especially after the recent introduction of the alternative

methods such as the methods proposed by Dong (2001) and Xiao & Yamada (2004). Some of these investigations are introduced here in chronological order:

As their work was referred earlier in this Section, Doerk et al. (2003) compared the following SHSS evaluation methods: surface stress extrapolation (SSE), through thickness stress linearization at the weld toe (TTWT), and the Dong method. They found that the methods generally give similar results and since the definition of structural stress is principally the same in all methods, the same S-N curves can be used regardless of the method used for evaluation of SHSS. They also confirmed the mesh-insensitivity claimed by the Dong method in case of 2D models. But, in case of 3D models all methods showed a scatter as a result of variations in the mesh size.

In a similar work, Poutiainen et al. (2004) compared the same methods as above research. They found that for 2D models all methods give virtually the same results and if one element is used through the thickness, all methods can be considered mesh-insensitive. In the case of 3D model, nodal averaging seemed to be very influential on the results of the TTWT and Dong methods. The Dong method was the most demanding method in terms of computational effort required for post processing. They also pointed out that SSE method is the most sensitive method to mesh variations.

Fricke & Kahl (2005) also carried out a comparison between three structural stress evaluation methods by applying the methods to different structural details. The investigated methods were surface stress extrapolation carried out by IIW regulations, Dong (2001) method, and Xiao & Yamada (2004) method. They found that element properties and sizes were the main reason for variations in the hot spot values, particularly in the case of modelling with shell elements. They also pointed out the beneficial effect of residual stresses on the fatigue lives of real specimens. This caused large differences between experiments and computed fatigue life.

Notaro et al. (2007) assessed the fatigue life of a complex welded detail which is in wide use in the shipbuilding industry using two SHSS evaluation methods. One method was the surface stress extrapolation and the other was the new method proposed by Xiao & Yamada (2004). They compared the analytical values to the experimental measurements and found an acceptable agreement between the analytical methods and the results from the tests.

Kim & Kang (2008) tested 12 specimens of a simple edge detail (type 'b' hot spot) with various dimensions and, based on FE analyses, computed the geometric stress according to both SSE and Dong method. They found that the Dong method results in lower geometric stress values than SSE. The fatigue life prediction using these methods was better than predictions based on the nominal stress method. They proposed that an even better fatigue life prediction is possible by introducing a thickness correction factor into the values obtained from the Dong method.

These investigations and similar works of other researchers have lead to adoption of the alternative SHSS evaluation methods in the newest draft of the IIW recommendations (2009 revision).

2.3.7 Hot spot S-N design curves

The ‘FAT class’ or ‘detail category’ is by definition the fatigue stress range that gives a fatigue life of two million cycles. The shape of fatigue strength S-N curves in IIW recommendations for the structural hot spot stress are similar to the direct nominal stress S-N curves and consist of a line with constant slope of $m=3.00$ (in a log-log scale) and a cut-off limit for the case of CAFL¹⁰ at the 5 million cycles. A schematic of the S-N curves is presented in Figure 2.15.

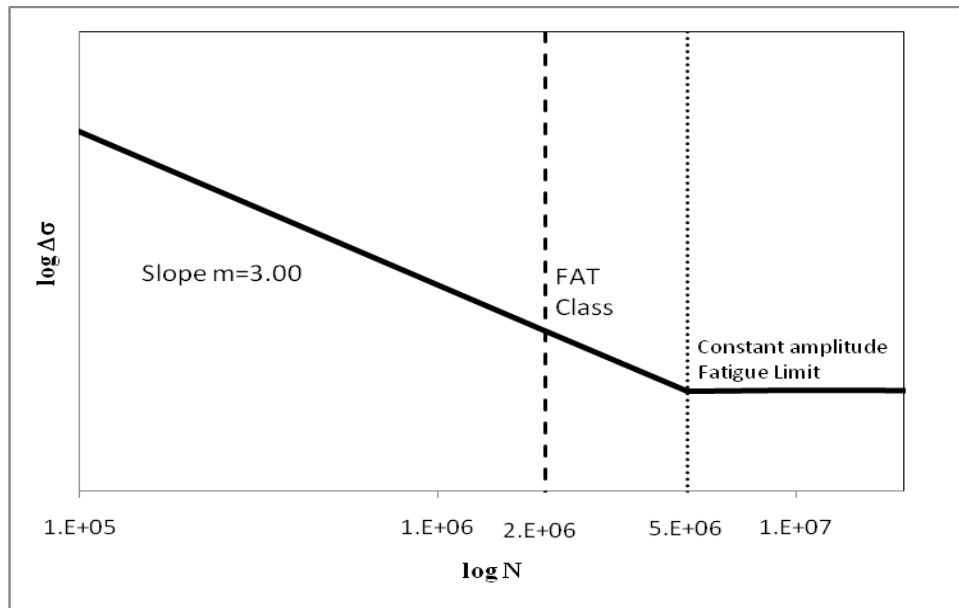


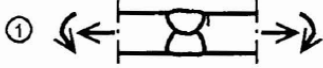

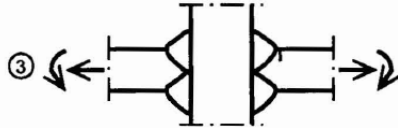
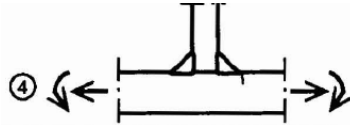


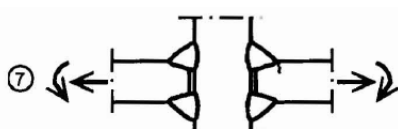
Figure 2.15 fatigue strength S-N curves for structural hot spot stress in steel.

Marquis and Kähönen (1996) performed a comparison between several S-N curves (recommended by design codes or proposed by various researches) versus experimental results. The older pre-standard Eurocode (ENV 1992) was also included in their study. They concluded that the pre-standard Eurocode S-N curves are significantly on the safe side. As a result, the last revision of Eurocode 3 has recommended the same fatigue resistance S-N curves as the IIW recommendations which gives slightly higher fatigue life for the components.

In contrast with nominal stress approach (See Section 2.2 and Figure 2.3), no standard details are associated with the curves. Instead, 7 types of welds are introduced and one S-N curve is recommended for each type. These are shown in the Table 2.4. It should be noticed that the effect of the misalignments are not included in these design S-N curves and as it was noted before, that effect should be taken into account in a proper way in the design process. Another effect that should be considered when using these S-N curves is the effect of component size on the fatigue strength of the component. This is done by introducing a reduction factor for plates more than 25 mm thick.

¹⁰ Constant Amplitude Fatigue Limit

Table 2.4 Detail categories for the structural hot spot stress method recommended with both Eurocode and IIW recommendations.

Detail category	Constructioal detail	Description	Requirements
112		1) Full penetration butt joint (Special quality)	1) - All welds ground flush to plate surface parallel to direction of the arrow. - Weld run-on and run-off pieces to be used and subsequently removed, plate edges to be ground flush in direction of stress. - Welded from both sides, checked by NDT.
100		2) Full penetration butt joint (Normal quality).	2) - Weld not ground flush - Weld run-on and run-off pieces to be used and subsequently removed, plate edges to be ground flush in direction of stress. - Welded from both sides.
100		3) Cruciform joint with full penetration K-butt welds.	3) Weld toe angle $\leq 60^\circ$
100		4) Non load-carrying fillet welds.	4) Weld toe angle $\leq 60^\circ$
100		5) Bracket ends, ends of longitudinal stiffeners	5) Weld toe angle $\leq 60^\circ$
100		6) Cover plate ends and similar joints	6) Weld toe angle $\leq 60^\circ$
90		7)cruciform joints with load-carrying fillet welds	7) Weld toe angle $\leq 60^\circ$

As Maddox (2002) states, one of the major research issues in the field of fatigue assessment using hot spot method is the choice of hot spot stress design S-N curves. Many research efforts have been done in this regard. For example, Maddox (2002) investigated a large number of hot spot S-N data for various structural details available in the literature including the data obtained during a major joint industry project (JIP) aiming at the design of floating production, storage and offloading (FSPO) units. He concluded that the analysed fatigue data support the assumption of FAT 90 design S-N curve when using the IIW “0.4t and 1.0t” extrapolation rule. In the framework of the phase II of above mentioned JIP project, Lotsberg & Sigurdsson (2006) confirmed the validity of the FAT 90 curve also for “0.5t and 1.5t” rule.

It is worth mentioning that both Eurocode and IIW recommendations allow using data from fatigue tests for derivation of design S-N curves for details similar to the tested specimens. For example, in an earlier research conducted by Kjellberg & Persson (1998) at the department of naval architecture and ocean engineering of Chalmers university of technology, the experimental fatigue data from testing of 11 different types of specimens were analysed and a design S-N curve with a slope of $m=3.40$ and fatigue class of FAT 85 was proposed for the design of the ship body’s structural details similar to the examined specimens.

3 Fatigue Tests

3.1 Orthotropic bridge decks

Orthotropic bridge decks consist of a deck plate stiffened by a system of orthogonal longitudinal and transverse stiffeners. The stiffeners could be of open or closed cross sections. These are shown in Figure 3.1. The resulting system is a light weight deck for steel road bridges and is especially efficient for use in long-span or suspension bridges, where the reduction in dead weight of the structure is more important. According to Kolstein (2007), Germany and Netherlands are the largest owners of steel bridges with orthotropic decks. Orthotropic bridge decks were introduced in 1950's. Their popularity was at its highest during 70's and then reduced afterwards. Kolstein (2007) states the decline in use of this system is related to the growing awareness of engineers to fatigue problems with orthotropic decks.

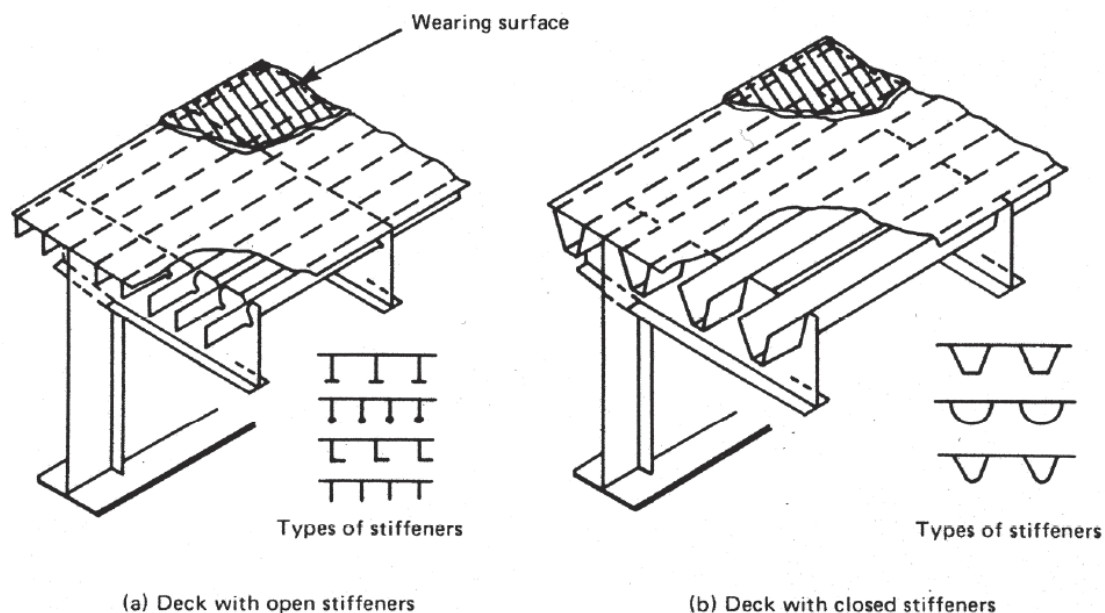


Figure 3.1 Two types of orthotropic bridge decks.

3.2 The assessed detail

A detail in orthotropic bridge decks with open stiffeners (also named troughs or ribs) was investigated in this study. That was the stiffener to crossbeam joint. This joint is the most complex joint in the orthotropic deck. Two highly stressed members cross each other in this location. As a part of his extensive study of fatigue in orthotropic bridge decks, Kolstein (2007) summarized the reported fatigue failures in this type of joints for the case of decks with closed stiffeners. The joint can be constructed in two ways:

- The cross beams being continuous and stiffeners being welded to them. This method was used in earlier designs. This reduces the possibility of cracking in the cross beam, but the weld between stiffener and cross beam is rather weak in fatigue loading.
- Keeping stiffeners continuous by making cut-outs in the cross beams. Besides, cope holes may be provided in the locations of top and bottom edges of the stiffener to improve the fatigue life.

In this study, the second type of the above types was assessed. Three full-scale specimens¹¹ were tested in the experimental part of the study. The dimensions of the specimens are shown in Figure 3.2. The joints between the stiffener, cross beam and deck plate were all fillet welded with a weld throat dimension of $a=5$ mm.

3.3 Test method

The specimens were tested in a way similar to the three point bending test, as shown in Figure 3.3 and Figure 3.4. Each specimen was held on two roller supports at the cross beam ends. The load was applied in a vertical plane passing through the mid-span of the cross beam by an actuator via a load cell and a loading beam. The loading beam divided the load into two equal parts and applied each part to one end of the stiffeners. The stiffeners were stiffened by two stiffeners at the point of application of concentrated load to prevent local deformations, as seen in Figure 3.3. This loading would cause a negative moment in the stiffener in the joint location, and a positive moment in the cross beam in that section. Specimens were first loaded statically with a small load to carry out elastic strain measurements via strain gages. Subsequently, high cycle fatigue testing with constant amplitude fatigue load was performed.

¹¹ A fourth specimen was also tested. It was loaded monotonically until failure to determine the collapse load.

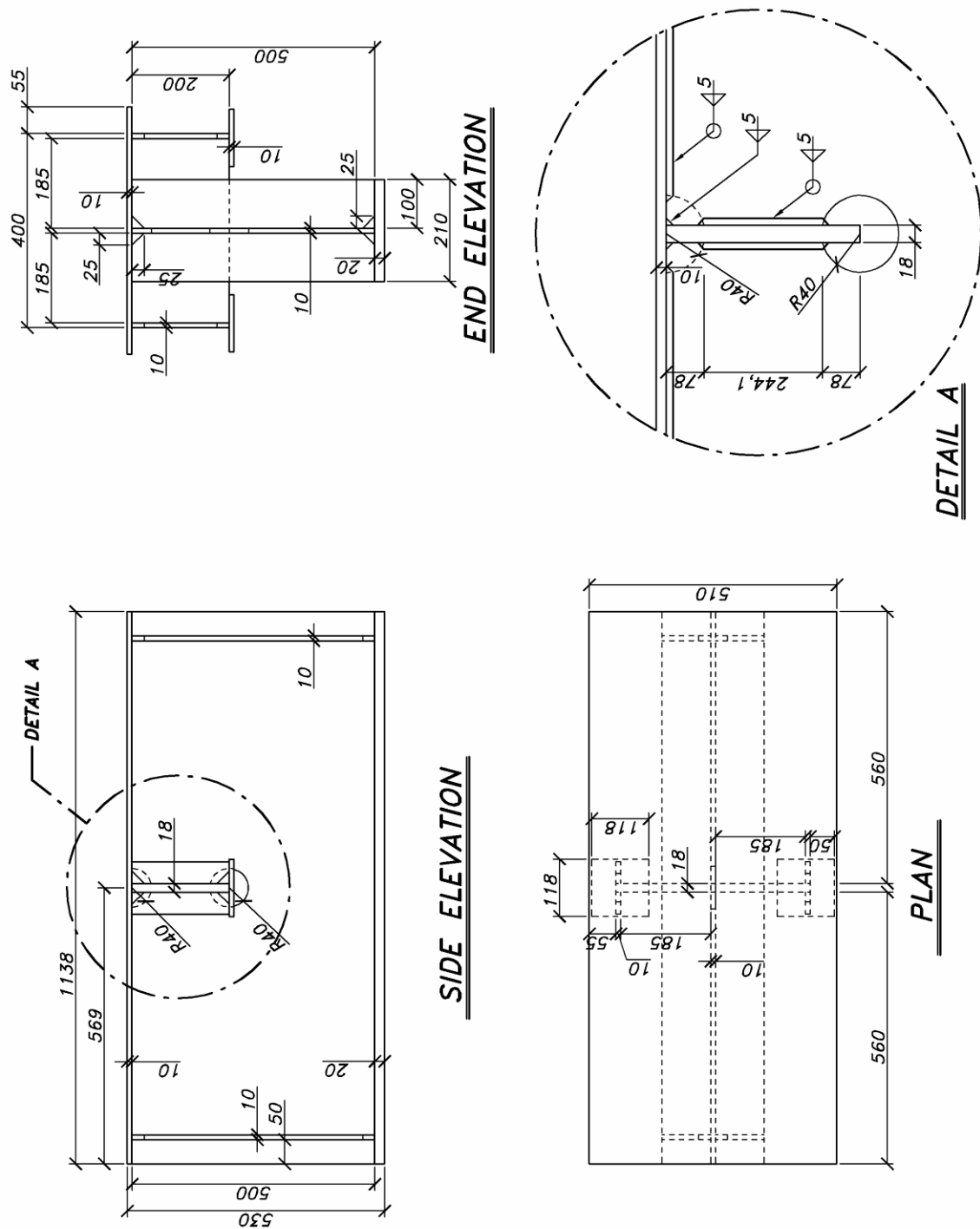


Figure 3.2 Dimensions of the tested specimens.

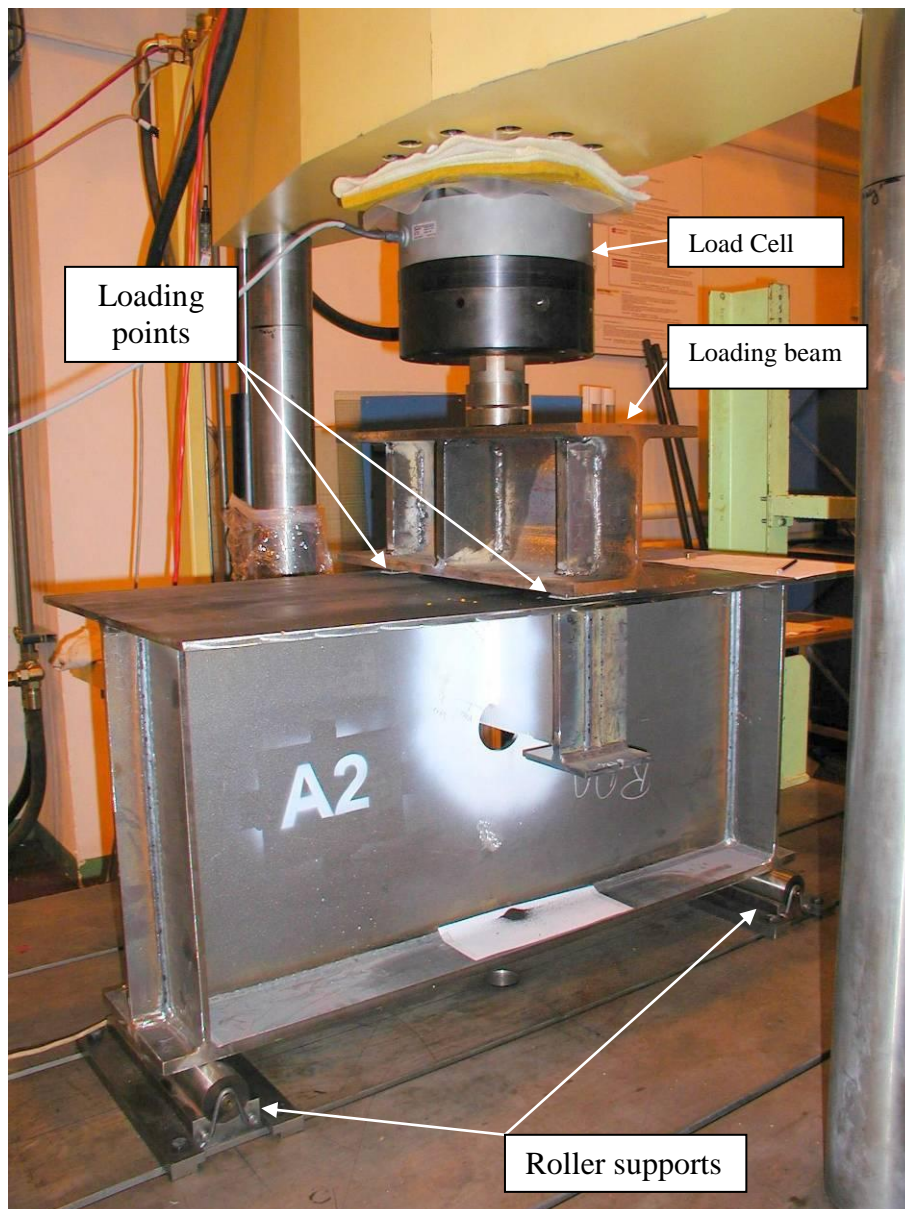


Figure 3.3 specimen mounted in the fatigue test machine.

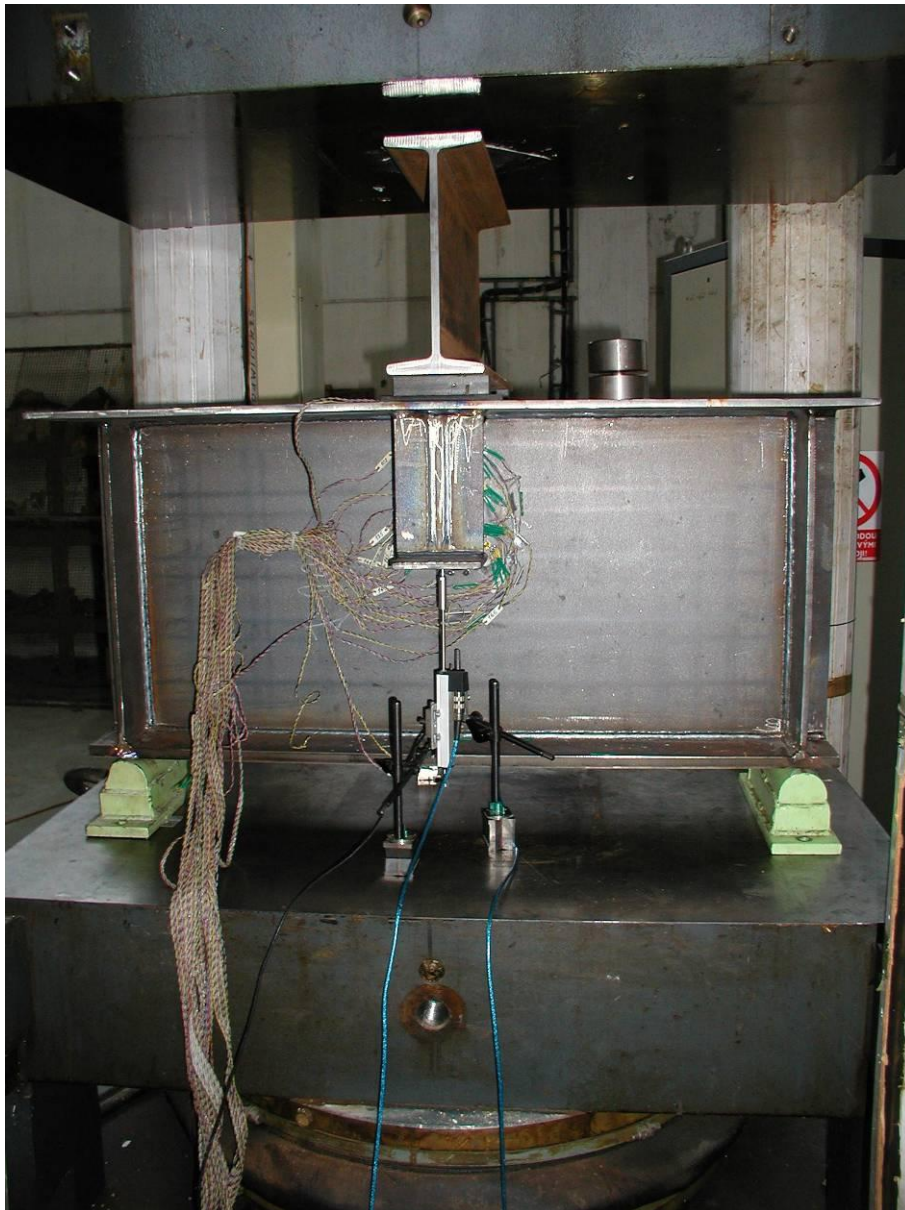


Figure 3.4 specimen mounted in the fatigue test machine.

3.4 Measurements

Strain measurements were taken during the static tests. The hot spot zones (i.e. placement of the strain gages) were located by a primary finite element analysis. The points on the weld toes with high values of principal stresses are prone to cracking. These zones are shown in Figure 3.5. It is worth noting that, according to FE analysis results, there is a possible cracking zone on the curved edge of the upper cope hole which cannot be predicted by the SHSS method. This is addressed in the limitations of the study in Chapter 2.

The model also predicted that the first fatigue cracks should initiate on the surface of the web of the crossbeam at the bottom of weld line (point A in Figure 3.5). This was the case for the specimen A4 (see Table 3.11 at the end of this chapter). However, the

stresses in the end of cross beam-to-deck connection were underestimated since the weld geometry at that hot spot was not modelled. During the experiments, this point was the first place for the cracks to initiate in the A2 and A3 specimens. The studied detail shows an example of a detail with several ‘competing’ hot spots.

From the data mentioned above, four hot spots were identified on the web of the cross beam (‘wb’ and ‘wt’ in Figure 3.6) and four hot spots on the deck plate (‘fl1’ and ‘fl2’ in Figure 3.6). Because of the symmetry of the detail, there are two of each of the above mentioned hot spots. ‘wb’ and ‘wt’ points are type ‘b’ hot spots and ‘fl1’ and ‘fl2’ points are of type ‘a’. Based on the finite element analysis, the cracking in point ‘fl1’ did not seem to be critical. However, some cracking was observed at the deck plate in this point. So, it was added to the list of the hot spots for further investigation.

The cracking might also initiate in the weld toe on the stiffener plate. But for the assessed detail, this was not the case, because of the relatively high thickness of the stiffener plate (18mm). This was shown also in finite element analysis and was verified in the experiments.

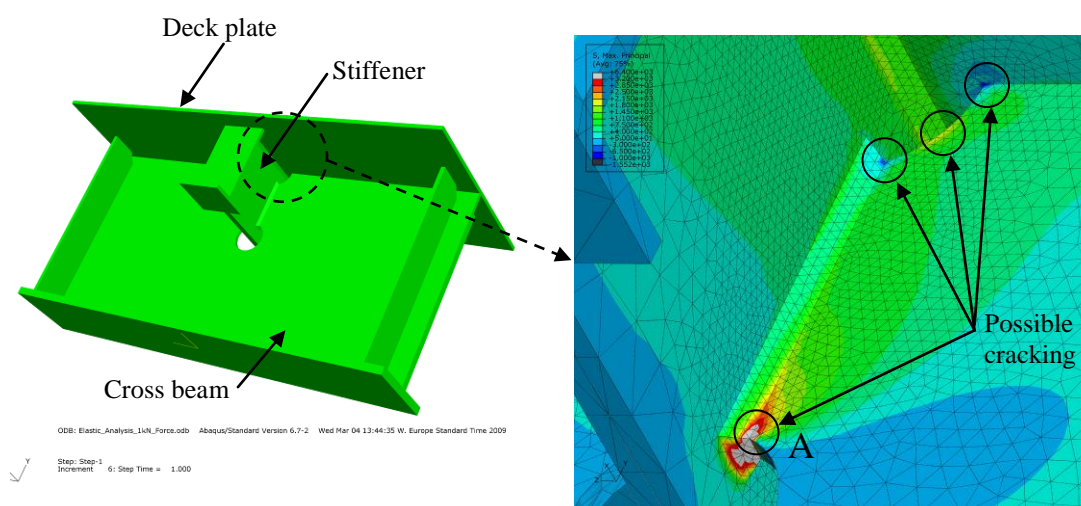


Figure 3.5 Identifying the hot spot locations from the FE analysis.

The stress profiles in the hot spot zones were measured with chain strain gages, as shown in Figure 3.7. This was done for specimen A4. Furthermore, two simple strain gages were installed on the plate surface opposite to the face where chain strain gages were installed. This way, the calculation of structural stress by surface stress extrapolation could be verified by two measurements. Given the complexity of the detail geometry in one hand and the irregularities in the weld geometry in the other hand, the placement of the strain gages on the desired location was an intricate job. This was specially the case for the type B hot spots, because the strain gradient in the hot spot is steeper and exact placement of strain gages in both directions, perpendicular to the weld and along the weld, is crucial. It also appeared in practice that the exact placement of simple strain gages in the prescribed extrapolation points is rather hard. Hence, the use of chain strain gages is recommended in all hot spot zones in future studies. As an example of the problems involved in placement of the strain gages on their theoretical location, Figure 3.8 shows the measured distances of

installed strain gage from the hot spot 'wb' on specimen A4. Note that the 2.5 mm vertical distance of the strain gage from the hot spot is hardly avoidable, because of the curvature of the plate edge at the cope hole.

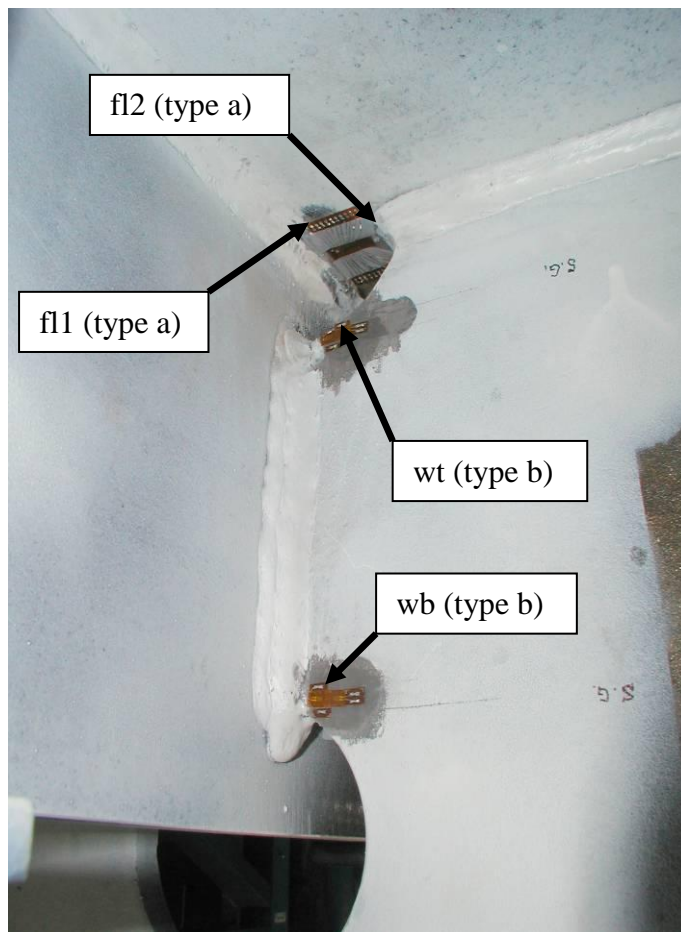


Figure 3.6 Assessed hot spot locations on the specimen.

Furthermore, since the 'fl1' and 'fl2' hot spots were too close to each other, it was not possible to install two strain gages in the area between these two points. So, just one chain strain gage was installed in the area at a distance $0.4t$ from the weld toe at hot spot 'fl1'.

Since the specimens A2 and A3 were tested before the start of this study, the arrangement of the strain gages did not conform to the requirements put by the SHSS method. The measurements on these specimens were made by rosette strain gages.

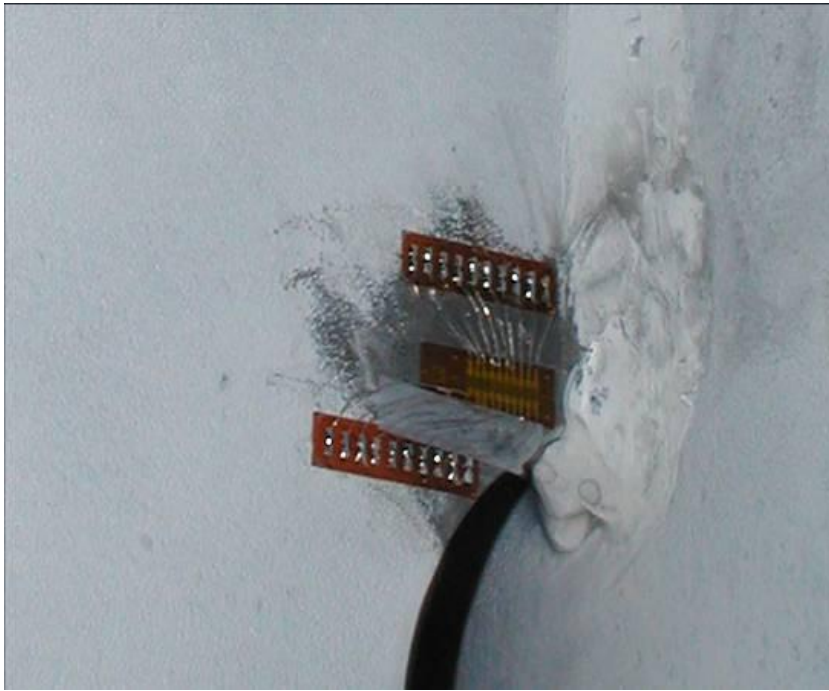


Figure 3.7 Chain strain gages installed on 'wb' hot spot on specimen A4 (before wiring).

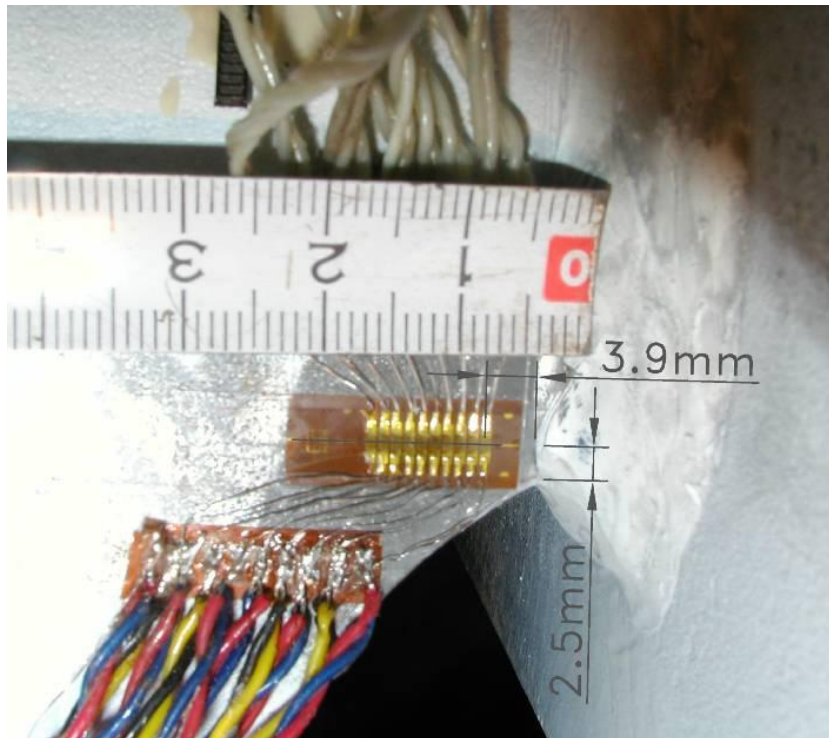


Figure 3.8 Measurement of the horizontal and vertical distance of the chain strain gage from the type 'b' hot spot ('wb' point - A4 specimen).

3.5 Specimens

3.5.1 Specimen A2

This specimen was first tested under a constant amplitude fatigue load with a load range of 200 kN. After about 5.5 million cycles, no visible crack was formed. So, the test continued with a load range of 400 kN for another 1.5 million cycles. The loading data is presented in Table 3.1.

Figure 3.9 and Figure 3.10 show the specimen after the test. Table 3.2 and Table 3.3 show the fatigue crack growth data for the cracks shown in the figures.

Table 3.1 Fatigue loading data for the specimen A2.

Maximum load [kN]	Minimum load [kN]	Load range [kN]	Load frequency Hz]	Number of cycles [n]
210	10	200	3	5 527 812
410	10	400	2	1 543 930

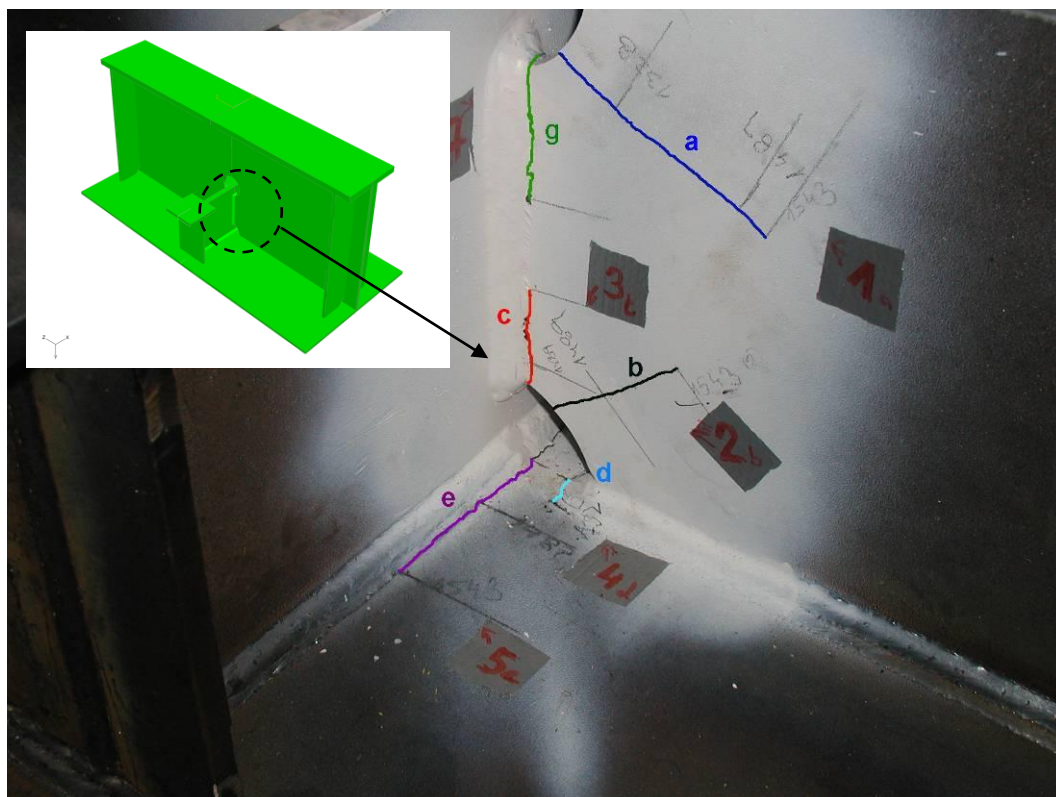


Figure 3.9 Fatigue cracks in specimen A2.

Table 3.2 Crack growth data - Specimen A2.

Crack	Crack a	Crack b	Crack c	Crack d	Crack e	Crack g
Hot spot	N/A	N/A	wt	fl2	fl1	wb
Cycles[n]	Length [mm]	Length [mm]	Length [mm]	Length [mm]	Length [mm]	Length [mm]
180000	0	0	0	0	0	0
305000	0	0	0	0	0	0
368000	0	0	0	0	0	0
552739	0	0	0	0	0	0
732330	0	0	0	0	0	0
907260	0	0	0	0	0	0
1123466	0	0	0	0	0	0
1136255	0	0	0	0	0	0
1308000	0	0	0	0	0	0
1328000	33,66	0	0	0	0	0
1489000	84	31,89	16,15	0	31,54	0
1543930	95,46	69,29	48,11	14,61	77,3	54,01

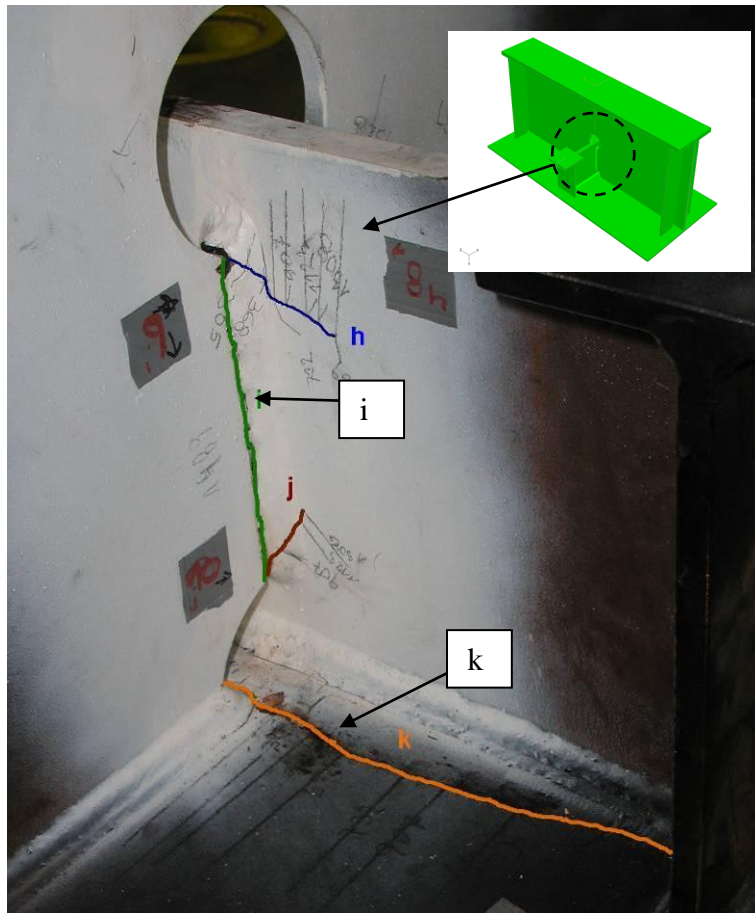


Figure 3.10 Fatigue cracks in specimen A2 (other side of the specimen).

Table 3.3 Crack growth data - Specimen A2, continued.

	Crack h	Crack i	Crack j	Crack k
Hot spot	wb	wb	wt	fl2
Cycles[n]	Length [mm]	Length [mm]	Length [mm]	Length [mm]
0	0	0	0	0
180000	0	0	0	20,51
305000	12,09	0	0	30,07
368000	19,76	0	0	38,59
552739	25,5	0	0	55,52
732330	32,93	0	0	81,58

907260	38,02	0	16,88	96,26
1123466	47,61	0	28,95	123,33
1136255	52,58	0	34,99	132,02
1308000	52,58	0	34,99	152,22
1328000	52,58	0	34,99	164,33
1489000	60,39	125	34,99	174,32
1543930	60,39	125	34,99	178,61

Figure 3.10 shows that the cracks ‘j’ and ‘h’ have initiated on the web plate surface of the cross beam. But their development pattern is rather complex. Instead of developing at the weld toe along the weld line (crack path i), they have grown through the weld itself and then through the thick web plate of the stiffener.

Crack growth data for cracks a and b (Table 3.2) reveals that the crack initiation in the curved parts of the cope holes, which are highly stressed but are not welded, occurs far more later than the cracking in hot spots

3.5.2 Specimen A3

This specimen was tested under a constant amplitude fatigue loading with a load range of 350 kN up to 5 million cycles. The loading data is presented in Table 3.4. Figure 3.11 to Figure 3.14 show the various cracks in the specimen after the test. The fatigue crack growth data for these cracks are presented in Table 3.5 to Table 3.7.

Table 3.4 Fatigue loading data for the specimen A3.

Maximum load [kN]	Minimum load [kN]	Load range [kN]	Number of cycles [n]
360	10	350	5 000 000

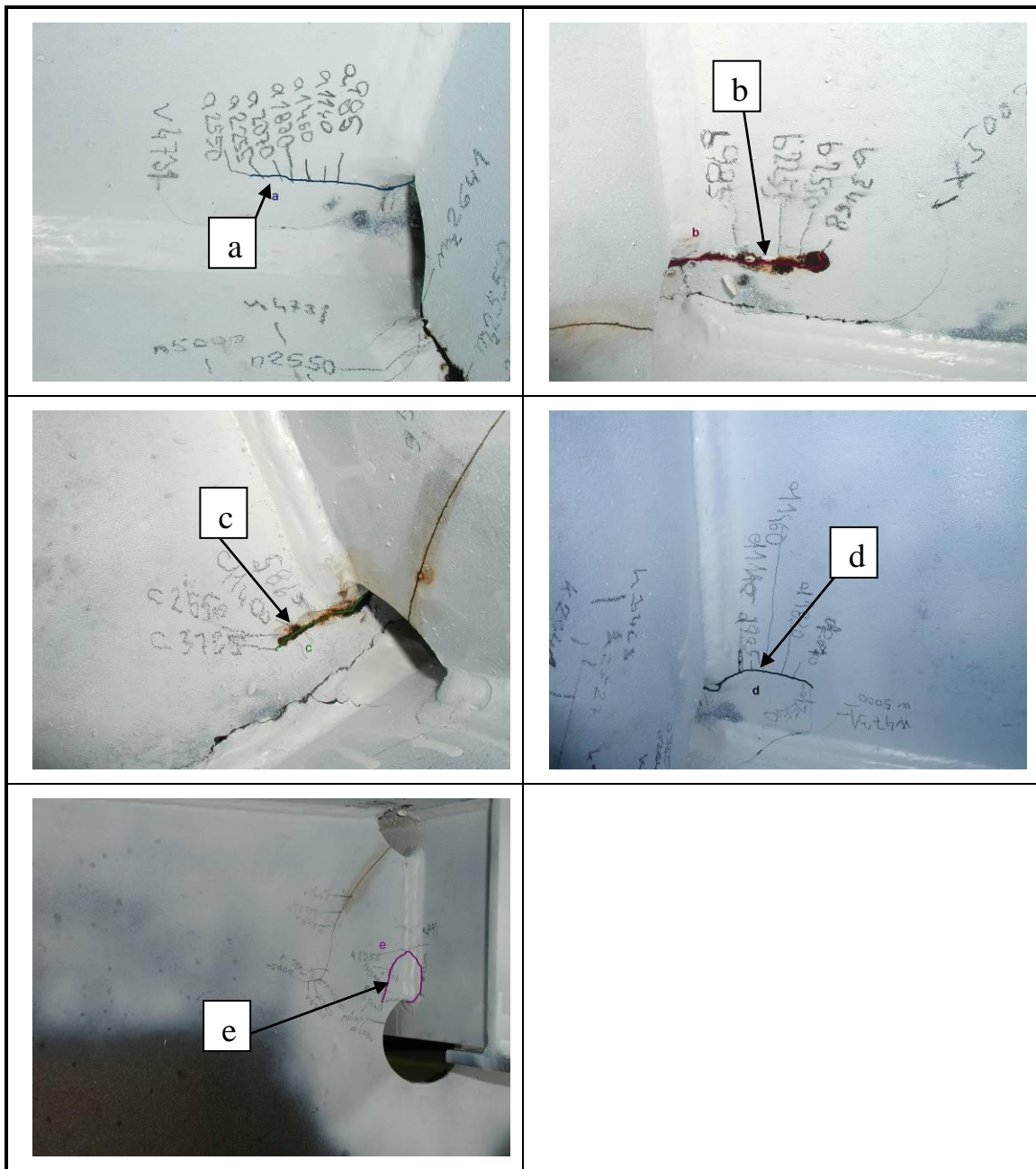


Figure 3.11 Fatigue cracks in specimen A3: (a)fl2 hot spot;(b)fl2 hot spot;(c)fl2 hot spot;(d)fl2 hot spot;(e) wb hot spot.

Table 3.5 Crack growth data - Specimen A3.

	Crack a	Crack b	Crack c	Crack d	Crack e
Hot spot	fl2	fl2	fl2	fl2	wb
Cycles[n]	length [mm]	length [mm]	length [mm]	length [mm]	length [mm]
0	0	0	0	0	0
985 000	18	22	20	30	0
1 085 000	18	22	20	30	5
1 140 000	23	30	20	35	5
1 330 000	23	30	20	35	15
1 460 000	28	30	20	35	15
1 830 000	33	30	20	43	15
1 871 000	33	30	20	43	15
1 935 000	33	30	20	43	15
2 070 000	37	30	20	49	15
2 255 000	43	35	20	49	63
2 527 000	43	35	20	54	63
2 550 000	47	41	33	54	63
2 641 000	47	41	33	54	63
2 886 000	47	41	33	54	63
3 065 000	47	41	33	54	63
3 139 000	47	41	33	54	63
3 468 000	47	46	33	54	88
3 719 000	47	46	33	54	88
3 785 000	47	46	36	54	88
3 963 000	47	46	36	54	88

4 139 000	47	46	36	54	92
4 370 000	47	46	36	54	92
4 731 000	47	46	36	54	92
5 000 000	47	46	36	54	122

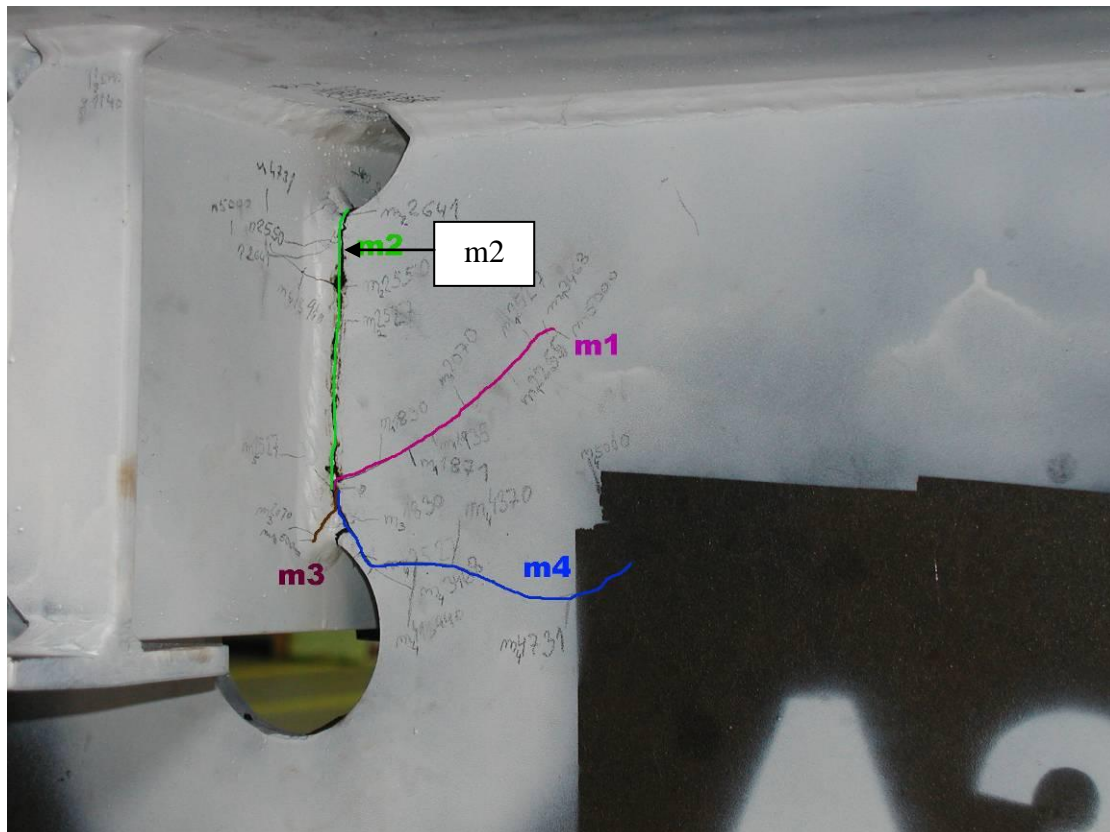


Figure 3.12 Fatigue cracks in specimen A3.

Table 3.6 Crack growth data - Specimen A3, continued.

	Crack m1	Crack m2	Crack m3	Crack m4
Hot spot	wb	wt	wb	wb
Cycles[n]	length [mm]	length [mm]	length [mm]	length [mm]
0	0	0	0	0
985 000	0	0	0	0

1 085 000	0	0	0	0
1 140 000	0	0	0	0
1 330 000	0	0	0	0
1 460 000	0	0	0	0
1 830 000	23	0	22	0
1 871 000	37	0	22	0
1 935 000	49	0	22	0
2 070 000	68	0	24	0
2 255 000	90	0	24	0
2 527 000	105	65	24	28
2 550 000	105	78	24	28
2 641 000	105	105	24	28
2 886 000	105	105	24	28
3 065 000	105	105	24	28
3 139 000	105	105	24	28
3 468 000	112	105	24	36
3 719 000	112	105	24	36
3 785 000	112	105	24	36
3 963 000	112	105	24	36
4 139 000	112	105	24	56
4 370 000	112	105	24	72
4 731 000	112	105	24	126
5 000 000	115	105	24	160

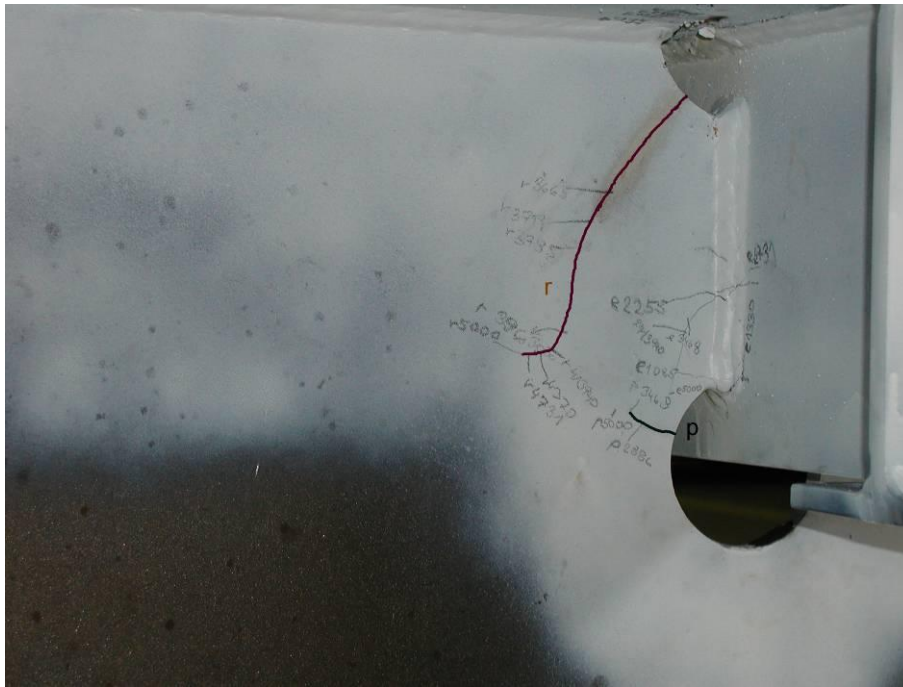


Figure 3.13 Fatigue cracks in specimen A3.



Figure 3.14 Fatigue cracks in specimen A3.

Table 3.7 Crack growth data - Specimen A3, continued.

	Crack p	Crack r	Crack v
Hot spot	N/A	N/A	f11
Cycles[n]	length [mm]	length [mm]	length [mm]
0	0	0	0
985 000	20	0	0
1 085 000	28	0	0
1 140 000	36	0	0
1 330 000	36	0	0
1 460 000	36	0	0
1 830 000	36	0	0
1 871 000	36	0	0
1 935 000	36	0	0
2 070 000	36	0	0
2 255 000	36	0	0
2 527 000	36	0	0
2 550 000	36	0	0
2 641 000	36	0	0
2 886 000	36	0	0
3 065 000	36	61	0
3 139 000	36	61	0
3 468 000	36	61	0
3 719 000	36	75	0
3 785 000	36	89	0
3 963 000	36	128	0
4 139 000	36	138	0

4 370 000	36	144	0
4 731 000	36	150	85
5 000 000	36	153	85

3.5.3 Specimen A4

The specimen was tested with a fatigue load range of 370 kN. The loading data is presented in Table 3.8.

Table 3.8 Fatigue loading data for the specimen A4.

Maximum load [kN]	Minimum load [kN]	Load range [kN]	Number of cycles [n]
10	380	370	Test in progress

This specimen was instrumented by chain strain gages in hot spot regions. The measurement method is given in Section 3.4. Following the IIW guidelines described in Section 2.3.5, the structural hot spot stress could be evaluated experimentally. Figure 3.15 shows the placement of strain gages on the specimen. Red numbers in bold on the figure show the channel numbers in the strain data output. Ranges of numbers denote chain strain gages. For example channels 51 to 60 were connected to the chain strain gage installed on the ‘wb’ hot spot. Moreover, channels 31-40 captured the chain strain gage output installed on the similar ‘wb’ hot spot on the other side of the specimen.

The stresses were calculated from the strain measurements using Equation 2-11. The ratios of the longitudinal and transverse strains ($\varepsilon_y/\varepsilon_x$) at hot spot regions were required for this calculation. These were calculated from the finite element analysis results (see section 2.3.5), and are shown in Table 3.9.

Table 3.9 $\varepsilon_y/\varepsilon_x$ ratios for hot spots.

Hot spot	wb	wt	fl1	fl2
$\varepsilon_y/\varepsilon_x$	-0.2149	-0.2081	-0.0673	Not Calculated

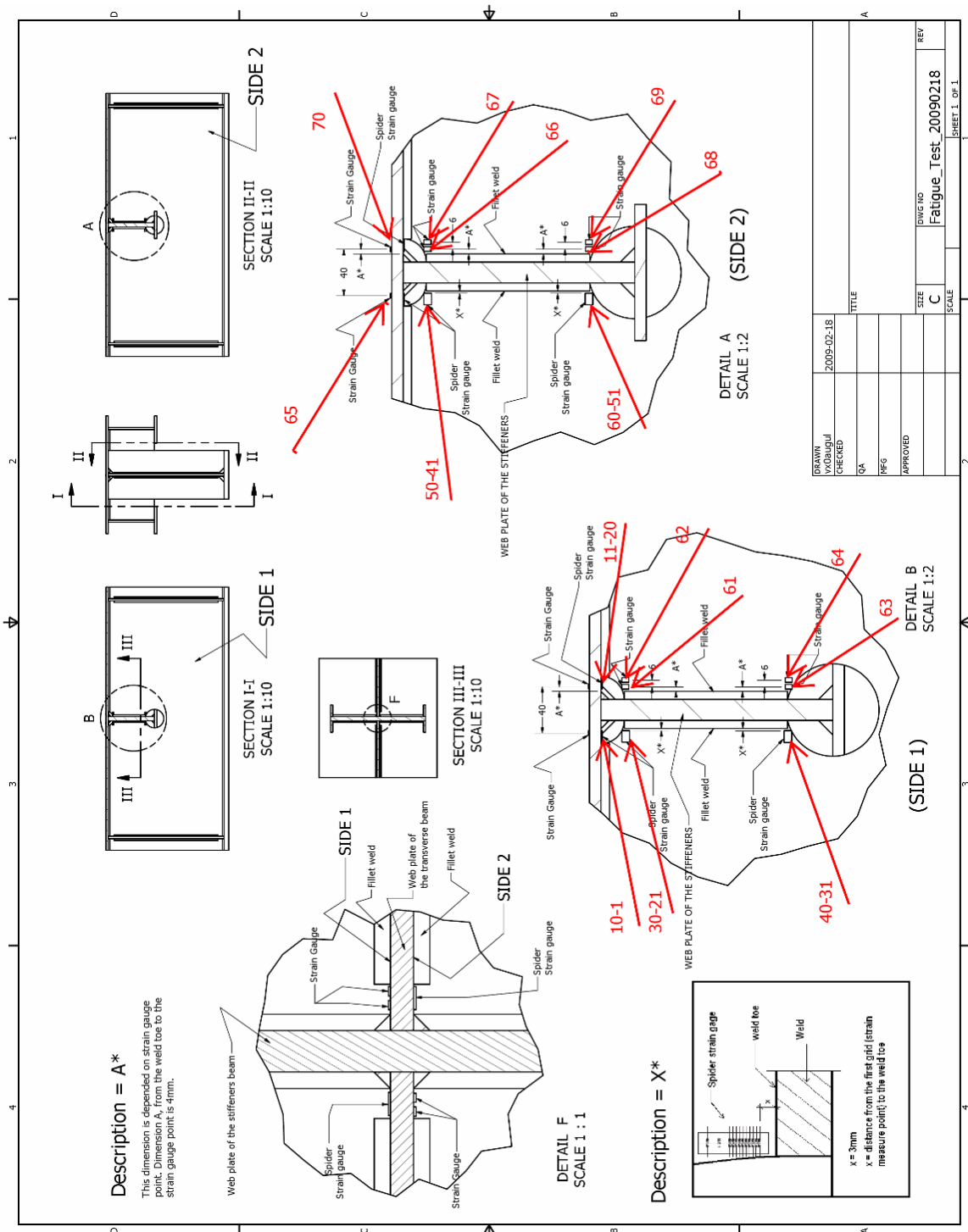


Figure 3.15 Placement of the strain gages on the specimen A4. Numbers in red denote the channel number in the strain data output. Ranges of numbers (e.g. 10-21) denote chain strain gages.

The stress profiles at the two sides of each hot spot are shown in Figure 3.16 to Figure 3.18 for hot spots 'wb', 'wt', and 'fl1'. The x-axis direction for the figures on left column is from right towards left. The extrapolated hot spot stresses are also indicated on the figures. Structural hot spot stresses for 'wt' and 'wb' are calculated from the

quadratic extrapolation of the stresses at 4 mm, 8 mm, and 12 mm from the weld toe, according to IIW guidelines.

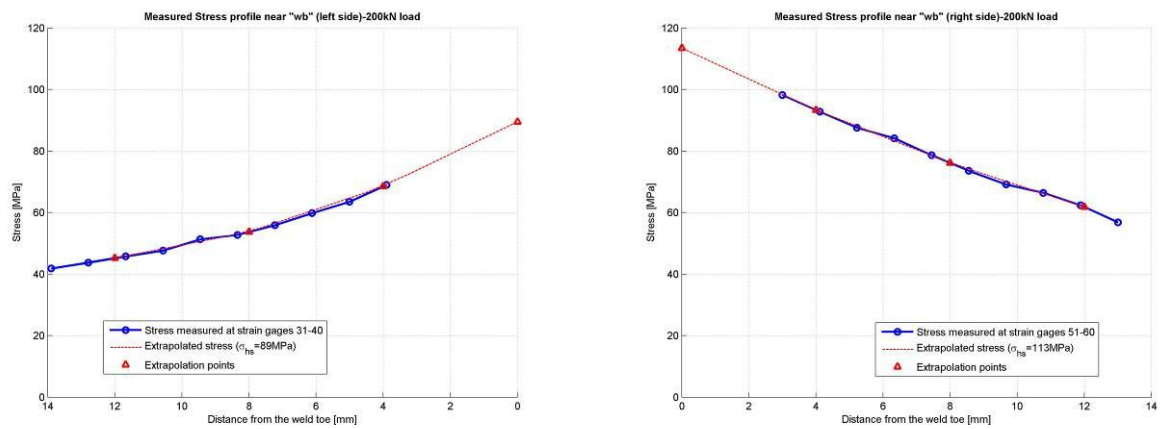


Figure 3.16 Measured stress profiles near the 'wb' hot spot (applied load:200kN).

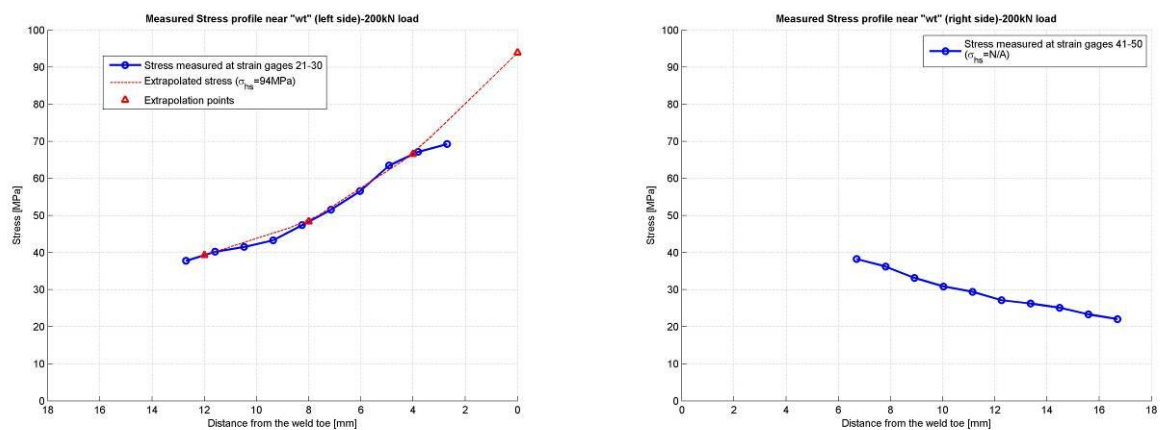


Figure 3.17 Measured stress profiles near the 'wt' hot spot (applied load:200kN).

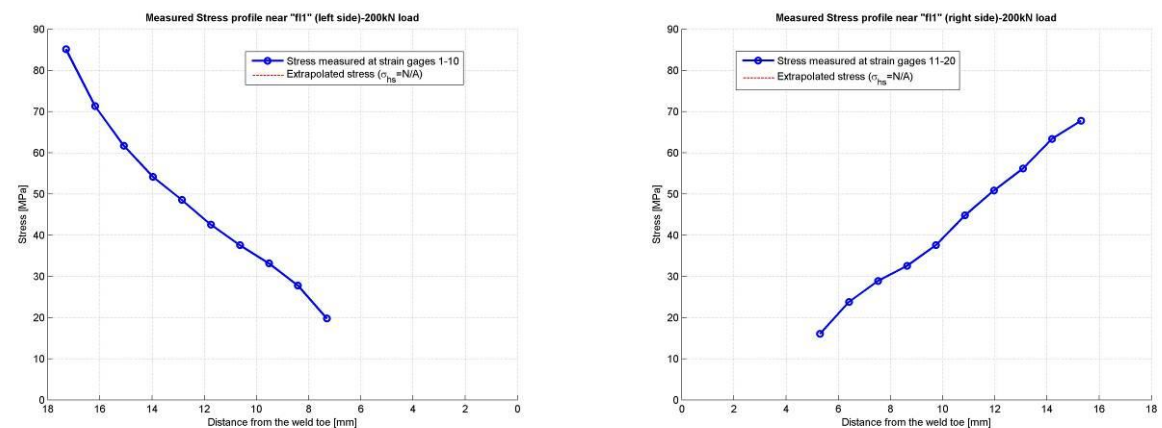


Figure 3.18 Measured stress profiles near the 'fl' hot spot (applied load:200kN).

For the right side of the ‘wt’ hot spot and both sides of the ‘fl1’ hot spot, the extrapolation was not possible, because the strains at 4 mm distance from the weld toe were not measured. The difference between the stress profiles at the two sides of each hot spot can be associated with the misalignments in the joint (see section 2.3.6). Table 3.10 shows a summary of experimentally evaluated SHSS values. The value for ‘wb’ in the table is selected as the average of the two evaluated values at the two sides of the hot spot.

Table 3.10 experimental SHSS values for different hot spots for a 200 kN load.

Hot spot	wb [*]	wt	fl1	fl2
σ_{hs} [MPa]	101	94	N/A	N/A

Since the test was in progress at the time of preparation of this thesis, the crack growth data could not be presented here. The observations showed that the first crack initiated in the ‘wb’ hot spot at 304 000 cycles, see Figure 3.19.



Figure 3.19 First observed fatigue crack on specimen A4 (Location: wb).

3.6 Summary of test results

A summary of the crack initiation data from the tests is presented in Table 3.11. For all specimens, the first crack in the joint was observed at the hot spots. For specimen A3, an early crack in the non-welded cope hole edge (crack p) was observed at the same time of cracking in a hot spot in the detail.

Table 3.11 Summary of crack initiation data for specimens A2 to A4.

Specimen	Load range [kN]	Number of cycles to cracking in hot spots [n]			
		wb	wt	fl1	fl2
A2*	400	$3.05 \cdot 10^5$	$9.07 \cdot 10^5$	$1.49 \cdot 10^6$	$1.80 \cdot 10^5$
A3	350	$1.09 \cdot 10^6$	$2.53 \cdot 10^6$	$4.73 \cdot 10^6$	$9.85 \cdot 10^5$
A4	370	$3.04 \cdot 10^5$	N/A	N/A	N/A

* Specimen A2 was first tested for 5 million cycles under a 200 kN load without any visible cracking.

4 Finite element modelling and analysis

Three main steps were taken in the FE modelling and analysis of the specimens. Those were pre-processing (modelling), processing (analysis), and post-processing. These steps are described in the following sections in this chapter. Various FE models were made to investigate the effect of different modelling techniques on the resulting SHSS values. These models and some preliminary results from the analyses are presented in this chapter. In addition, some modelling and post-processing issues were observed that has been addressed in this chapter.

4.1 Modelling

The finite element analysis program ABAQUS version 6.7.2 (ABAQUS, 2007) was used for numerical modelling¹².

Geometry: The geometry of the models was based on the theoretical dimensions. For shell element models the geometry was based on the mid-planes of the plates in the physical part. For solid element models and one of shell element models, only a quarter of the physical part was modelled because the part was symmetric in two directions. Later on, it appeared that using the symmetry to reduce the model size could affect the stresses in shell element models. This is due to the fact that the symmetry plane passes through the mid plane of some plates in the joint. Therefore, these plates should be modelled with a shell thickness of half of the plate thickness. This causes some difference in the stress results from the quarter-model and whole-model of the part. So, the whole geometry of the part was modelled in other shell element models.

Weld geometry was not modelled in two of shell element models. An investigation on a more simple joint detail revealed that weld modelling had significant effect on the SHSS values when a geometric feature (such as a cope hole) exists at the weld toe location. This investigation is presented in Appendix D. Therefore, two other shell element models (i.e. SW04 and TS02 models) were built with the weld geometry modelled. Weld modelling was carried out using the techniques explained in section 2.3.6. Weld geometry was also modelled in solid element models. The geometry of the fillet welds in solid element models was generated by chamfering two intersecting volumes (e.g. web plate and stiffener) in ABAQUS. There was a minor problem in this procedure. When the chamfer was passing through the curved edge of cope holes, some small extra edges were created in the corners, see Figure 4.1. These small edges prevented the correct generation of structured mesh in the subsequent steps. To correct the topology of the model and remove these edges, the ‘small edge removal tool’ available in ABAQUS was used. Later in the modelling phase it appeared that a more convenient way to model the weld geometry would be generation of weld volume by ‘extrude’, ‘revolve’, and ‘sweep’ operations available in the part modelling module of the program. These operations provide more control and better accuracy in

¹² At the beginning of the study, also I-DEAS computer aided engineering package was considered for use in the analysis. Later on, ABAQUS was selected because of the good post-processing options and better availability of the documentation at the department.

generation of the weld geometry. The weld geometry in the shell element models was created using this latter method.

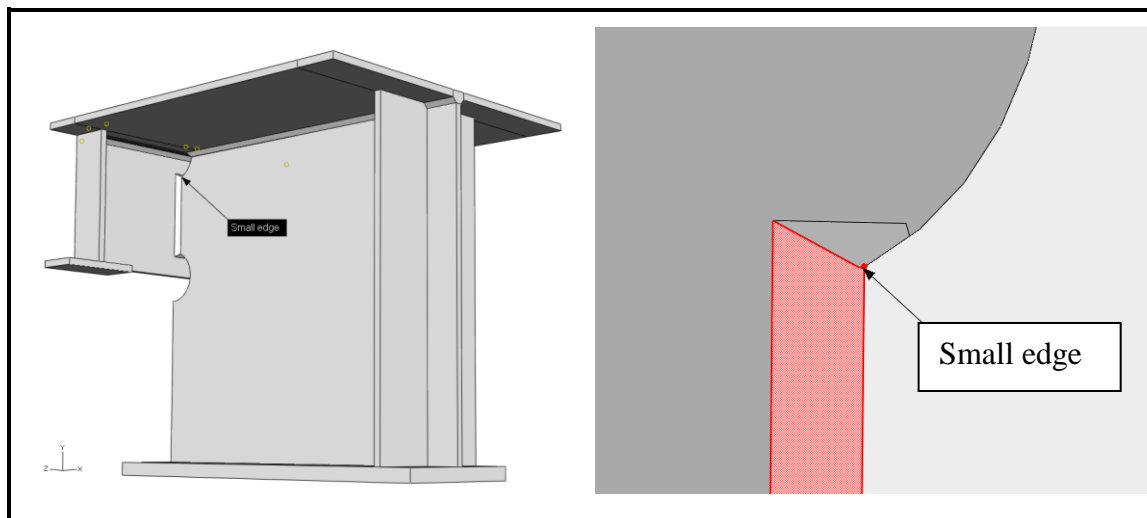


Figure 4.1 Modelling of the weld geometry.

Material properties: Typical steel mechanical properties ($E = 210\text{GPa}$ and $\nu = 0.30$) were used for the material properties. Only elastic properties needed to be considered.

Loading and boundary conditions: A unit load of 1 kN was applied to the model in the form of uniform vertical pressure applied right on the top of the stiffeners. Since one quarter of the model was modelled, this was equal to a 4 kN load on the specimen. The analysis was linear elastic and the stresses were linearly proportional to the loading. So, to calculate the stresses for other loading values, the analysis results were multiplied by the ratio of the desired load to the reference load (i.e. 4 kN). Boundary conditions consisted of: (a) restraint against vertical displacement along the roller support line; and (b) symmetry boundary conditions on the planes of symmetry of the physical model. The loading and boundary conditions are shown in Figure 4.2.

Meshing and element type: The first model, which was used for preliminary evaluation, was meshed with the tetrahedral elements (free mesh). All other models were meshed with prismatic elements (structured mesh) which complies with the IIW guidelines. To place the nodes exactly on the prescribed extrapolation points, the model volume was divided to 'partitions'. Then every partition could be meshed with different mesh densities. This is shown in Figure 4.3 and Figure 4.4. 10-node solid elements (C3D10) were used for free meshing. For structured mesh 20-node solid elements with reduced integration (C3D20R) and 8-node shell elements (S8R) were used.

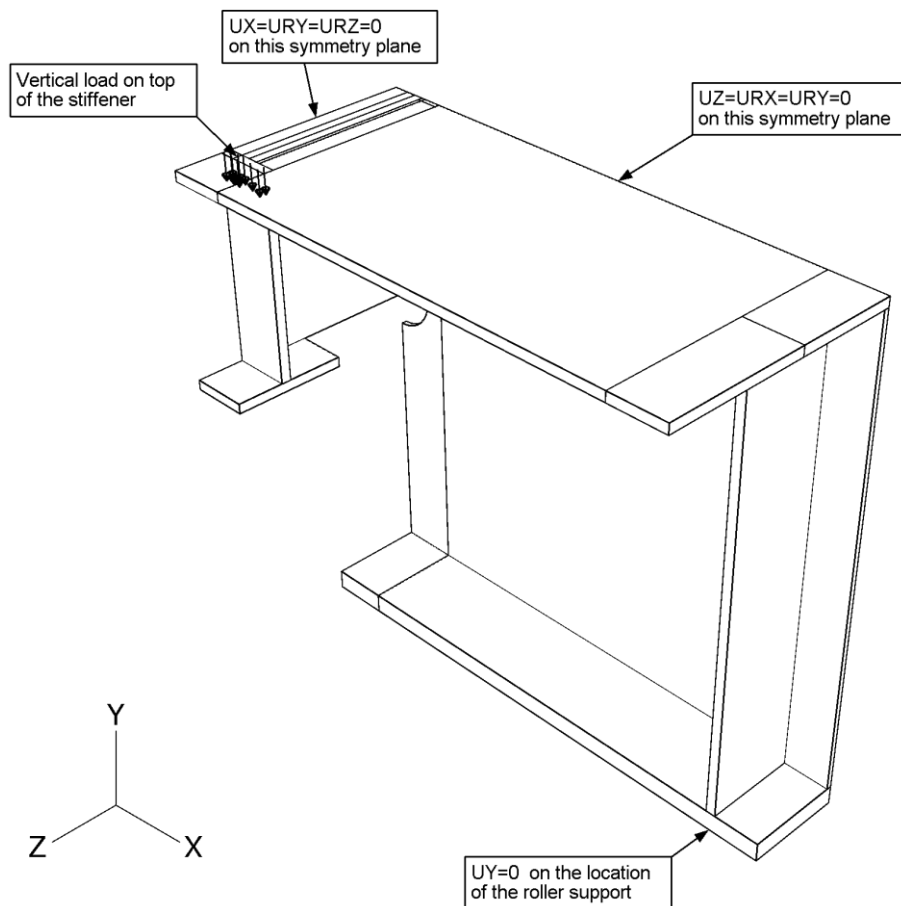


Figure 4.2 Loading and Boundary conditions for the FE models

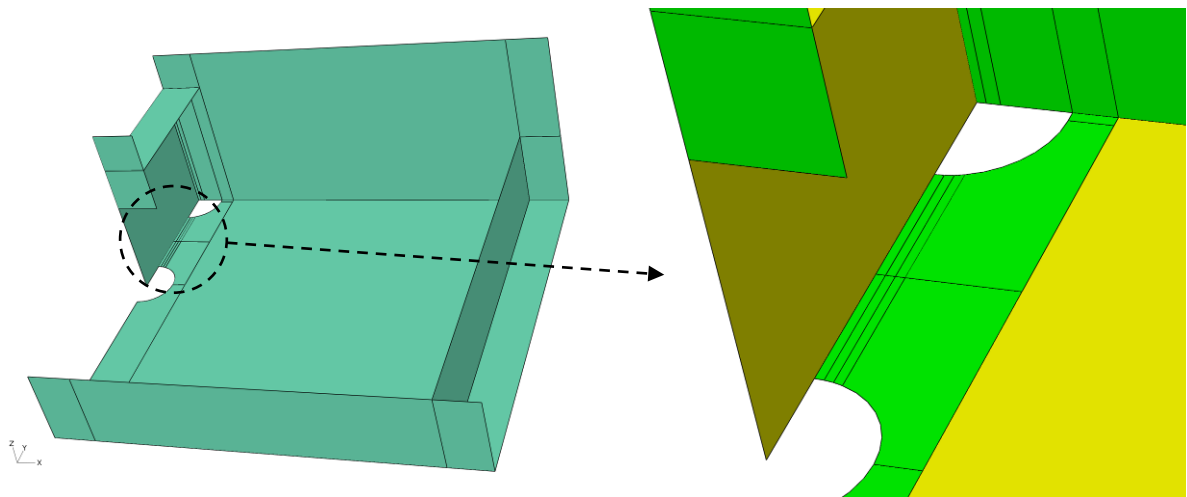


Figure 4.3 Partitioned model and close-up view at the hot spots region.

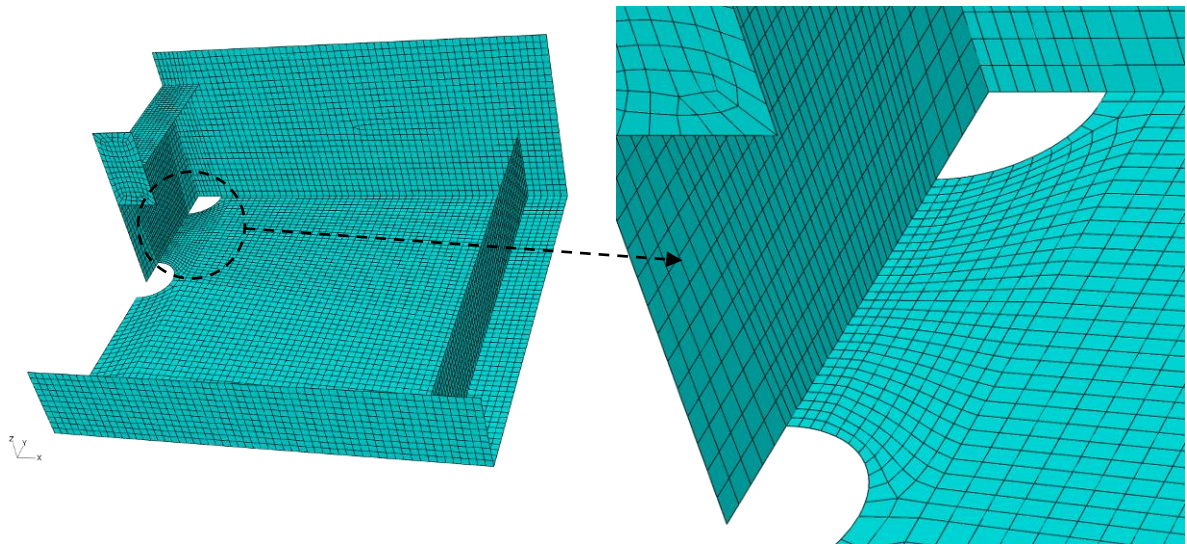


Figure 4.4 Structured mesh on model following the partitioning shown on Figure 4.3.

4.2 Description of the models

4.2.1 Model FR

This model was used for primary analysis of the test specimen and to determine the highly stressed regions in the joint. Therefore, minimal meshing rules were applied in building this model. The model was meshed with free meshing method. 10-node tetrahedral solid elements (C3D10) were used. The mesh density was increased in the joint region to increase the accuracy of the results. Figure 4.5 and Figure 4.6 show the mesh pattern in the whole model and in the joint, respectively. From the maximum principal stress plot in Figure 4.7, it can be seen that the joint region is the most highly stressed zone in the model, as it was expected. Further investigation of the joint region (Figure 4.8) shows that the 'wb' hot spot is more likely to be a point for crack initiation, because of the high principal stress values.

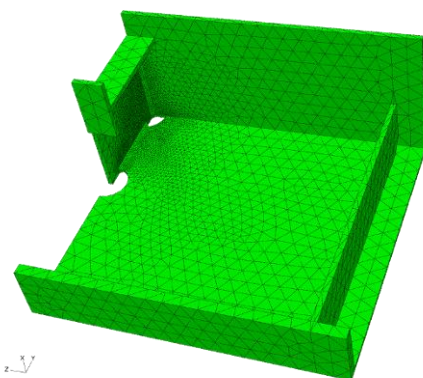


Figure 4.5 Free mesh on the model FR.

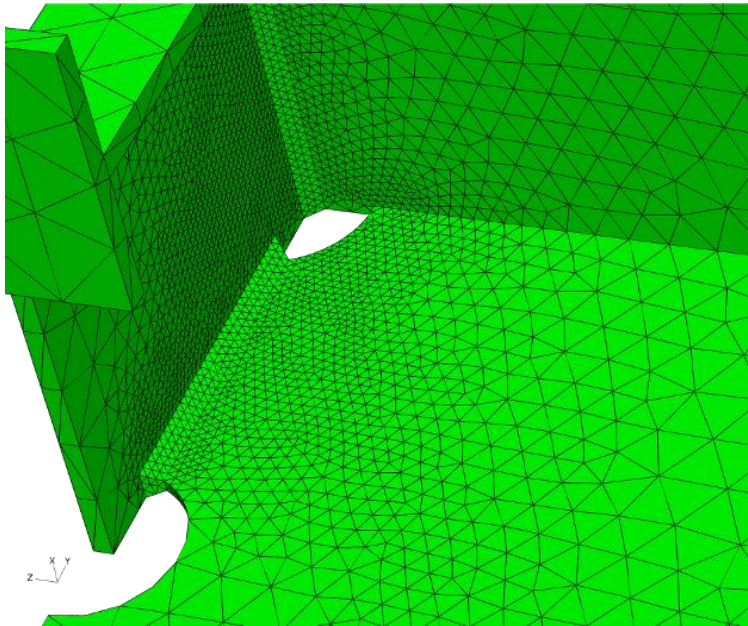


Figure 4.6 Close-up of the mesh in the joint region, FR model.

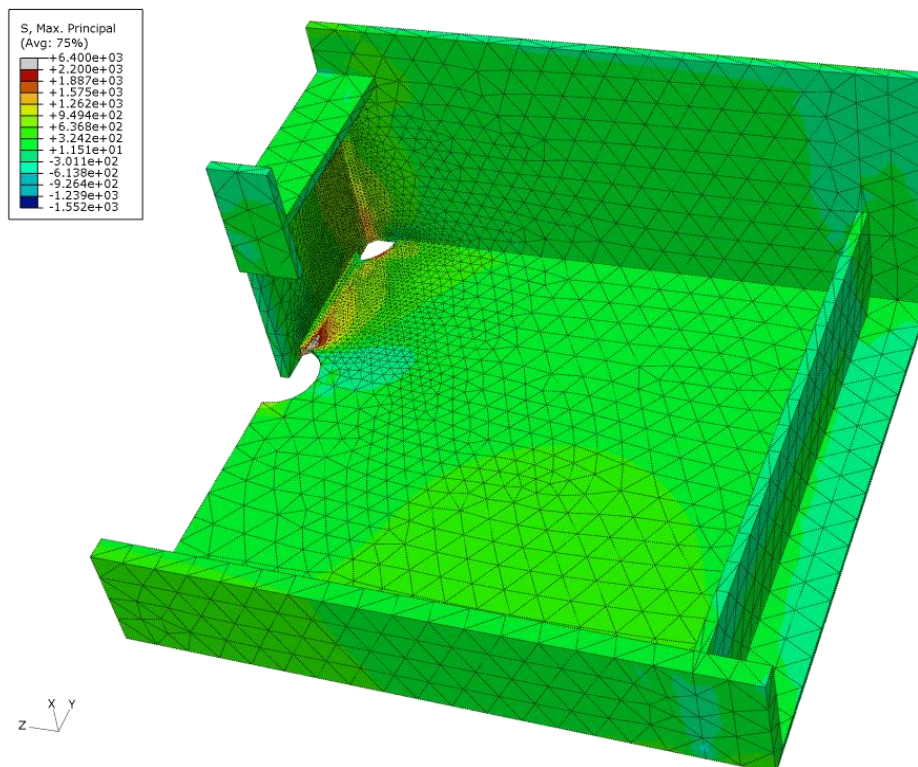


Figure 4.7 Maximum principal stress plot, FR model.

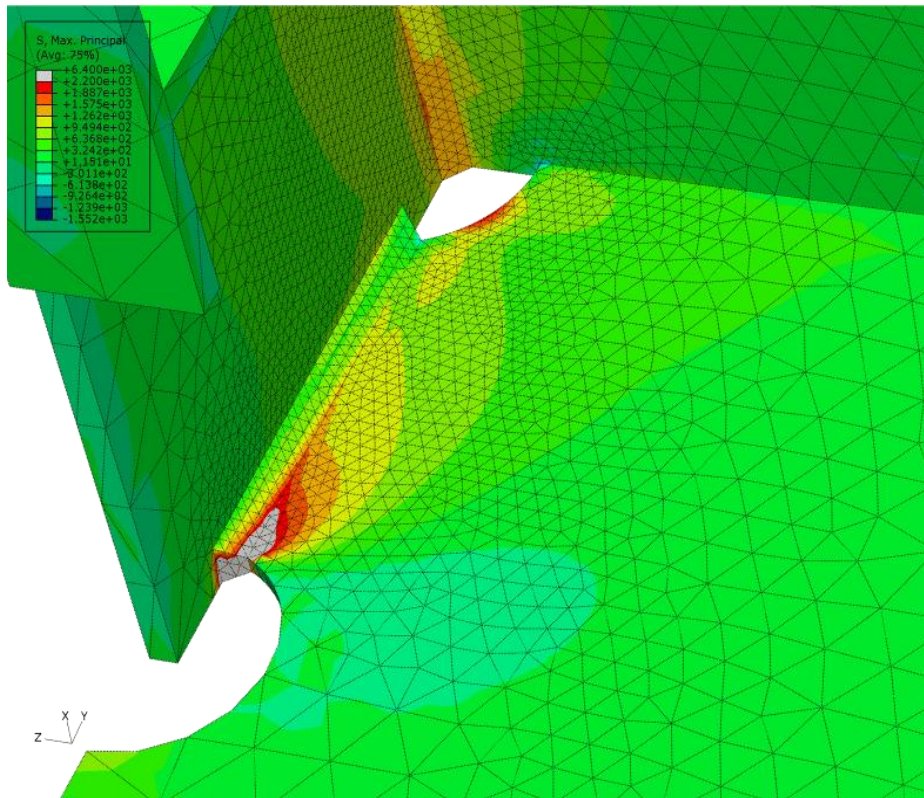


Figure 4.8 Close-up of the maximum principal stress plot in the joint region, FR model.

This model was not used further in the studies because the use of tetrahedral elements is not recommended (although not prohibited) in the SHSS guidelines.

4.2.2 Model SH10

This model, shown in Figure 4.9, was made based on the IIW recommendations for analysis with coarse mesh shell element models (see section 2.3.6.2). This model was the only shell element model in which a quarter of the physical specimen was modelled (see Section 4.1). As shown in close-up view of the model in Figure 4.10, the maximum element size at the type 'a' hot spot regions was $10\text{mm} \times 10\text{mm}$ (i.e. $t \times t$), and in type 'b' hot spots ('wb' and 'wt'), it was $10\text{mm} \times 10\text{mm}$. The weld geometry was not modelled.

Figure 4.11 shows the deflected shape of the model under loading. Verification data for the model is presented in the section 4.2.9. Figure 4.12 shows the plot of S11, which is the stress component perpendicular to the weld toe *at the top layer (surface) of the shell elements*¹³. This plot and similar plots from other models were used in extraction of the stress profiles at the weld toe region. As an example, the line denoted

¹³ S11 is the stress component at x-direction ($S11 \equiv S_x$). In the studied model, this corresponds to the stress component perpendicular to the weld toe for all four hot spots investigated.

by ‘start’ and ‘end’ on the model in Figure 4.10 was the path to extract the stress profile for the ‘wb’ hot spot. This will be described later in this chapter.

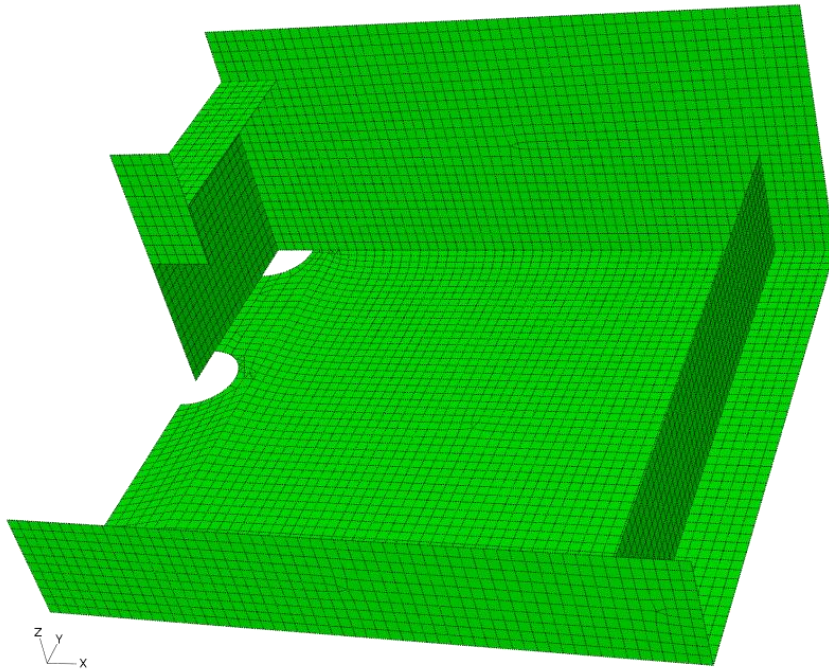


Figure 4.9 Structured mesh with shell elements, SH10 model.

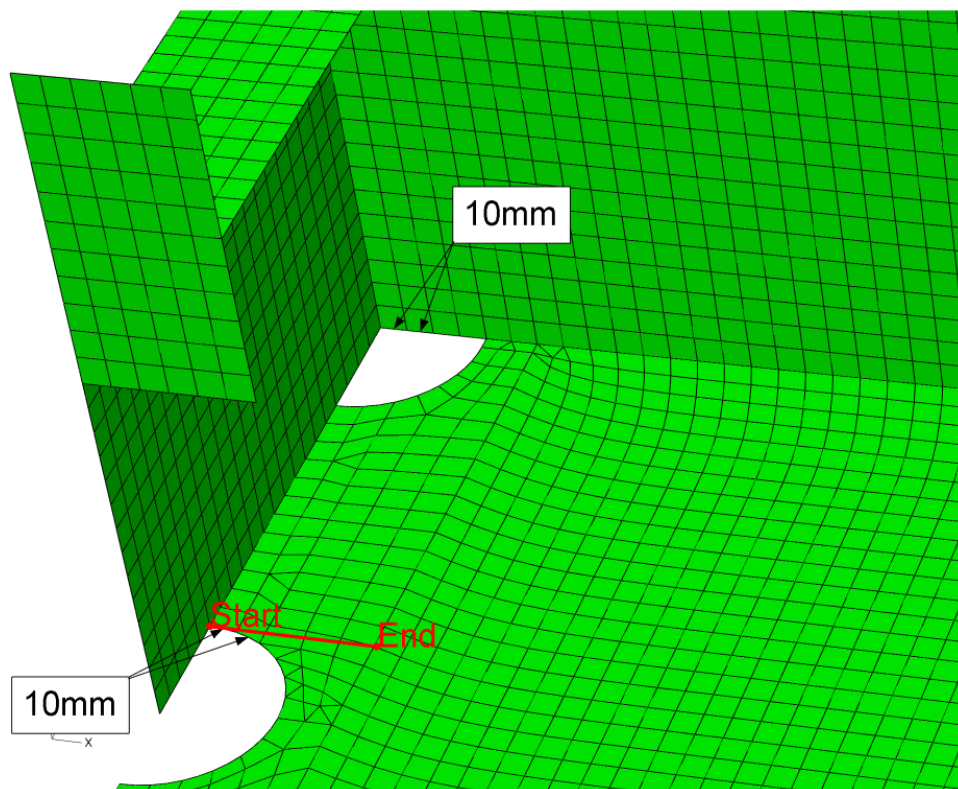


Figure 4.10 Close-up of the mesh in the joint region, SH10 model.

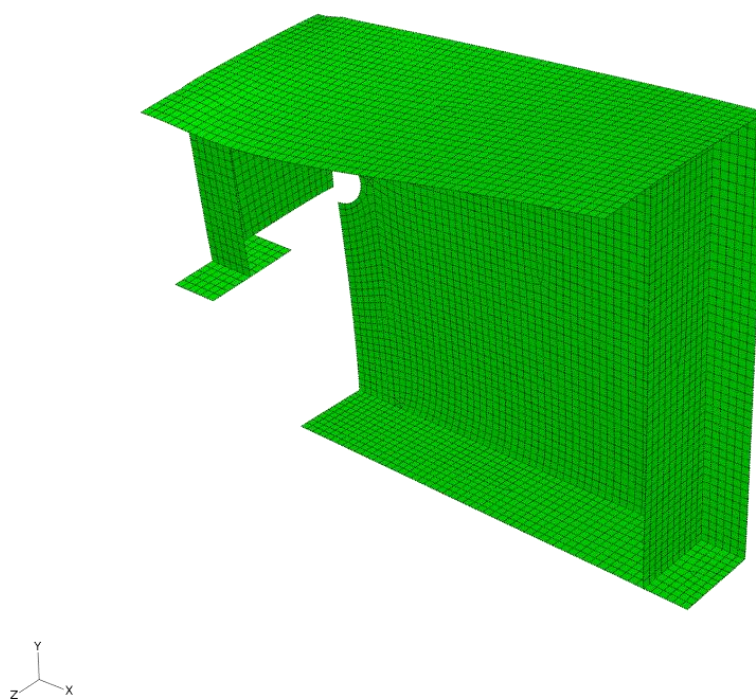


Figure 4.11 Deformed shape, SH10 model.

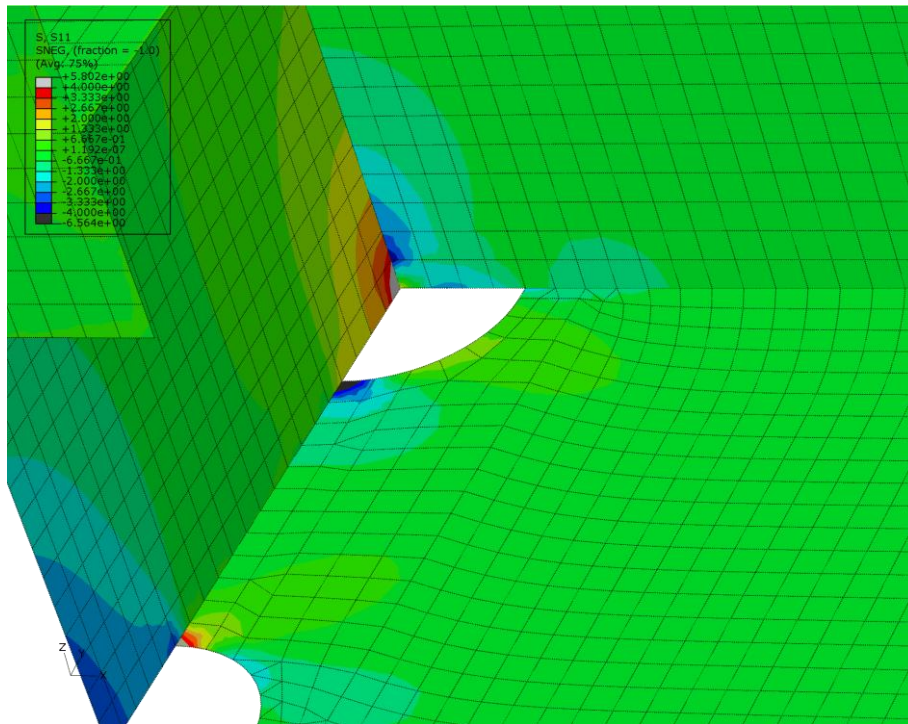


Figure 4.12 Close-up of the S_{11} plot (stress component perpendicular to the weld line) in the joint region, SH10 model.

4.2.3 Model SH04

This model was made with shell elements. Instead of modelling a quarter of the physical part, whole specimen was modelled to reduce the issues addressed earlier in Section 4.1. Finite element mesh was generally similar to the SH10 model. However, the mesh was modified such that nodal points coincided with the extrapolation points for calculation of SHSS¹⁴. The mesh was also refined at the joint region, see Figure 4.13. The refinement was based on the IIW recommendations for modelling with the fine mesh. The element size at the type ‘a’ hot spot region was $4\text{mm} \times 4\text{mm}$ (i.e. $0.4t \times 0.4t$) and $10\text{mm} \times 10\text{mm}$ (i.e. $t \times t$) in the elements adjacent to those elements. For type ‘b’ hot spots (‘wb’ and ‘wt’), the mesh size was $4\text{mm} \times 4\text{mm}$ for at least three consecutive elements near the weld toe, as shown in close-up view of the model in Figure 4.13. The weld geometry was not modelled.

Figure 4.14 and Figure 4.15 show the plot of the stress component perpendicular to the weld toe and maximum principal stress, respectively. Definitely, these stresses are *at the top layer (surface) of the shell elements*.

¹⁴ For a more detailed explanation of the role of these extra nodal points, see the description of the OP04 model (Section 4.2.6) and Figure 4.23.

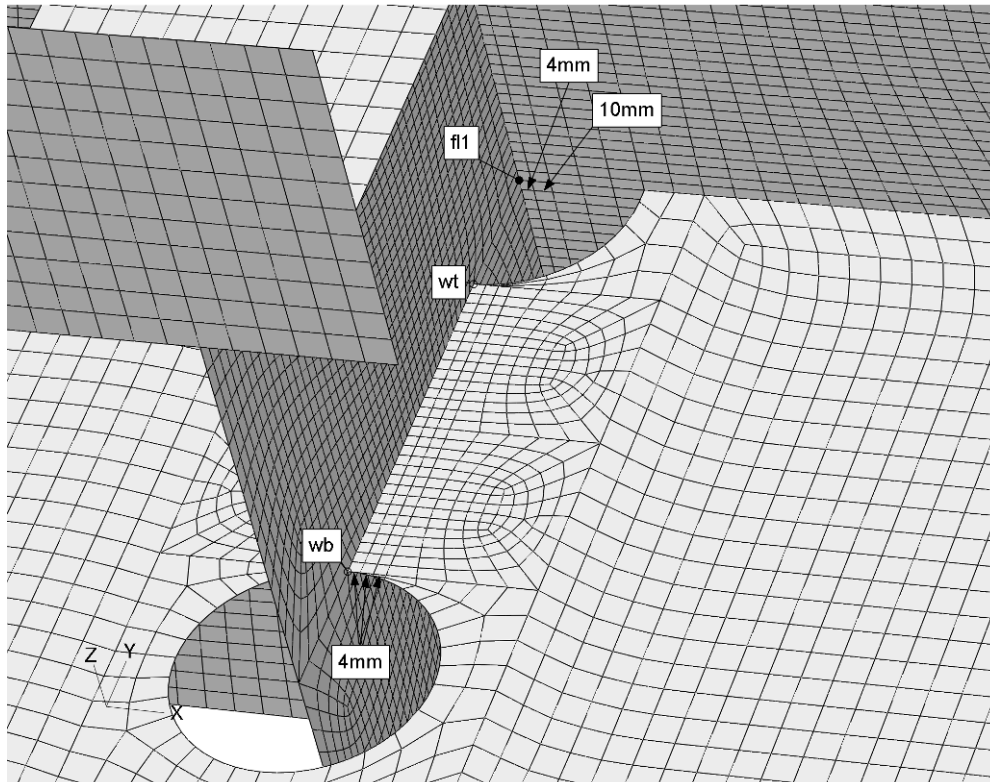


Figure 4.13 Mesh in the joint region, SH04 model.

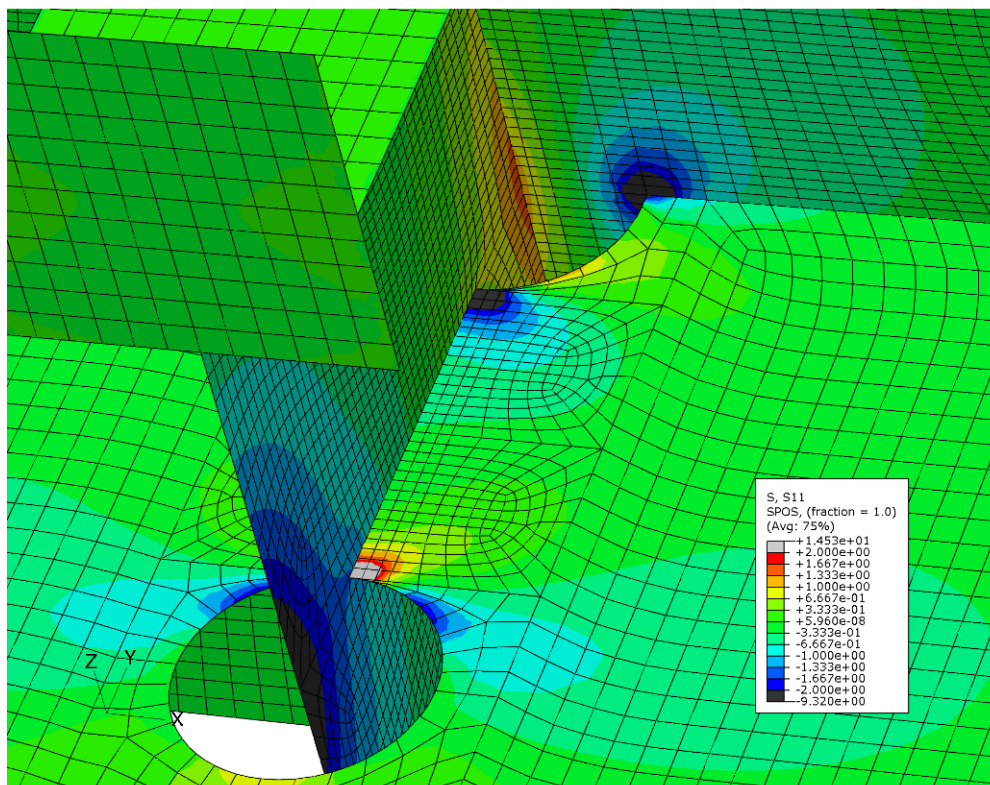


Figure 4.14 S11 plot in the joint region, SH04 model.

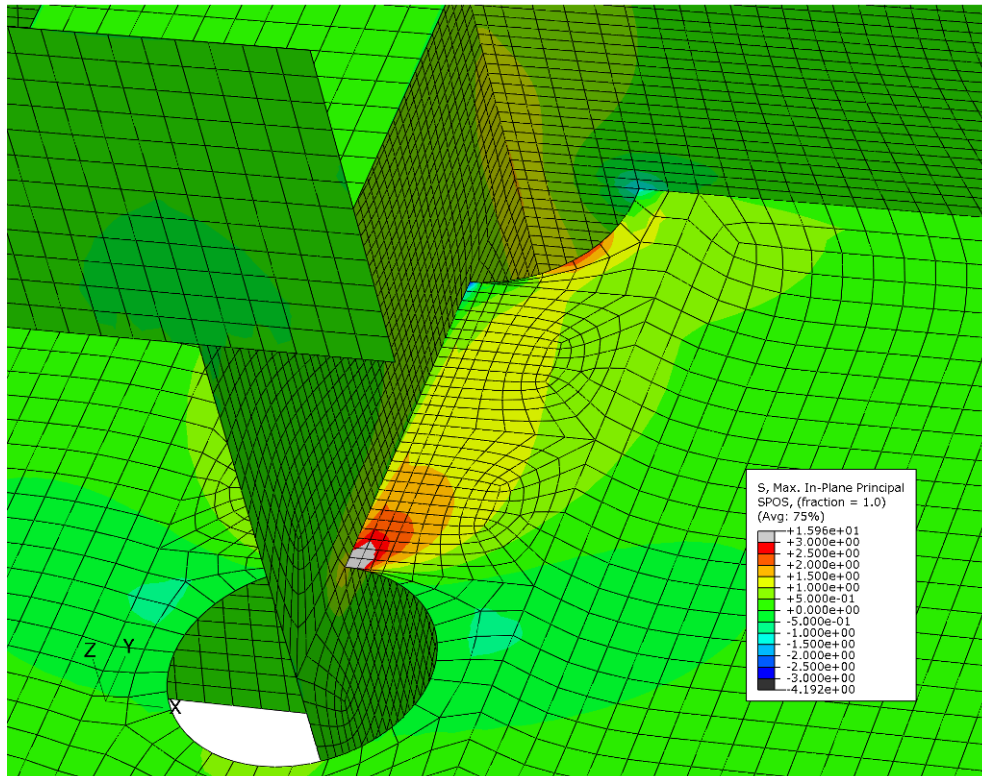


Figure 4.15 Maximum principal stress plot in the joint region, SH04 model.

4.2.4 Model BR10

This was the first model made with solid elements. It was made based on IIW recommendations for modelling with coarse mesh. That is, $10\text{mm} \times 10\text{mm}$ (i.e. $t \times t$) elements in 'fl1' region and $10\text{mm} \times 10\text{mm}$ elements in the 'wt' and 'wb' regions. The number of elements through the plate thickness was set to one. The welds were also modelled as described in section 4.1. The weld at 'fl2' hot spot was not modelled.

Contour plots of stress component perpendicular to the weld toe and maximum principal stress are presented in Figure 4.17 and Figure 4.18, respectively.

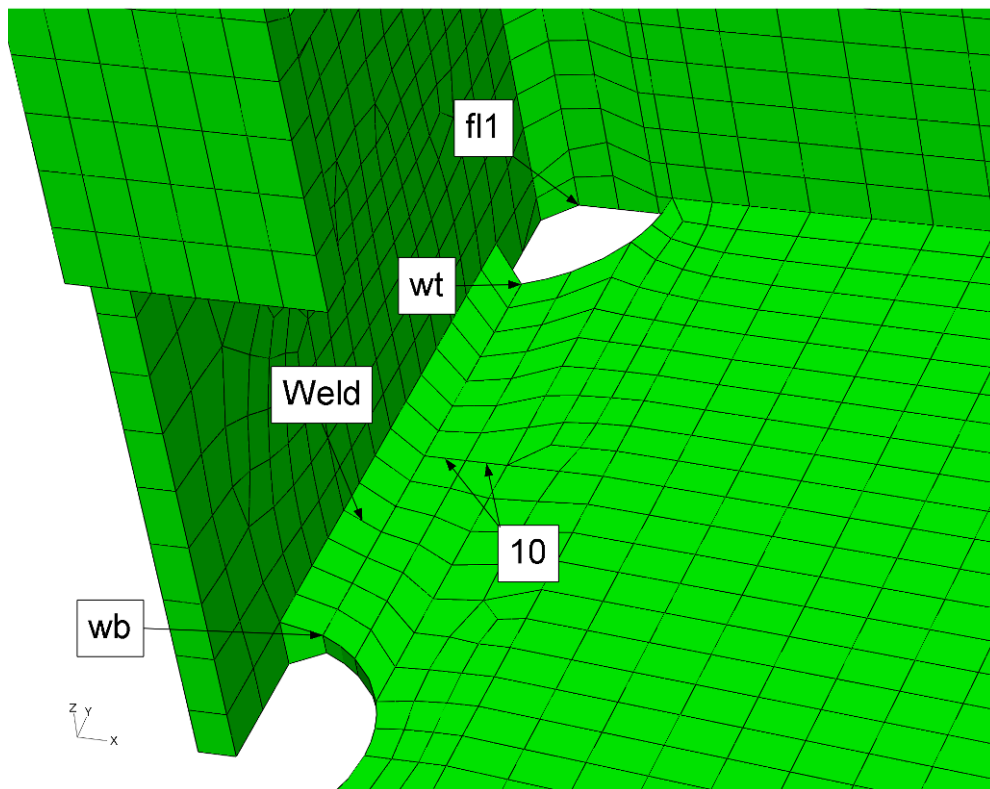


Figure 4.16 FE mesh in the joint region, BR10 model.

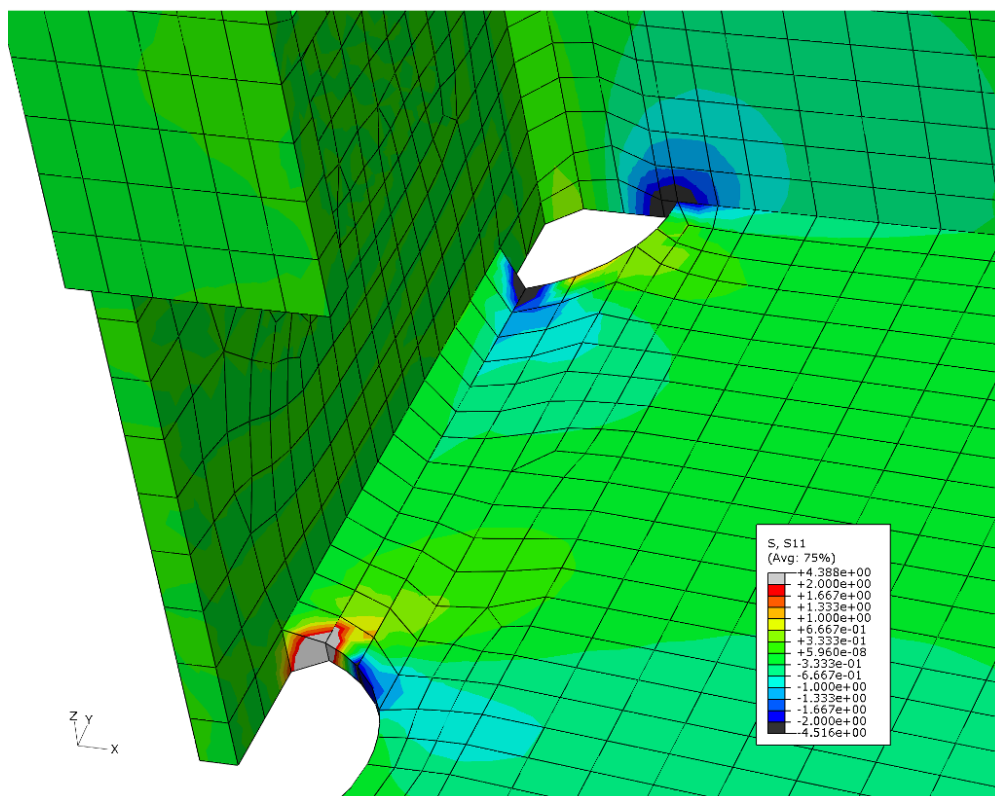


Figure 4.17 S11 plot in the joint region, BR10 model.

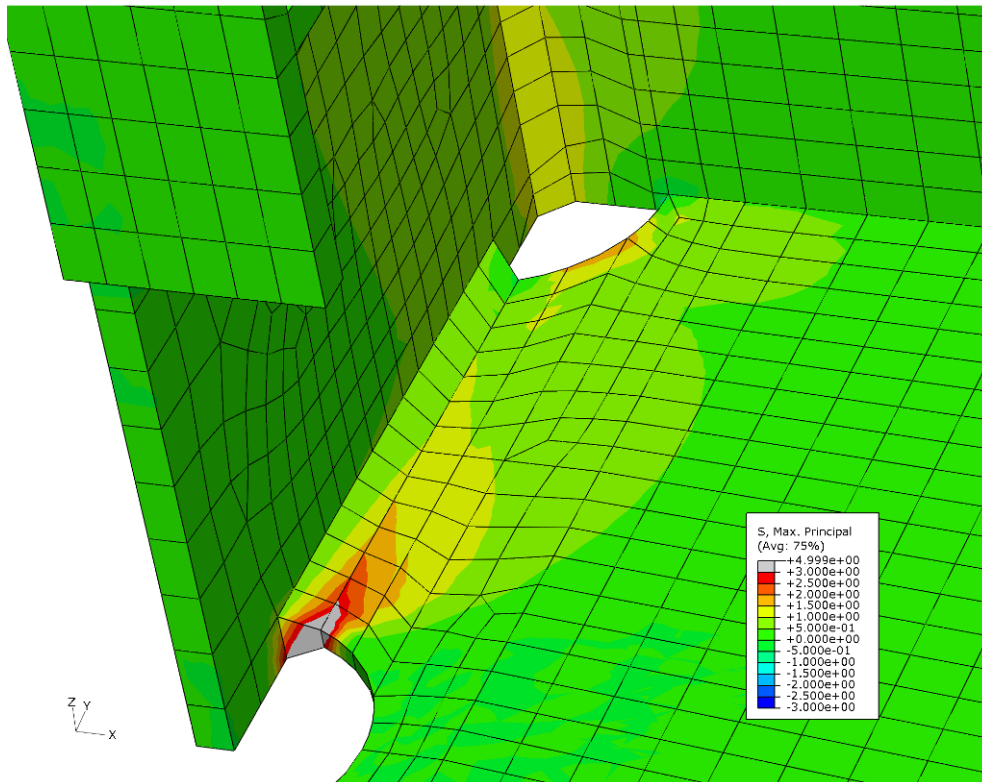


Figure 4.18 Maximum principal stress plot in the joint region, BR10 model.

4.2.5 Model BR04

This model was similar to the BR10 model, but the mesh at the hot spot regions was refined. The element size at the type 'a' hot spot region was $0.4t * 0.4t$ and $t * t$ in the elements adjacent to those elements. For type 'b' hot spots ('wb' and 'wt'), the mesh size was $4mm * 4mm$ for three consecutive elements near the weld toe, as shown in close-up view of the model in Figure 4.13. Contour plots of stresses are presented in Figure 4.20 and Figure 4.21

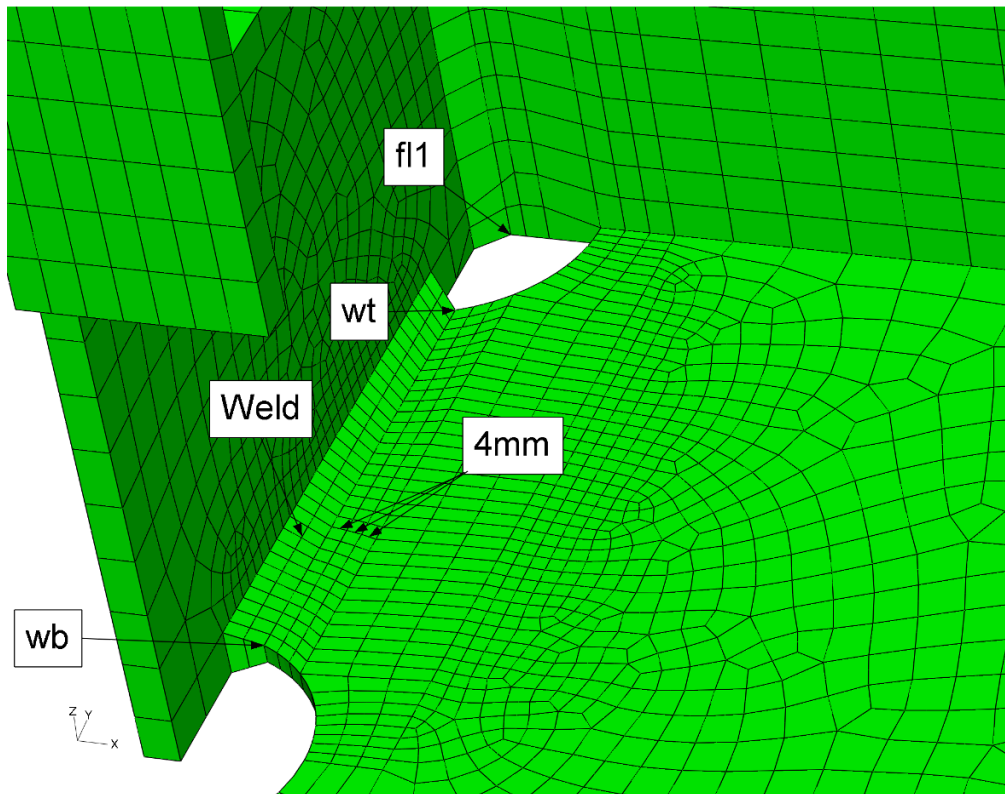


Figure 4.19 Meshing in the joint region, BR04 model.

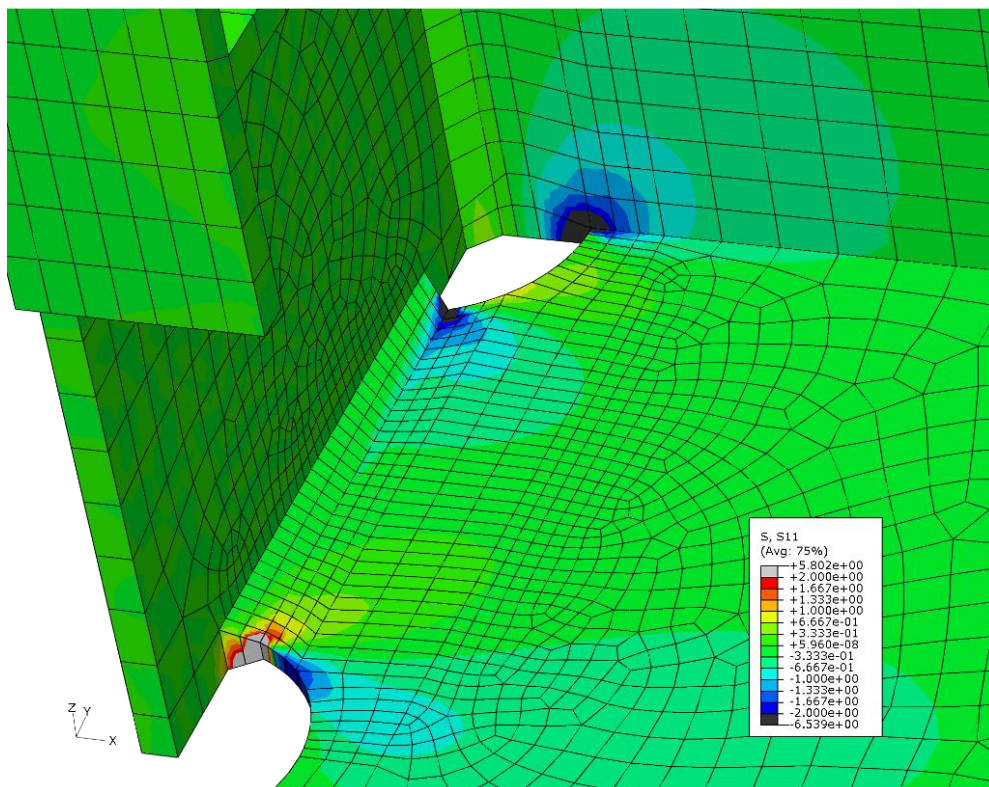


Figure 4.20 S11 plot in the joint region, BR04 model.

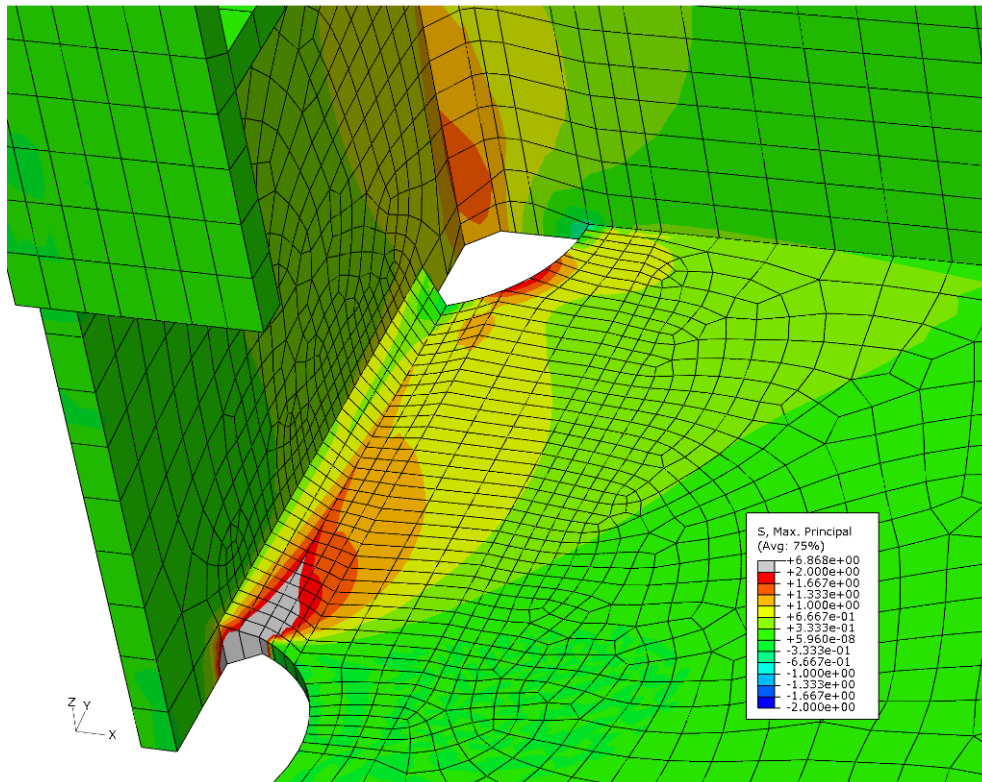


Figure 4.21 Maximum principal stress plot in the joint region, BR04 model.

4.2.6 Model OP04

To improve the accuracy of the results, the OP04 model was made on the basis of model BR04, see Figure 4.22. All welds were modelled. FE mesh at 'wb' and 'wt' regions was improved to comply better with the IIW recommendations. The improvement in meshing can be seen and compared to that of BR04 model in Figure 4.25. It can be seen in Figure 4.25a that although the extrapolation points reside on the edges of elements and are 4 mm, 8 mm, and 12 mm away from the weld toe, they are not exactly on node locations. This would make the program to interpolate the nodal results to calculate the stresses at the desired extrapolation points, which results in loss of accuracy. The modified mesh of OP04 model in Figure 4.25b has nodes on the extrapolation points. The stresses and strains in these nodes are calculated from the primary field variable in the FE analysis and are not interpolated. Figure 4.24 shows the stress profiles for two models. The improvement in the stress profile can be observed in Figure 4.24. As it will be shown in Section 5.1.1, this correction in the stress profile had considerable effect on the SHSS value at the 'wb' and 'wt' hot spots.

The close-up view of the mesh in the joint region is shown in Figure 4.25. Contour plots of the stresses in the joint region can be seen in Figure 4.26 and Figure 4.27. Figure 4.28 shows the vector plot of principal stresses at the weld toes.

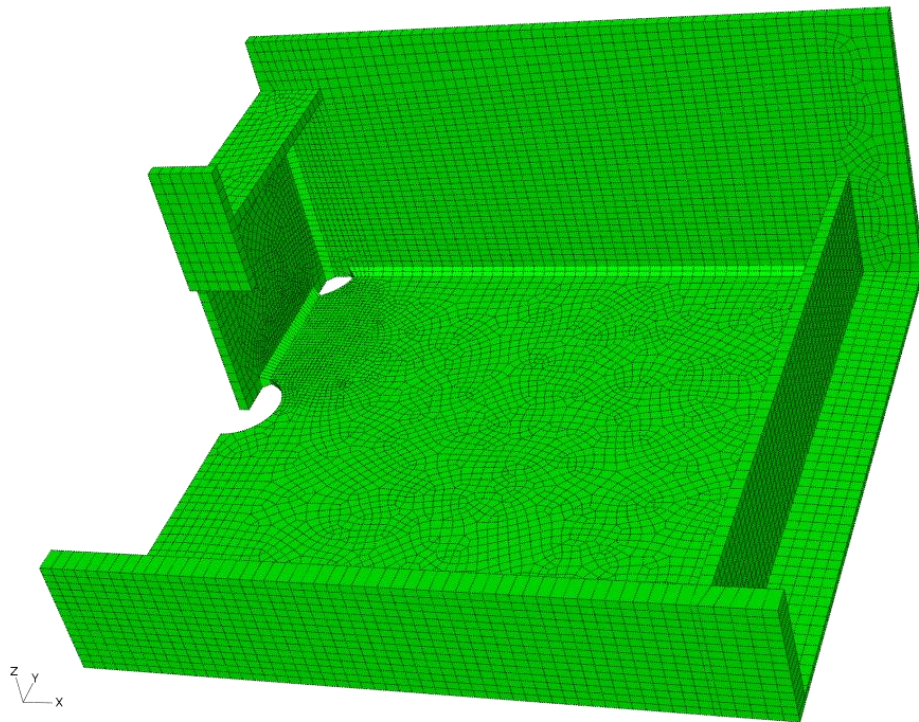
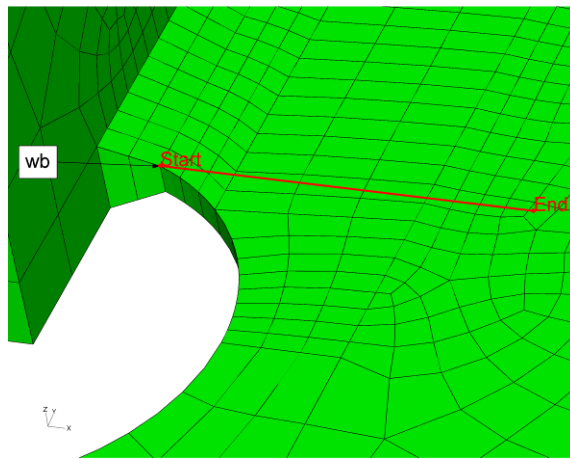
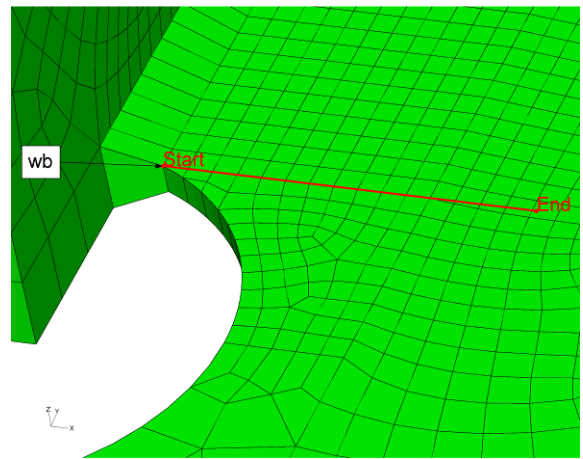


Figure 4.22 Structured mesh with solid elements, OP04 model.



(a)



(b)

Figure 4.23 comparison of the mesh details in two models: (a) model BR04, (b) model OP04

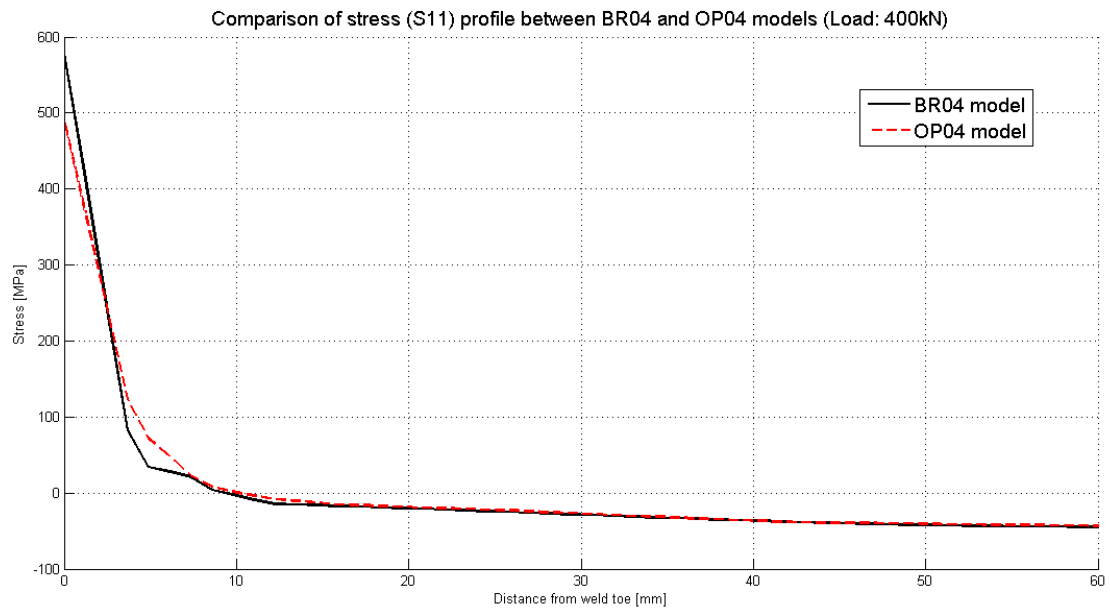


Figure 4.24 Stress (S11) profiles at 'wb' hot spots for two models (BR04 and OP04)

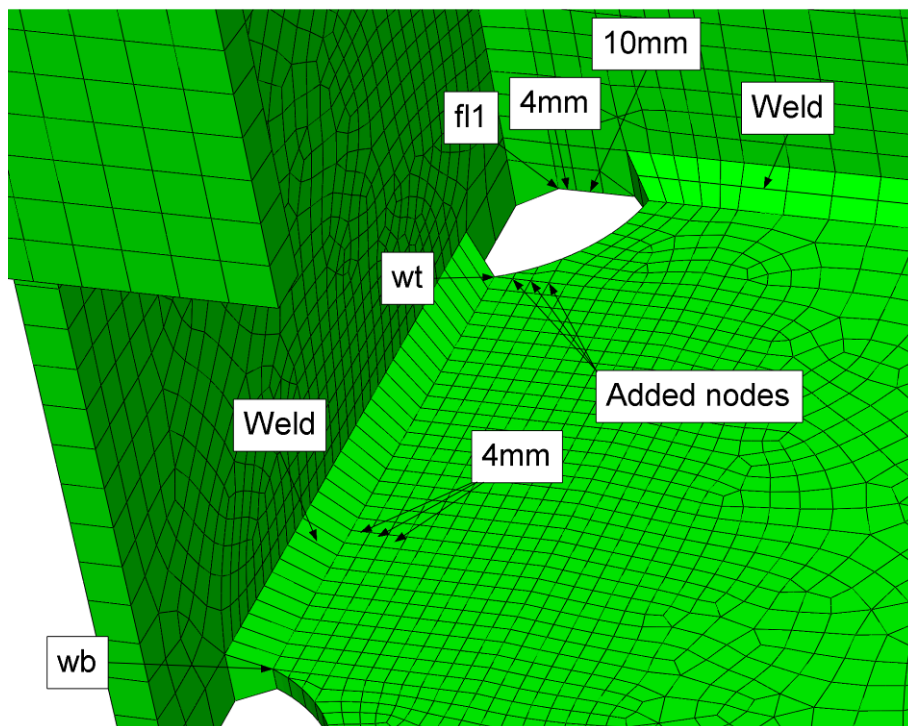


Figure 4.25 Close-up of the mesh in the joint region, OP04 model.

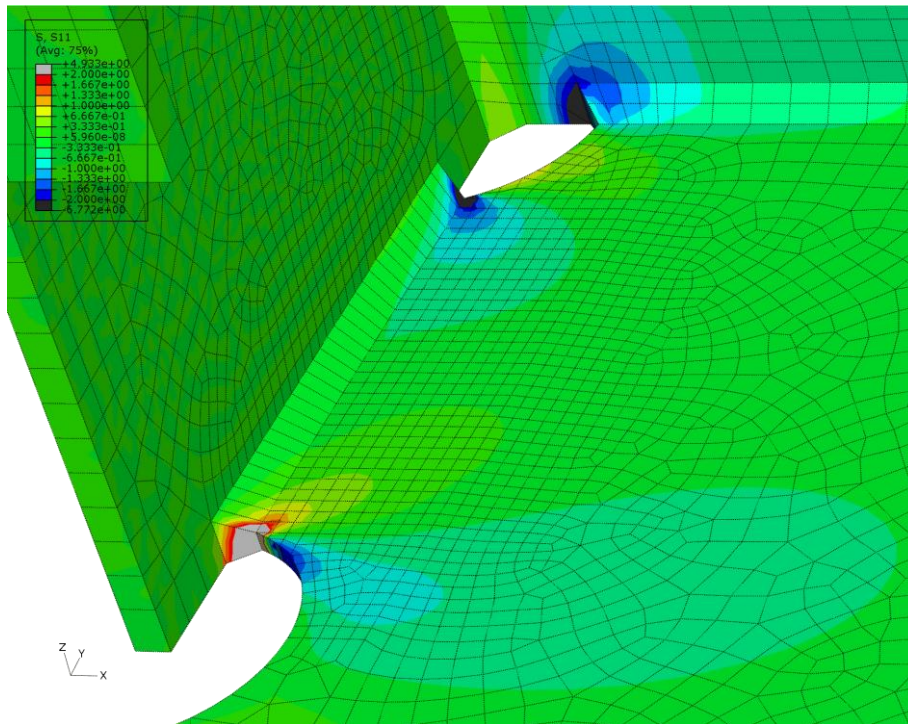


Figure 4.26 *S11 plot (stress component perpendicular to the weld line) in the joint region, OP04 model.*

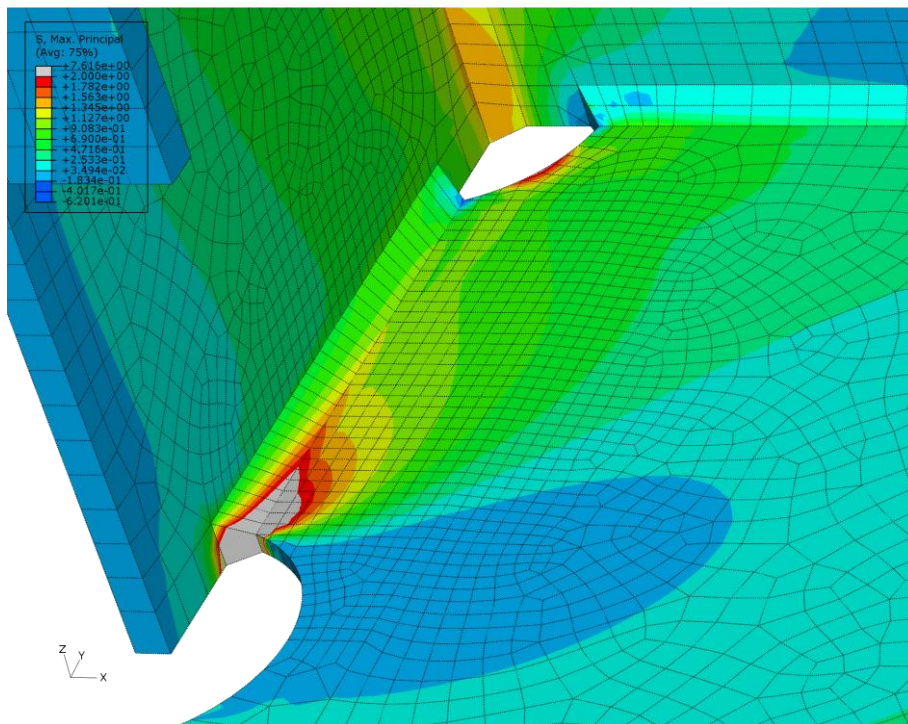


Figure 4.27 *Maximum principal stress plot in the joint region, OP04 model.*

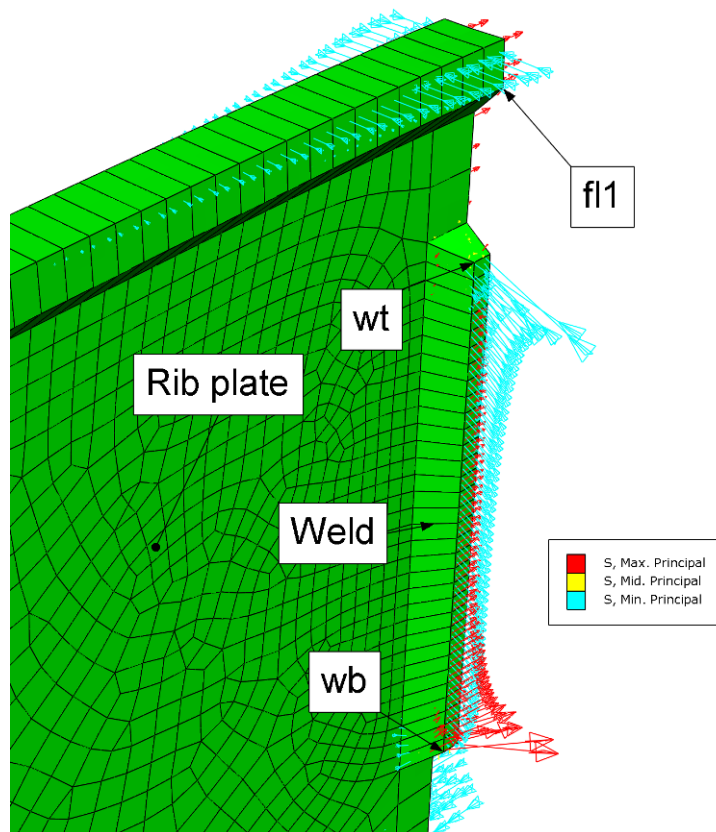


Figure 4.28 principal stresses directions at the weld toes.

4.2.7 Model SW04

As mentioned earlier in Section 4.1, the SW04 model and TS02 model were improved models of the original fine-mesh shell element model (SW04). The improvement was made by introducing welds into the finite element model. This was necessary because the SHSS values from the SH04 model were unrealistically high, compared to the SHSS values from both the solid element model (OP04) and the experimental measurements.

From this model, IIW recommendations for fine-meshed models were applied. Whole specimen was modelled. Welds were modelled with inclined shell elements (see Figure 4.29). IIW accepts this modelling technique provided that 'proper' stiffness for the oblique shell elements is selected. The thickness (that controls the stiffness) of the elements was selected equal to the weld throat thickness (i.e. $a = 5\text{mm}$). This value was selected according to the recommendations of Eriksson et al. (2003). They pointed out that this method underestimates the weld stiffness.

Figure 4.30 and Figure 4.31 show the plot of the stress component perpendicular to the weld toe and maximum principal stress, respectively.

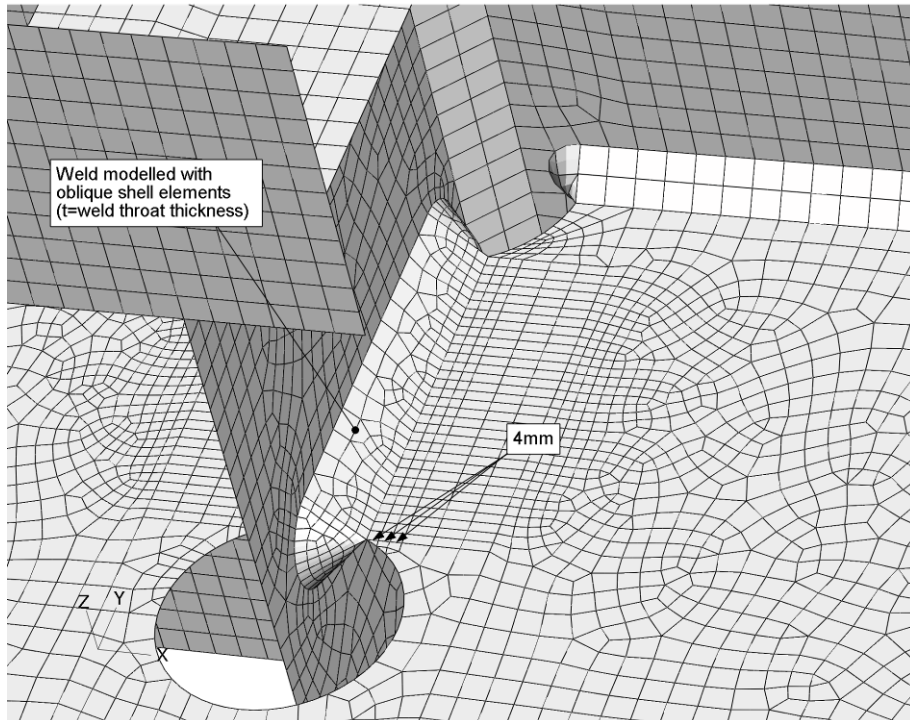


Figure 4.29 weld modelling with oblique shell elements, SW04 model.

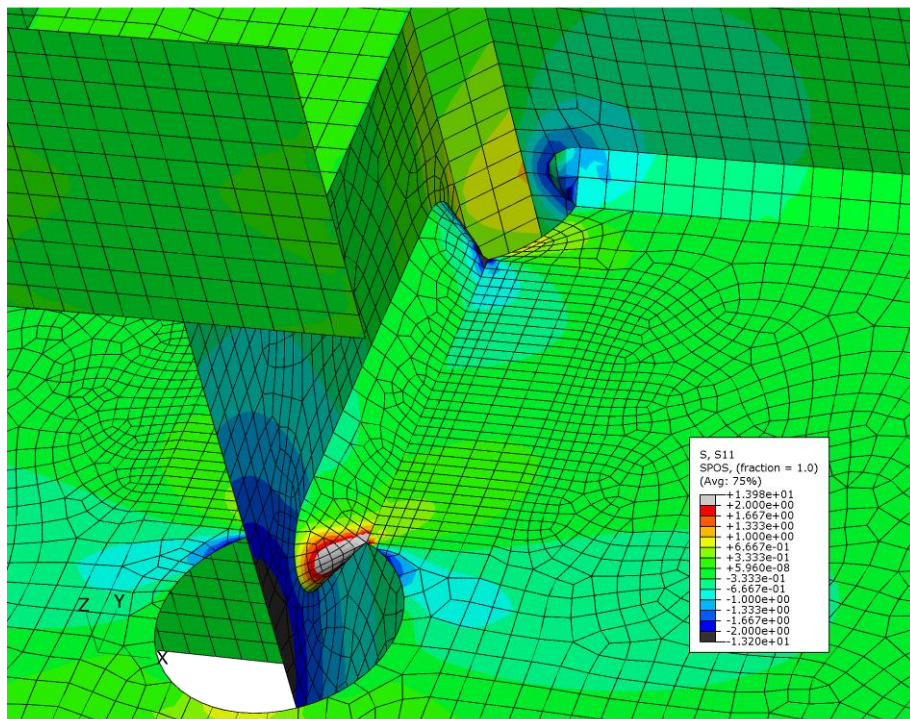


Figure 4.30 S11 plot (stress component perpendicular to the weld line) in the joint region, SW04 model.

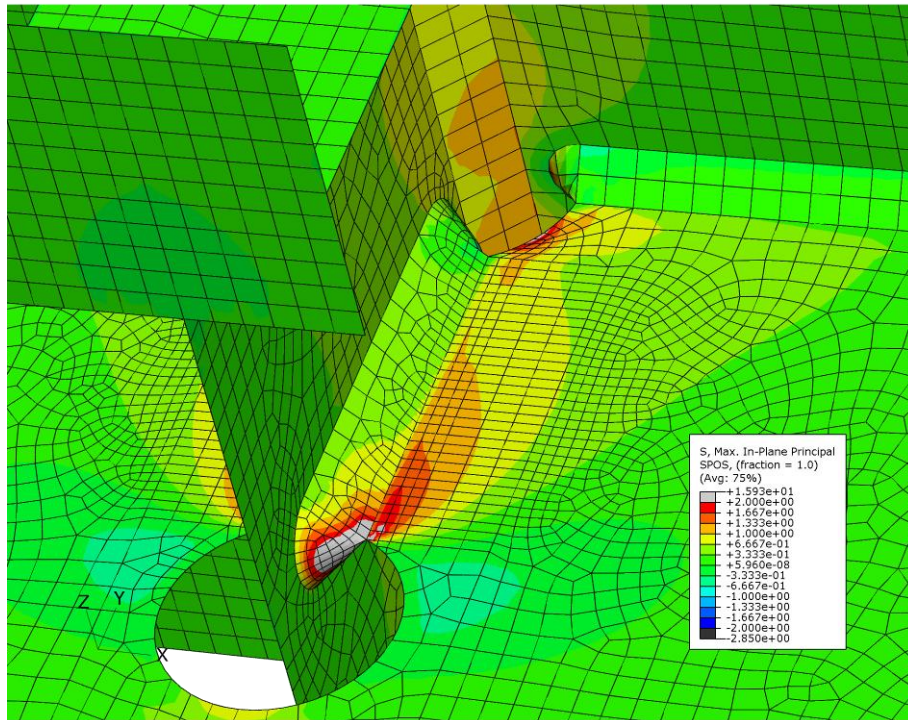


Figure 4.31 Maximum principal stress plot in the joint region, SW04 model.

4.2.8 Model TS02

The weld was modelled in this shell element model by increasing the thickness of the elements in the weld region. Eriksson et al. (2003) suggest using this technique for modelling of fillet welds in shell element models. The increased thickness for the elements in the weld region is calculated according to the method shown in Figure 4.32.

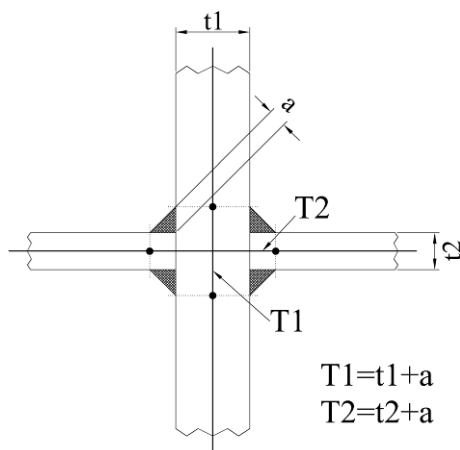


Figure 4.32 Calculation of increased thickness for shell elements in the weld region (Eriksson et al. 2003).

Figure 4.33 shows the regions within the welded area where shell elements with increased thickness were used. The extrapolation should be carried out into the transition point, where the thickness of shell elements changed. In order to maintain the stress singularity in this point and to have a better approximation of the joint geometry, the corner where the cope hole connects to the stiffener plate, was modified. This can be seen in Figure 4.33. The mesh size at the type 'b' regions was $2\text{mm} \times 2\text{mm}$ which is smaller than IIW recommended values for fine-meshed models. Whole physical part was modelled. A close up view of the finite element mesh at joint region can be seen in Figure 4.34.

The plot of the stress component perpendicular to the weld toe and maximum principal stress are depicted in Figure 4.35 and Figure 4.36, respectively.

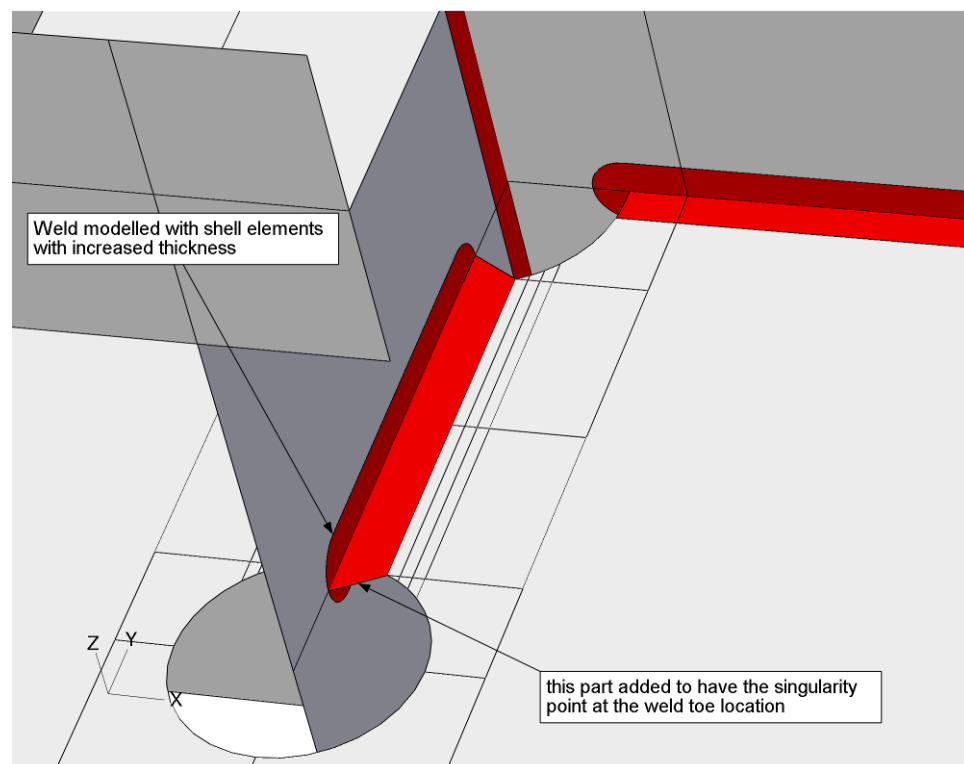


Figure 4.33 Weld modelling with thickened shell elements, TS02 model. Shaded areas show regions which were modelled with thickened shell elements.

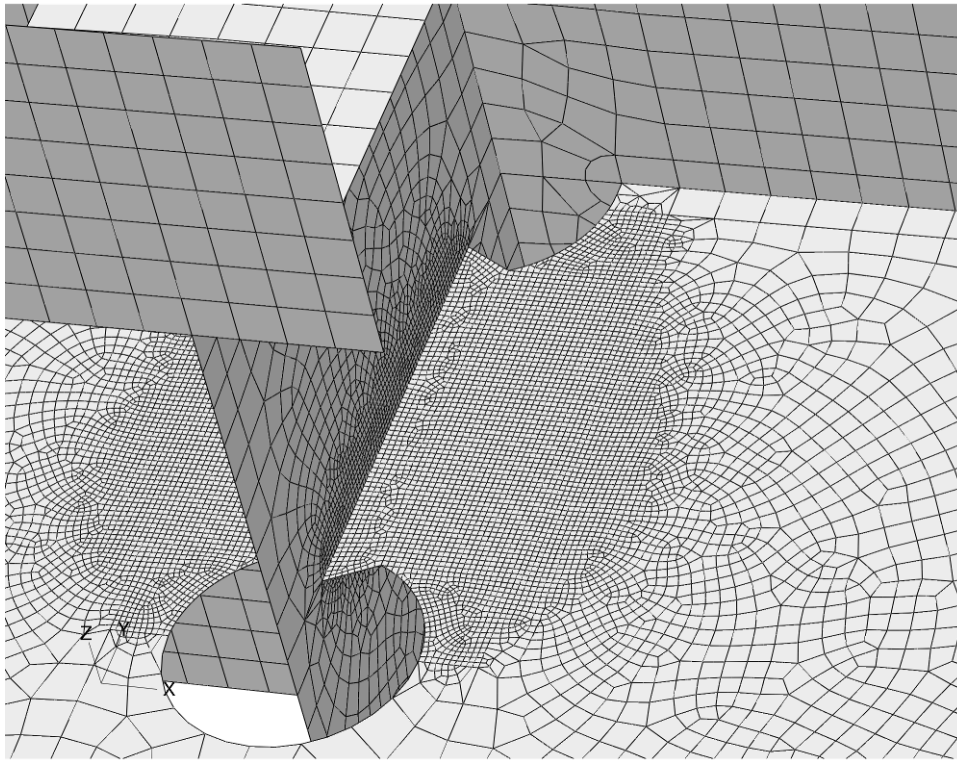


Figure 4.34 FE mesh in the joint region, TS02 model.

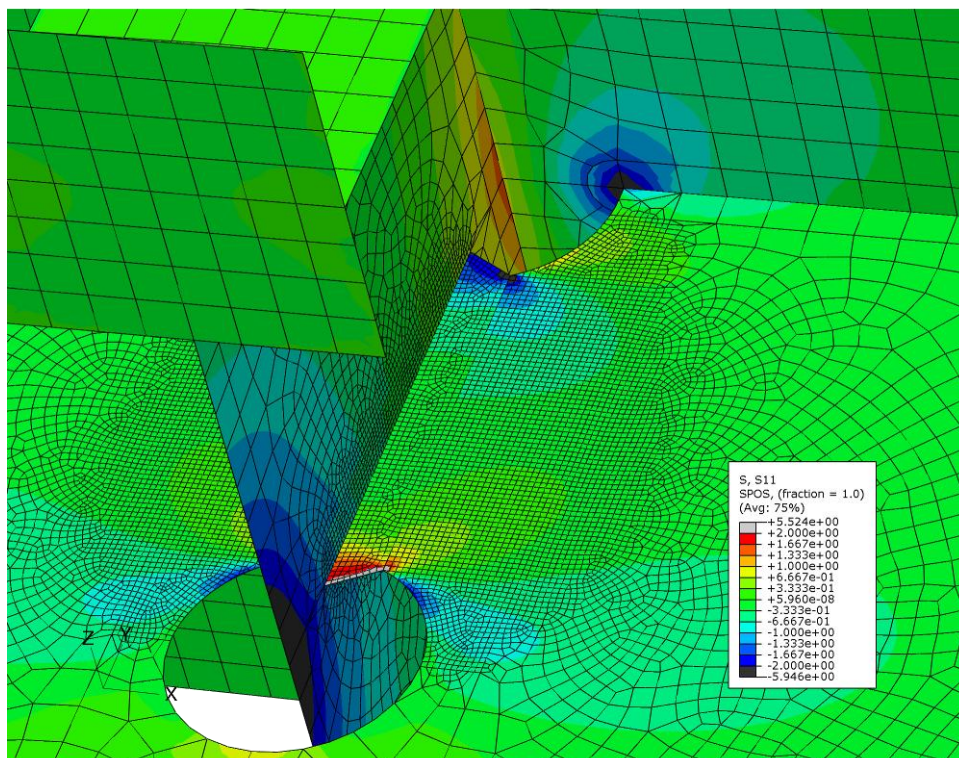


Figure 4.35 S11 plot (stress component perpendicular to the weld line) in the joint region, TS02 model.

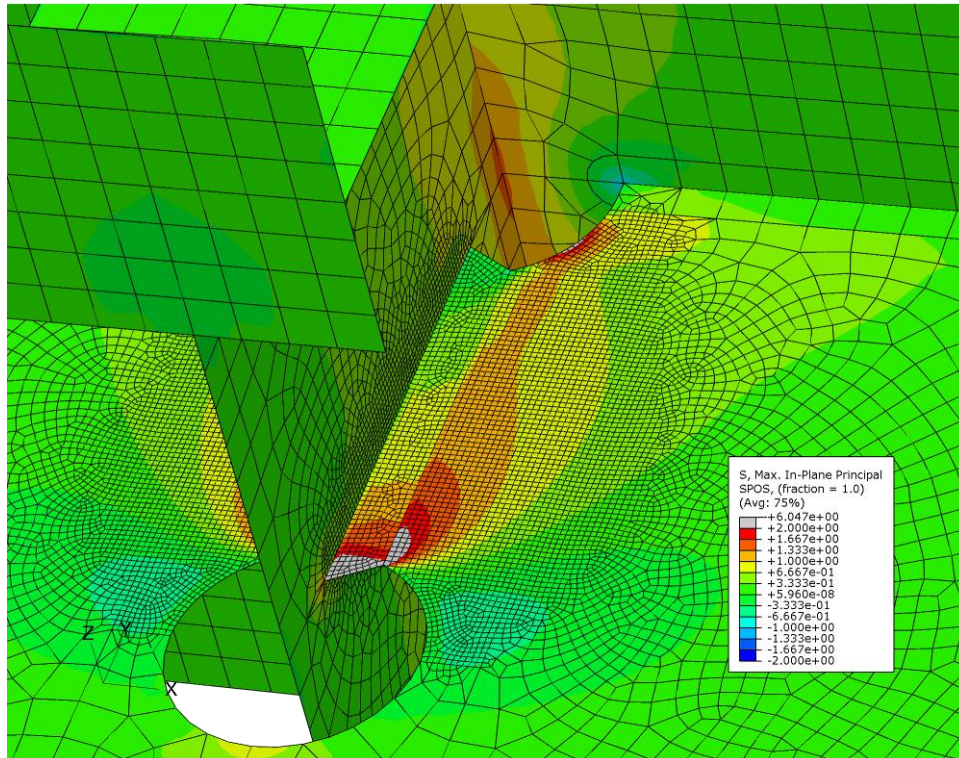


Figure 4.36 Maximum principal stress plot in the joint region, TS02 model.

4.2.9 Verification of the models

The deformed shape of the structure was used as an initial check of the models, for example see Figure 4.11. Another check would be the sum of reaction forces at the supports. It should be equal to the external applied force. The stresses and displacements in some key points of the models were also compared to the hand calculations. These calculations are presented in Appendix B. For a 400 kN loading, the bending stress in the bottom flange of the cross beam at mid-span was $\sigma_{bf}=40.81$ MPa. The maximum deflection of the cross beam at that point was estimated as $\delta_{max}=0.315$ mm. Table 4.1 shows the values of maximum deflection at mid-span, bending stress in the outmost fibre of lower flange at the mid-span of cross beam, and sum of support reactions for all of the models. To calculate the stress at the lower flange, nodal stresses across the flange at the mid-span section were read from analysis results and then were averaged.

The table shows that maximum deflection at mid-span and total equilibrium forces for all models correspond well with the theoretical values. However, bending stress calculated from the results of the model SH10 is 17% underestimated. Further inspection revealed that this error has occurred because of the use of symmetry in construction of this shell element model. Therefore, reduction in model size by the use of the symmetry should be carried out carefully to reduce the risk of modelling errors. This is specially the case in shell element models when the symmetry plane passes through the mid-plane of the structural plates.

Table 4.1 Verification of the models.

Model	δ_{\max} [mm]	σ_{bf} [Mpa]	Sum of support reactions [kN]
SH10	0.3300	34	4x100
SH04	0.3000	40	400
BR10	0.3000	41	4x99.9991
BR04	0.3000	41	4x99.9991
OP04	0.3000	41	4x100
SW04	0.29	40	400
TS02	0.30	40	400

4.3 Analysis of the models

The analysis type was linear elastic and the models were medium-sized in number of nodes and elements. Therefore, the computation was not very time consuming. Default solver options of the ABAQUS were used.

To have a measure of the computational effort needed for each model, some information regarding the size of the models is presented in Table 4.2. It should be noted that user's time (the time spent to make the model) was the largest part of the analysis time. This was the case specially in the models in which weld geometry was modelled. The user's time spent on making the OP04 or SW04 model was considerably more than simpler models, like SH04 model.

The computational size of the model can become more critical when modelling full-scale real structures, such as a whole bridge deck. In those cases, sub-modelling techniques may become handy.

Table 4.2 Comparison of the computational size of the model.

Model	Type	Mesh size	Element type	Number of nodes	Number of elements
SH10	Shell	Coarse	S8R	19027	6247
SH04	Shell	Fine	S8R	87201	28941

BR10	Solid	Coarse	C3D20R	25561	3578
BR04	Solid	Fine	C3D20R	35281	4958
OP04	Solid	Fine	C3D20R	68890	9785
SW04	Shell	Fine	S8R	66548	22406
TS02	Shell	Fine	S8R	62152	20736

4.4 Post-processing of the results

The stress profiles at the weld toes (hot spots) were calculated from the stress field results by defining paths at hot spot regions in the direction perpendicular to the weld toe (see Figure 4.10 and Figure 4.23) and then extracting the stress data on those paths. It is worth noting that Niemi et al. (2006) recommend disabling stress averaging option available in finite element analysis programs. This option is turned on by default in ABAQUS. However, in the case studied here, turning off this option resulted in two different stress values in a single point in some locations (see Figure 4.37). The extra stress value did not seem to be reasonable, since the stress field should be continuous. So, the stress averaging option was left turned on in the analyses performed here. The only difference was observed in the weld toe itself ($x = 0$) for some models. The stress was not evaluated correctly in these points due to the stress averaging with neighbouring elements. However, this did not affect the structural hot spot stress values, because the reported stress at the weld toe is not of interest in the SHSS method.

These stress profiles were then exported into a Microsoft Excel worksheet in the form of two column data, one column being the distance from the weld toe, and the other being the stresses at that point. A third column was added to the worksheet. This column included control parameters like extrapolation type (linear or quadratic) and locations of extrapolation points. Finally, a MATLAB code read the data in the worksheet and performed the extrapolation and calculated structural hot spot stress. Appendix C includes the source of this MATLAB code, which is named HS-Fatigue. The resulted stress profiles and structural hot spot stresses are presented in Chapter 5.

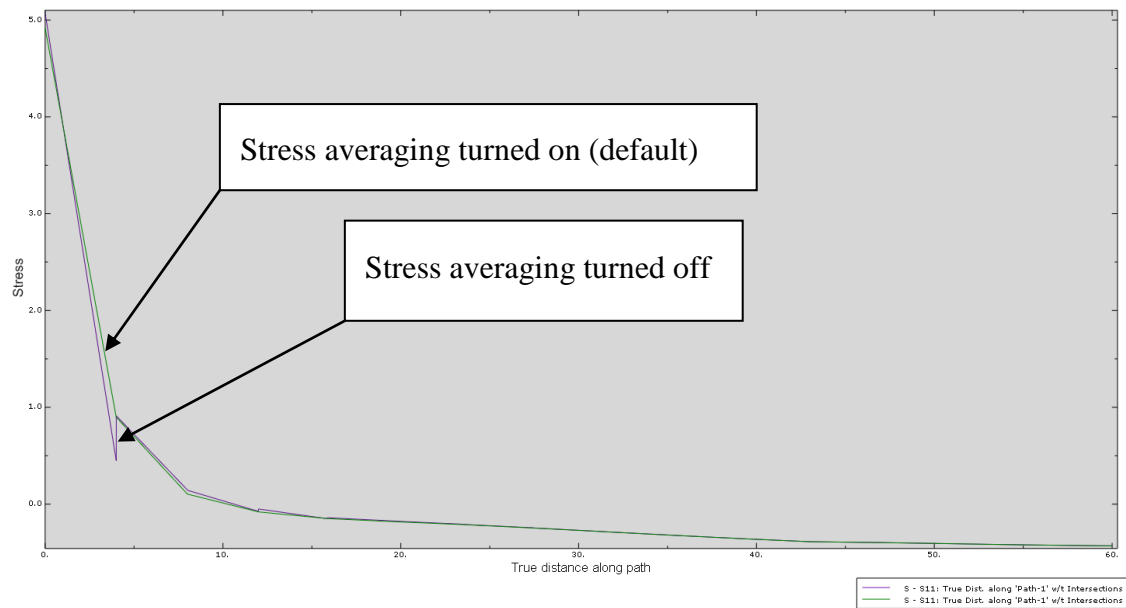


Figure 4.37 Effect of stress averaging on the stress profiles.

5 Fatigue life assessment of specimens

In this chapter, fatigue life predictions for the specimens based on the structural hot spot stress method are presented. The evaluated hot spot stresses are also compared to the measured hot spot stresses for one of the details ('wb' hot spot). Moreover, real fatigue life of the specimens is compared to their predicted life based on the nominal stress method according to Eurocode.

5.1 Structural hot spot stress method

5.1.1 Calculation of SHSS from finite element analysis results

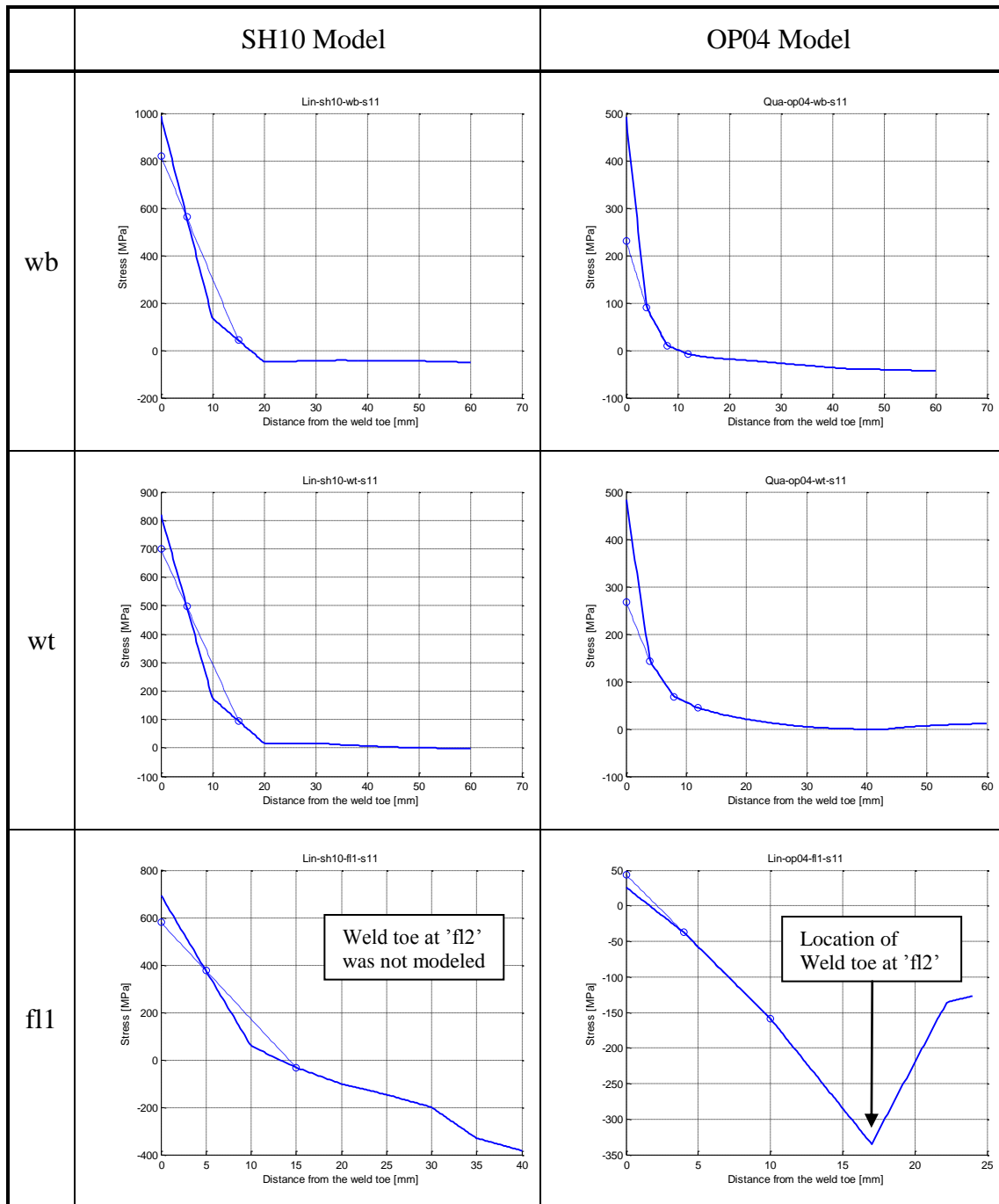
The post-processed results of the finite element analysis are presented here. The post-processing stage was described in Section 4.4. Table 5.1 shows the stress profiles for two of the models (SH10 and OP04) at three hot spots: 'wb', 'wt' and 'fl1'. The finite element mesh of the models was not suitable for calculation of structural hot spot stress at 'fl2' hot spot. Hence, that hot spot is not investigated further in this study. The rise in the stress values at the fl1 in about 20 mm from the weld toe in the table is because of the weld at 'fl2'. It should be noted that the origin of horizontal axis for shell element models in these graphs is on the mid plane of the stiffener plate, while the origin for solid element models is located at the weld toe.

5.1.2 Comparison of SHSS values from finite element models to experimental measurements

To validate the finite element models, the SHSS values from the models were compared to their corresponding values from the strain measurements on the specimens. Figure 5.1 shows the stress profiles for the OP04 and SH04 models together with stress profiles from the strain measurements. The measured stress profiles are the same as the profiles shown in Figure 3.16 and Figure 3.17, but multiplied by a factor of 2 to account for the 400 kN load. It can be seen that the extrapolated hot spot stresses from OP04 model are in acceptable agreement with the measurements in both 'wb' and 'wt' hot spot. This might have been even better if the misalignments in the studied cruciform joint were introduced into the finite element model. On the other hand, shell element model (SH04) resulted in unrealistically high SHSS values which are not acceptable.

Above said, it seemed that solid element model OP04 had sufficient accuracy to be used as a benchmark for comparing the results from the other models. Besides, some modifications in the shell element model were made (mainly by including the weld into the model) to improve the accuracy of the results from this model. This resulted in the two models SW04 and TS02 which was described in detail in the last chapter. In the following section, the stress profiles and evaluated SHSS values from various finite element models are presented and compared to the 'benchmark' (i.e. OP04) model.

Table 5.1 *S11 stress profiles at three hot spots for two models (SH10 and OP04) for 400kN loading (abscissa: distance from the weld toe (for OP04) or distance from the mid-plane of the stiffener (SH10 model) in mm, ordinate: S11 stress in MPa).*



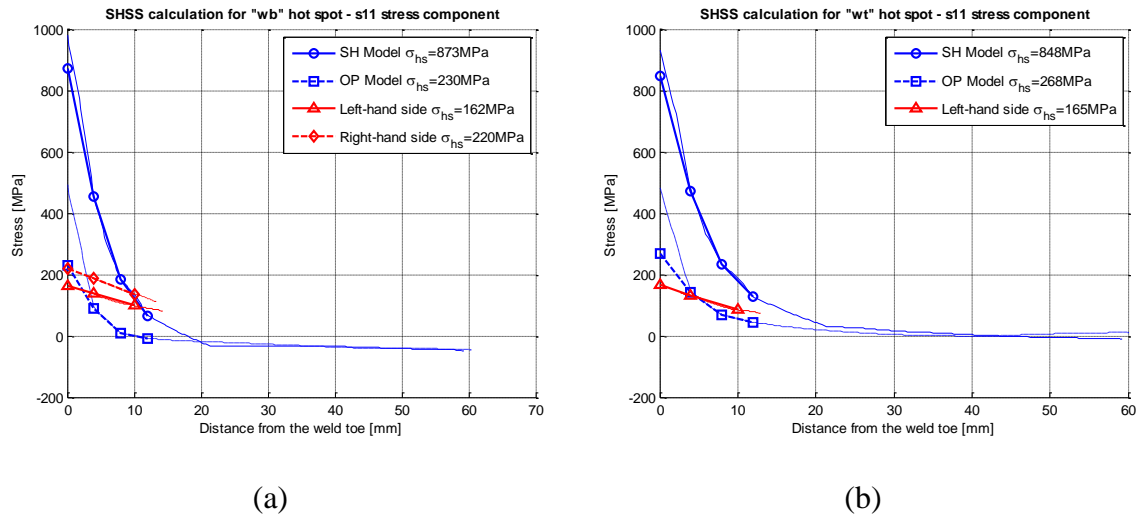


Figure 5.1 Stress profiles from the measurements vs. stress profiles and hot spot stresses from the finite element analysis (SH04 and OP04 models); (a) 'wb' hot spot, (b) 'wt' hot spot.

5.1.3 Comparison of the SHSS values for all finite element models

Figure 5.2 and Figure 5.3 show the summary of the S11 (stress component perpendicular to the weld toe) and principal stress profiles for the 'wb' hot spot, respectively. Far enough from the weld toe (about 30 mm) all stress profiles are practically the same. But in the near-field region different models give different stress profiles. Consequently, the extrapolated SHSS results from these profiles show considerable variation. As it was shown in the Section 5.1.2, shell element models without welds (SH10 and SH04 models) gave unreasonable results which were very high. It should be added that only one quarter of the physical specimen was modelled in the shell element model SH10 (see Section 4.1). This also led to even less accurate results for this model.

Gradient of the stress field in type 'b' hot spots is steeper than type 'a' hot spots. This supports the idea that the modelling of weld will reduce the extrapolated hot spot stress; since the extrapolation will be performed onto a point farther from the mid-plane. This was also supported by the case study of a simple cruciform joint which is described in appendix D. In that case, the agreement between the shell element model and solid element model was very good when the welds were included into the shell element model in the form of oblique shell elements. Having this in mind, it was expected to have a good agreement between improved shell element models (SW04 and TS02) and OP04 model. But, as it can be seen in the figures, both of the improved shell element models resulted in SHSS values which were considerably lower than the OP04 model. Thus, it seems that when a geometric feature (like a cope-hole in our case) exists in the weld toe region, the weld modelling techniques in shell element models may not give results with acceptable accuracy. Furthermore, their results may be underestimated and on the unsafe side. This was the case in our study.

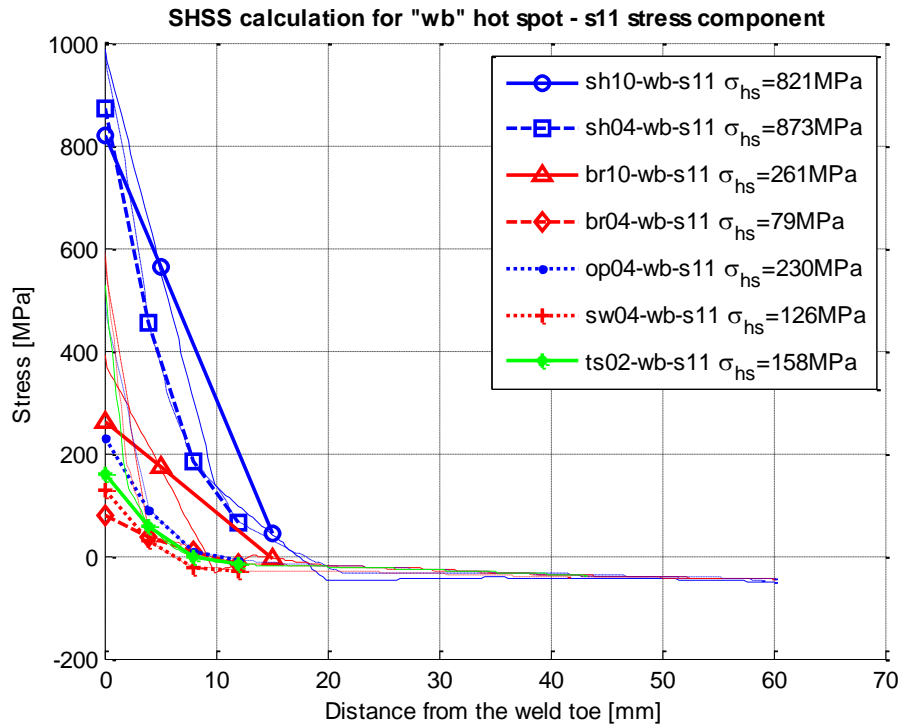


Figure 5.2 Summary of S11 (stress component perpendicular to the weld toe) stress profiles at 'wb' hot spot for five models (load:400 kN).

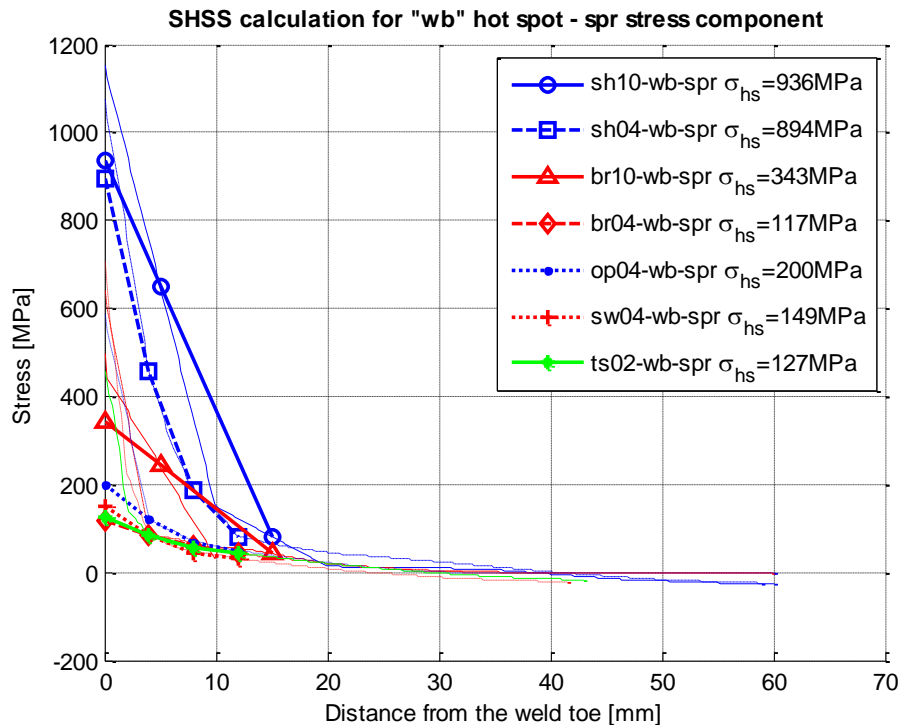


Figure 5.3 Summary of maximum principal stress profiles at 'wb' hot spot for five models (load:400 kN).

The difference in SHSS values for BR04 and OP04 models can be associated with the interpolation issue discussed earlier in section 4.2.6. It is interesting to observe the considerable impact of a relatively minor mesh correction in the final results of the calculations for these two solid element models.

It can be seen that the structural hot spot stress value at 'wb' based on the principal stresses ($\sigma_{hs} = 200MPa$) is less than the value based on normal stresses ($S11, \sigma_{hs} = 230MPa$) for model OP04. So, in this case the hot spot stress value according to Eurocode is different from the SHSS value according to the IIW recommendations (See Section 2.3.4).

Figure 5.4 and Figure 5.5 show the summary of the S11 (stress component perpendicular to the weld toe) and principal stress profiles for the 'wt' hot spot, respectively. Again, the same trend can be observed: shell element models (without welds modelled) result in higher structural hot spot stress values. Part of the variation in solid element results can be associated with the fact that for BR10 and BR04 models the extrapolation points are not coincident with the nodal points of the finite element mesh. Modified shell element models (SH04 and TS02) again give considerably lower SHSS values than the OP04 model.

Figure 5.6 and Figure 5.7 show the summary of the S11 (stress component perpendicular to the weld toe) and principal stress profiles for the 'fl1' hot spot, respectively. Figures show a trend approximately similar to previous investigated hot spots. Shell element models (without weld modelled) overestimate the SHSS value to unreasonable values. This shows the importance of the modelling of the weld in the regions where two adjacent welds exist. The stiffness of the plate in between the two welds varies considerably if the welds are or are not included in the model. The results from the modified shell element models are not included in the graphs for this hot spot because in the last stages of the research the focus was more on the investigation of type 'b' hot spots 'wt' and 'wb'.

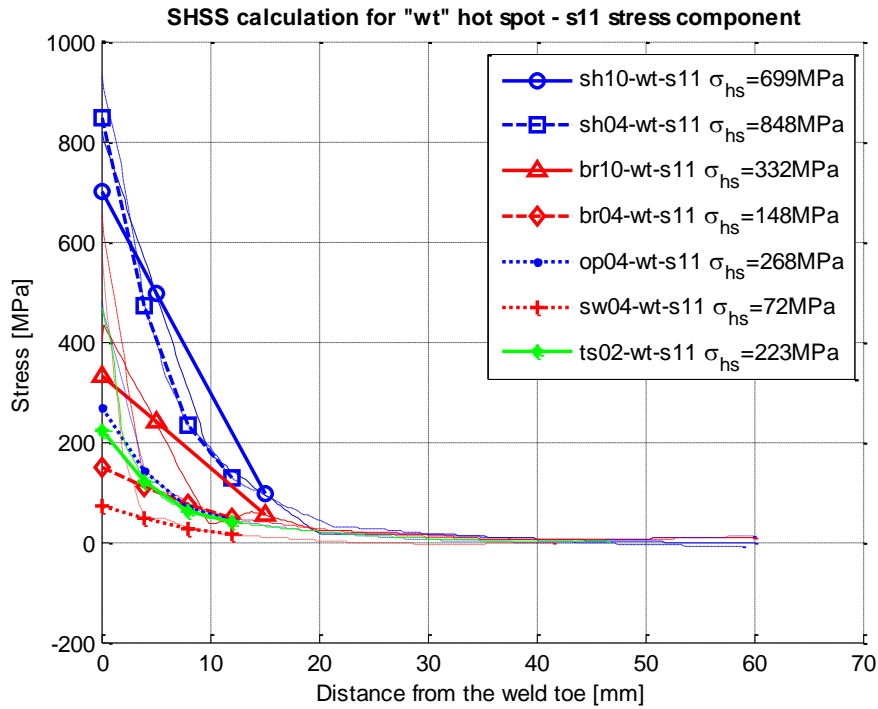


Figure 5.4 Summary of S_{11} stress profiles at 'wt' hot spot for five models (load:400 kN).

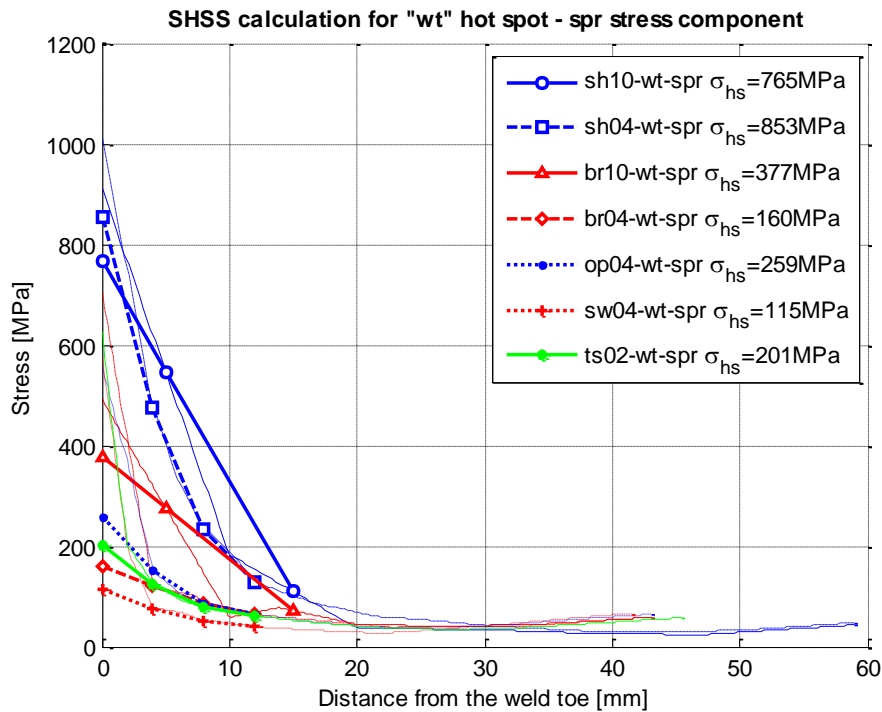


Figure 5.5 Summary of maximum principal stress profiles at 'wt' hot spot for five models (load:400 kN). Note the abnormality in the SHSS value of the SH04 model.

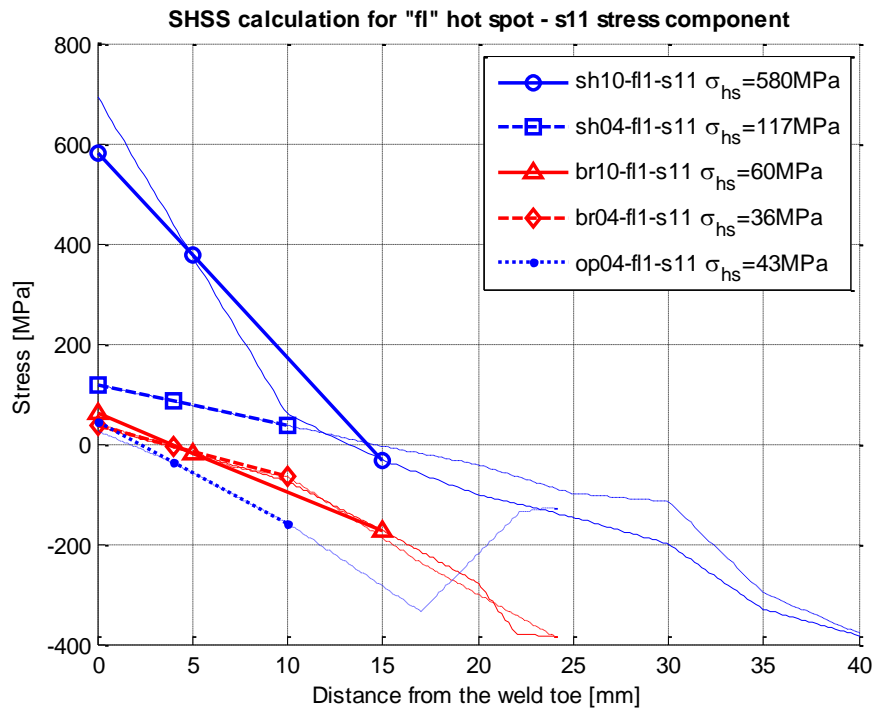


Figure 5.6 Summary of S11 stress profiles at 'fl' hot spot for five models (load:400 kN).

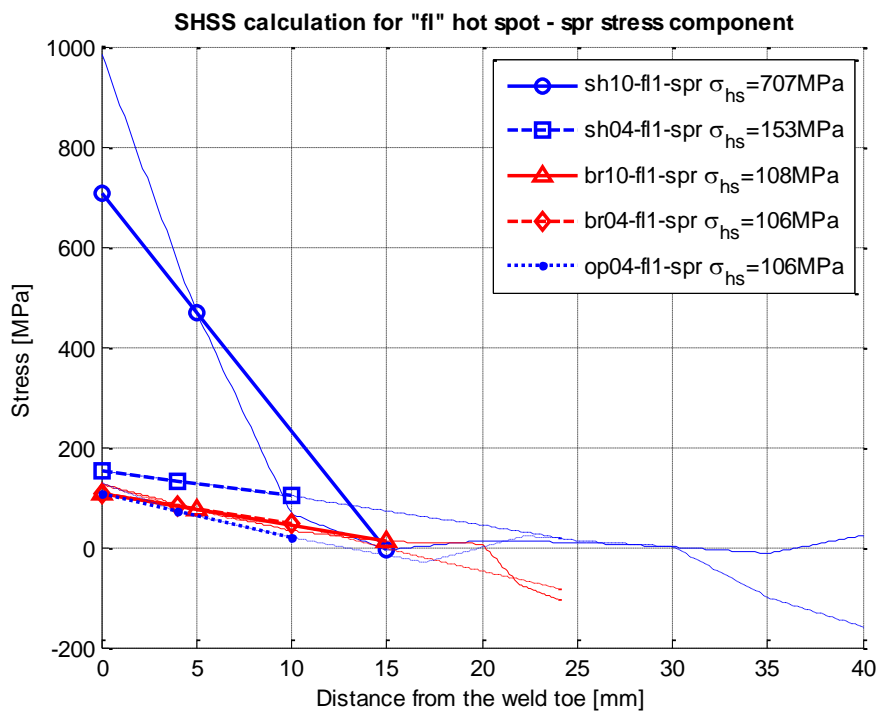


Figure 5.7 Summary of maximum principal stress profiles at 'fl' hot spot for five models (load:400 kN).

5.1.4 Comparison of numerical and experimental results

Cracks in the 'wb' hot spot region were generally the earliest cracks observed in the specimens (See Table 3.11). Thus we will investigate it further in this section. Table 5.2 summarizes the hot spot values and the corresponding predicted fatigue lives for different models together with the experimental hot spot value for 'wb' measured on specimen A4.

As stated before, the OP04 model is more reliable than the other models in evaluation of the SHSS values. Thus, it was selected to construct the S-N plot of the structural hot spot stress evaluation results, shown in Figure 5.8. The figure shows fatigue life data for crack initiation in the location of bottom cope-hole edge on the web of cross beam. The S-N curve is that of detail category 90, corresponding to the cruciform joint (see Table 2.4). The data points are derived from the experiment and from the FE analysis: The structural hot spot stress range (y-coordinate) of the points is that of OP04 model and the number of cycles (x-coordinate) is as of the number of cycles to crack initiation in 'wb' point in the test (see Table 3.11). Specimen a2 was tested under two load different ranges 200 kN and 400 kN. The equivalent SHSS stress range for this specimen was calculated using Palmgren-Miner linear damage accumulation rule. The figure shows that the results of the SHSS method are on the safe side in this case. It should be noted that no partial load and/or resistance factor were used in the calculations, because the modelling of the real behaviour was of interest.

Table 5.2 Comparison of numerical and experimental SHSS values at 'wb' hot spot.

Model	Load [kN]	Based on S11		Based on principal stress	
		σ_{hs} [MPa]	Endurance [N]	σ_{hs} [MPa]	Endurance [N]
SH10	400	821.0	2.63E+03	936.0	1.78E+03
	350	718.4	3.93E+03	819.0	2.65E+03
	370	759.4	3.33E+03	865.8	2.25E+03
SH04	400	873.0	2.19E+03	894.0	2.04E+03
	350	763.9	3.27E+03	782.3	3.05E+03
	370	807.5	2.77E+03	827.0	2.58E+03
BR10	400	261.0	8.20E+04	343.0	3.61E+04
	350	228.4	1.22E+05	300.1	5.39E+04
	370	241.4	1.04E+05	317.3	4.57E+04

BR04	400	79.0	2.96E+06	117.0	9.10E+05
	350	69.1	4.41E+06	102.4	1.36E+06
	370	73.1	3.74E+06	108.2	1.15E+06
OP04	400	230.0	1.20E+05	200.0	1.82E+05
	350	201.3	1.79E+05	175.0	2.72E+05
	370	212.8	1.51E+05	185.0	2.30E+05
SW04	400	126.0	7.29E+05	149.0	4.41E+05
	350	110.3	1.09E+06	130.4	6.58E+05
	370	116.6	9.21E+05	137.8	5.57E+05
TS02	400	158.0	3.70E+05	127.0	7.12E+05
	350	138.3	5.52E+05	111.1	1.06E+06
	370	146.2	4.67E+05	117.5	8.99E+05
Test (Specimen A4)	400	202.0	1.77E+05	-	
	350	176.8	2.64E+05	-	
	370	186.9	2.24E+05	-	

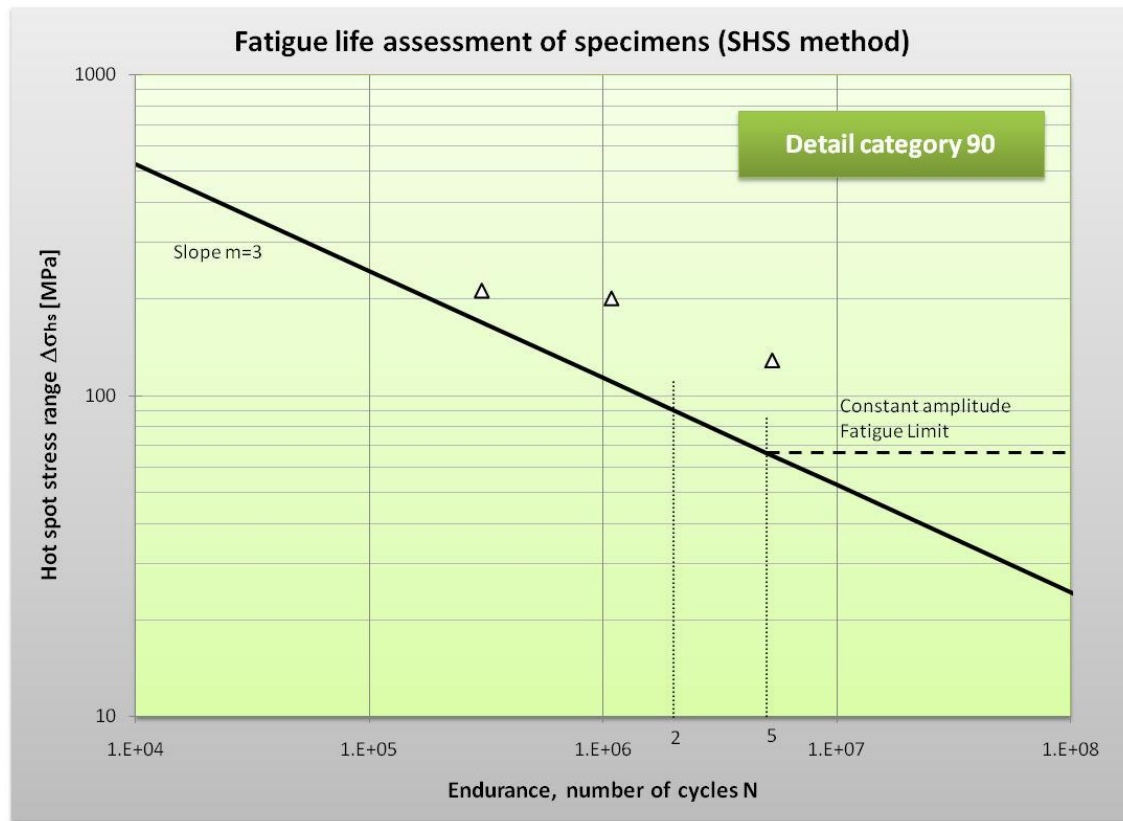


Figure 5.8 Structural hot spot stress S-N curve for the tested specimens, 'wb' hot spot (SHSS values derived from model OP04).

5.2 Nominal stress method

Chapter 9 of Eurocode 3 (2005) has introduced detail categories for orthotropic bridge decks with open and closed stringers (stiffeners). Table 5.3 shows a part of Table 8.9 of the Eurocode corresponding to the detail categories for the orthotropic bridge decks with open stiffeners. According to this table, an equivalent stress range $\Delta\sigma_{eq}$ should be calculated as a combination of the direct (normal) stress range and shear stress range at the stiffener. This equivalent stress range is then used as nominal stress range in the appropriate S-N curve (which is, in this case, detail category 56).

The calculations are carried out for the fatigue loading of specimen A2. That is, a fatigue load range of 200 kN applied for 5 million cycles, followed by a load range of 400 kN applied for 380'000 cycles. The detailed calculations are presented in Appendix A of this report. Table 5.4 shows summary of calculated damage ratios for specimen A2. It should be noted that the partial load and resistance factors were set to unity in the calculations. This was done in order to attain a realistic fatigue life which would be comparable to the results from the experiment.

Table 5.3 Detail categories for orthotropic decks with open stiffeners, from Table 8.9 of Eurocode 3 (2005).

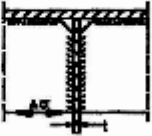
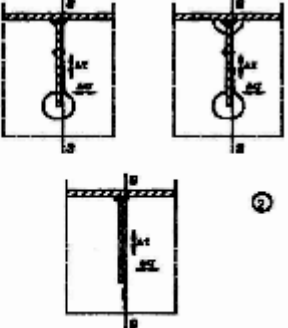
Detail category	Constructional detail		Description	Requirements
S0	$t \leq 12\text{mm}$		1) Connection of longitudinal stringer to cross girder.	1) Assessment based on the direct stress range $\Delta\sigma$ in the stringer.
S1	$t > 12\text{mm}$		2) Connection of continuous longitudinal stringer to cross girder. $\Delta\sigma = \frac{\Delta M_x}{W_{pl,x}}$ $\Delta\tau = \frac{\Delta V_x}{A_{web,x}}$ Check also stress range between stringers as defined in EN 1993-2.	2) Assessment based on combining the shear stress range $\Delta\tau$ and direct stress range $\Delta\sigma$ in the web of the cross girder, as an equivalent stress range: $\Delta\sigma_{eq} = \frac{1}{2} (\Delta\sigma + \sqrt{\Delta\sigma^2 + 4\Delta\tau^2})$

Table 5.4 Calculated damage ratios for different cracking locations (hot spots) in specimen A2, based on nominal stress method.

Hot spot location	wb	wt	fl2
Damage ratio	0.415	0.802	0.039

The damage ratio predicted by the nominal stress method for the ‘wt’ point ($D=0.802$) was larger than the damage ratio for the ‘wb’ ($D=0.415$) and ‘fl2’ point ($D=0.039$). This is contrary to the predictions made by the FE analyses and also observed fatigue cracking in the experiment. It seems that Eurocode 3 guidelines are not clear in this regard. It does not prescribe any critical point in the section for evaluation of the equivalent stress range ($\Delta\sigma_{eq}$).

The damage calculated for ‘fl2’ hot spot (that is, point C in the Appendix A) seems under-estimated, since the shear lag effect in the deck plate is not considered in the simplified hand calculations.

For A2 specimen, which was tested under the highest load range among the specimens, the calculated damage ratios were less than 1 for all hot spots. So, according to nominal stress method, the fatigue cracking in ‘wb’ and ‘fl2’ was unlikely to occur. The damage ratio at ‘wt’ ($D=0.802$) was high enough to anticipate cracking. It is emphasized that the partial load and resistance factors are not considered in the calculations.

The results of fatigue assessment based on nominal stress method are summarized in Figure 5.9. The figure shows S-N curve for cracking in web of cross beam (detail category 56) together with the data points from the test. The nominal stress range (y-coordinate) of the points is the equivalent stress range for point B (i.e. 'wt') as calculated in Appendix A and the number of cycles (x-coordinate) is as of the number of cycles to crack initiation in the test (see Table 3.11). The figure shows that the nominal stress method underestimates the damage and thus, overestimates the fatigue life of the specimens, which is on the unsafe side.

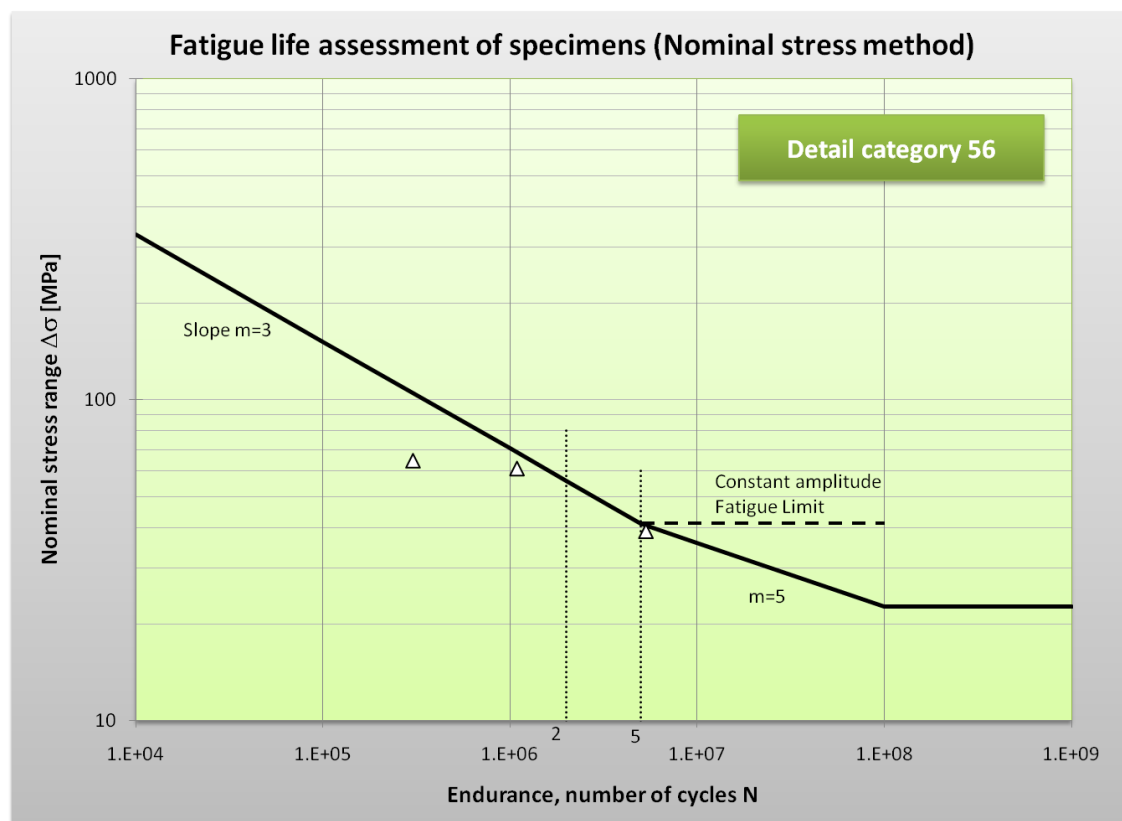


Figure 5.9 Nominal stress S-N curve for the tested specimens.

6 Conclusion

Structural hot spot stress method (SHSS) utilizes the advantages of finite element method for fatigue assessment of welded steel details. This enables the method to assess more types and variations of details compared to the conventional nominal stress method. The method has been in use for about 30 years in other engineering disciplines such as offshore and marine structures and automotive engineering. It has been used also in fatigue life assessment of welded joints of hollow core sections and some bridge structures. With the introduction of the method into Eurocode 3, it is expected that the application of the method in the fatigue assessment of civil engineering steel structures will increase.

The application of structural hot spot stress on fatigue life assessment of a welded bridge detail was studied in this project. The studied detail was a fillet-welded stiffener-to-cross beam joint which is typical in the orthotropic steel bridge decks. Root cracking in the fillet welds was not considered, and it did not occur in the experiments, neither. Three full-scale specimens of the detail were made and tested under constant amplitude fatigue loads. Structural hot spot stress was evaluated experimentally on one of these models, namely specimen A4. In the numerical part of the study, six different finite element models of the physical part were made. Finite element modelling was carried out in accordance with IIW recommendations. Structural hot spot stresses for each model were calculated. The accuracy of the models was assessed by comparing these SHSS values to the experimental values. Finally, the testing and analysis results were put into relevant fatigue strength S-N curve recommended by the Eurocode, to compare the fatigue life as predicted by the code to the fatigue life in the tests. This comparison was also done for the relevant S-N curve for the nominal stress method.

In the modelling phase the following issues were observed:

- The modelling of the welds in the software used in this study, and similar general purpose FEA software, is a tedious task. The modelling of the weld in a way complying with the SHSS method requirements is not straightforward and easy to implement, especially in the case of using shell element models. Considering popularity of welded structures and growing need to model them with the FEM, it will be desirable to implement more robust modelling options for creating and analysing FE models of welded structures. Also, proper post-processing tools will pave the way of regular use of the SHSS method in the design office.
- Although it was not an issue in this study, it should be noted that fulfilment of some of IIW requirements in FE modelling can be problematic. For example consider these three conditions: requirements for the mesh size, having one element through the thickness, and elements' aspect ratios not exceeding the maximum allowed value. Satisfying all these three conditions at the same time can be troublesome in some cases. Also, in the case of edge details (type 'b' hot spots) with curved edges, it is not clear how the extrapolation can be carried out. For example, for an attachment end with a soft end (similar to the details discussed in Fricke & Doerk 2006), the extrapolation could pass the curved edge of the plate.

- User's time spent for modelling the geometry of the part and proper meshing of the model was considerably more than the analysis time. Since the analysis type was linear elastic, the analysis time was not very long even for fine-mesh solid element model OP04 which was the largest in the number of elements. In contrast, the user's time for solid element models was much more than shell element models, because of more details that should be introduced into the solid models.

In the post-processing of the results and calculation of SHSS for different models following remarks can be made:

- Structural hot spot stress values calculated from the solid model with fine mesh (OP04 model) were about 14 percent higher than the mean of experimentally measured values, which is acceptable, considering the effect of misalignments in the real specimen. Especially considering the case that the strains on the specimen were measured at a 2.5 mm transverse distance from the hot spot location, because of the practical issues.
- Structural hot spot stress values at 'wb' hot spot calculated from OP04 model were used in the proper fatigue strength curve (detail category 90) of the Eurocode. The predicted fatigue lives for three specimens were less than their actual fatigue lives. This means that SHSS results are on the safe side in the studied case. Conversely, nominal stress method overestimated the fatigue lives of all of three specimens, which is on the unsafe side. Albeit this was without considering any partial load or resistance factor in the calculations.
- Comparison of SHSS results from the two fine mesh models BR04 and OP04 showed that the coincidence of extrapolation points and nodal points has a dramatic effect in the results.
- For the case studied in this research, SHSS values computed from shell element models without welds modelled were significantly larger than the measured values and from the values from more accurate solid element. In contrary, introducing the welds into the shell element models resulted in considerably lower SHSS values which were, again, unacceptable. Hence, shell element models for fatigue evaluation of complex details should be verified by more accurate analyses and/or tests.
- In the case study of a single cruciform joint in Appendix D, shell element model (with welds included) had a very good agreement with the solid element model. As mentioned before, this was not the case in the FE models of the studied specimen. Comparing these two cases, it seems that the presence of a geometric feature (like a cope hole or curved edge) in the hot spot region might be the cause for the difference in the results. In these cases, the stiffness of the weld has a considerable effect on the results and proper modelling of this stiffness becomes more important. Therefore, it is suggested that solid element models being used for these situations.
- The gradient of the stress field is steeper in type 'b' hot spots than type 'a'. In addition, the structural stress and nonlinear notch stress components cannot be fully separated in type 'b' hot spots (for type 'a' hot spots these two

component can be separated; see Equations 2.4 to 2.6). Consequently, SHSS values for Type 'b' hot spots are more sensitive to the meshing options than type 'a' hot spots. So, the meshing and the results should be overlooked when analysing type 'b' hot spots.

In this research, the structural hot spot stress was calculated with surface stress extrapolation (SSE) technique. It is suggested that other alternative techniques for evaluation of SHSS be examined. Through thickness stress linearization at the weld toe (TTWT), the Dong (2001) method and Xiao & Yamada (2004) method are of special interest. The outcome of these techniques can be compared to the SSE technique to determine the most accurate and efficient method. In particular, the sensitivity of the models to the mesh density can be assessed.

The experimental work described in this thesis is currently in progress at the ITAM. Another type of specimens with different geometry and thinner stiffener is going to be tested. In this case, the detail will potentially have some more hot spots located on the stiffener plate. It is advisable that the fatigue life of these specimens also being evaluated using SHSS method.

Another issue observed in this study was that Eurocode 3 guidelines regarding the use of SHSS method (or geometric stress method, as Eurocode names it) provide little information on how the modelling should be done. To fill these gaps, IIW recommendations were used. Since the modelling specifications are of critical importance in validity of results, it is proposed that complementary recommendations be introduced into the Chapter 9 of the Eurocode 3.

All in all, SHSS method, when used with a fine-mesh solid element FE model, was used successfully in estimation of the fatigue life of the studied detail in this research. However, it was observed that modelling technique (element type, mesh size, and mesh details) had considerable impact on the results. The user's effort for constructing the model is higher than regular finite element analyses, but still it is acceptable. Following the IIW guidelines accompanied with some experience in FE modelling of welded details can ensure reliable results.

7 References

- ABAQUS, Inc., 2007. *ABAQUS Analysis: User's Manual, Version 6.7*, Dassault systèmes.
- Biot, M. et al., 2001. An investigation of fatigue damage: Numerical approaches and experimental validation. In *Proceedings of the International Conference on Offshore Mechanics and Arctic Engineering - OMAE*. pp. 79-86.
- Chan, T.H.T., Guo, L. & LI, Z.X., 2003. Finite element modelling for fatigue stress analysis of large suspension bridges. *Journal of Sound and Vibration*, 261(3), 443-464.
- Doerk, O., Fricke, W. & Weissenborn, C., 2003. Comparison of different calculation methods for structural stresses at welded joints. *International Journal of Fatigue*, 25(5), 359-369.
- Dong, P., 2001. A structural stress definition and numerical implementation for fatigue analysis of welded joints. *International Journal of Fatigue*, 23(10), 865-876.
- Eriksson, Å. et al., 2003. *Weld evaluation using FEM : a guide to fatigue-loaded structures*, Stockholm: Industrilitteratur.
- ESDEP, 1993. Extracts from the European Convention for Constructional Steelwork (ESDEP), chapter 12. Available at: <http://www.esdep.org/members/master/toc.htm> [Accessed January 24, 2009].
- European standard, 2005. *Eurocode 3: Design of steel structures - Part 1-9: Fatigue*, Brussels: European Committee for Standardization.
- Fricke, W., 2002. Evaluation of Hot Spot Stresses in Complex Welded Structures. In *Proceedings of The IIW fatigue seminar, Commission XIII, International Institute of Welding, Tokyo*.
- Fricke, W., 2003. Fatigue analysis of welded joints: state of development. *Marine Structures*, 16(3), 185-200.
- Fricke, W. et al., 2008. Round robin study on structural hot-spot and effective notch stress analysis. *Ships and Offshore Structures*, 3(4), 335-345.

- Fricke, W. & Doerk, O., 2006. Simplified approach to fatigue strength assessment of fillet-welded attachment ends. *International Journal of Fatigue*, 28(2), 141-150.
- Fricke, W. & Kahl, A., 2005. Comparison of different structural stress approaches for fatigue assessment of welded ship structures. *Marine Structures*, 18(7-8), 473-488.
- Hobbacher, A., 2003. *Recommendations for Fatigue Design of Welded Joints and Components IIW Document XIII-1965-03, XV-1127-03*, Paris.
- Hobbacher, A.F., 2009. The new IIW recommendations for fatigue assessment of welded joints and components—A comprehensive code recently updated. *International Journal of Fatigue*, 31(1), 50-58.
- Kim, M. & Kang, S., 2008. Testing and analysis of fatigue behaviour in edge details: a comparative study using hot spot and structural stresses. *Proceedings of the Institution of Mechanical Engineers, Part C: Journal of Mechanical Engineering Science*, 222(12), 2351-2363.
- Kjellberg, M. & Persson, A., 1998. *The development of a hot spot stress based design S-N curve for ship structural details*, Master's thesis, Chalmers University of technology, Göteborg.
- Kolstein, M.H., 2007. *Fatigue classification of welded joints in orthotropic steel bridge decks*. PhD dissertation, Delft University of Technology.
- Lindemark, T. et al., 2009. Fatigue Capacity of Stiffener to Web Frame Connections. In *Proceedings of OMAE2009*. Honolulu, Hawaii, USA: ASME.
- Lotsberg, I. & Sigurdsson, G., 2006. Hot Spot Stress S-N Curve for Fatigue Analysis of Plated Structures. *Journal of Offshore Mechanics and Arctic Engineering*, 128(4), 330-336.
- Maddox, S.J., 2002. Hot-Spot Stress Design Curves for Fatigue Assessment of Welded Structures. *International Journal of Offshore and Polar Engineering*, 12(2), 134-141.
- Maddox, S.J., 1991. *Fatigue strength of welded structures* Second edition., Cambridge, England: Woodhead Publishing.

- Marquis, G. & Kähönen, A., 1996. *Fatigue testing and analysis using the hot spot method*.
- Marquis, G. & Samuelsson, J., 2005. Modelling and fatigue life assessment of complex structures. *Materialwissenschaft und Werkstofftechnik*, 36(11), 678-684.
- Miki, C. & Tateishi, K., 1997. Fatigue strength of cope hole details in steel bridges. *International Journal of Fatigue*, 19(6), 445-455.
- Niemi, E., Fricke, W. & Maddox, S.J., 2006. *Fatigue Analysis of Welded Components: Designer's Guide to the Structural Hot-spot Stress Approach*, Woodhead Pub.
- Niemi, E. & Marquis, G., 2002. Introduction to the structural stress approach to fatigue analysis of plate structures. In *Proceedings of the IIW fatigue seminar*. pp. 73–90.
- Niemi, E. & Marquis, G.B., 2003. Structural hot spot stress method for fatigue analysis of welded components. *Metal structures—Design, Fabrication, and Economy*, 90-77017.
- Notaro, G. et al., 2007. An application of the hot spot stress approach to a complex structural detail. In Guedes Soares & Koley, eds. *Maritime Industry, Ocean Engineering and Coastal Resources*. London: Taylor & Francis Group, pp. 245-256.
- Poutiainen, I., Tanskanen, P. & Marquis, G., 2004. Finite element methods for structural hot spot stress determination—a comparison of procedures. *International Journal of Fatigue*, 26(11), 1147-1157.
- Radaj, D., 1996. Review of fatigue strength assessment of nonwelded and welded structures based on local parameters. *International Journal of Fatigue*, 18(3), 153-170.
- Radaj, D., Sonsino, C. & Fricke, W., 2009. Recent developments in local concepts of fatigue assessment of welded joints. *International Journal of Fatigue*, 31(1), 2-11.
- Radaj, D., Sonsino, C.M. & Fricke, W., 2006. *Fatigue assessment of welded joints by*

local approaches Second., Cambridge, England: Woodhead.

Schumacher, A. & Nussbaumer, A., 2006. Experimental study on the fatigue behaviour of welded tubular K-joints for bridges. *Engineering Structures*, 28(5), 745-755.

Xiao, Z.G. & Yamada, K., 2004. A method of determining geometric stress for fatigue strength evaluation of steel welded joints. *International Journal of Fatigue*, 26(12), 1277-1293.

8 Appendix A: Calculations for nominal stress method

Fatigue life assessment of the test specimen based on nominal stress method

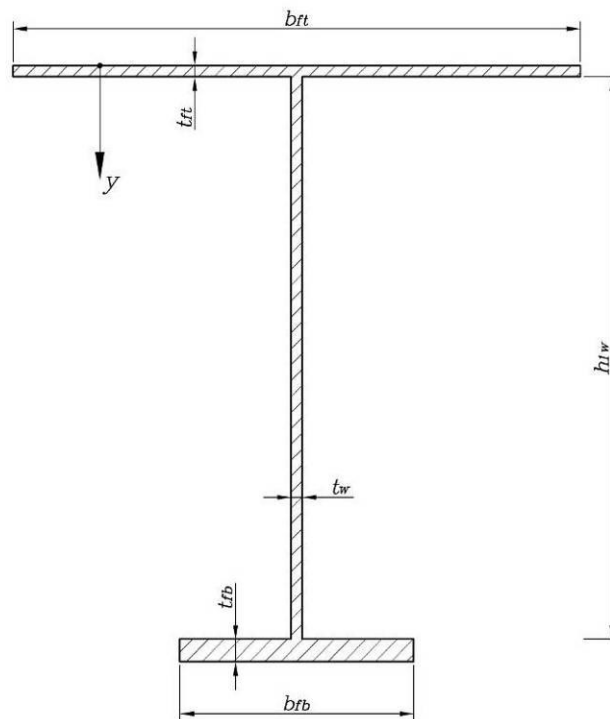
the calculation is based on Chapter 9 of Eurocode 3. the detail is category 56 based on table 8.9 of the code (orthotropic decks with open stringers)

Cross section dimensions:

$$b_{ft} := 510\text{mm} \quad t_{ft} := 10\text{mm}$$

$$b_{fb} := 210\text{mm} \quad t_{fb} := 20\text{mm}$$

$$h_{lw} := 500\text{mm} \quad t_w := 10\text{mm}$$



$$y_{ft} := \frac{t_{ft}}{2} \quad y_w := \frac{h_{lw}}{2} + t_{ft} \quad y_{fb} := t_{ft} + h_{lw} + \frac{t_{fb}}{2}$$

$$y_{ft} = 5 \cdot \text{mm} \quad y_w = 260 \cdot \text{mm} \quad y_{fb} = 520 \cdot \text{mm}$$

Cross section properties:

$$A_{\text{beam}} := b_{ft} \cdot t_{ft} + h_{lw} \cdot t_w + b_{fb} \cdot t_{fb} \quad A_{\text{beam}} = 1.43 \times 10^4 \cdot \text{mm}^2$$

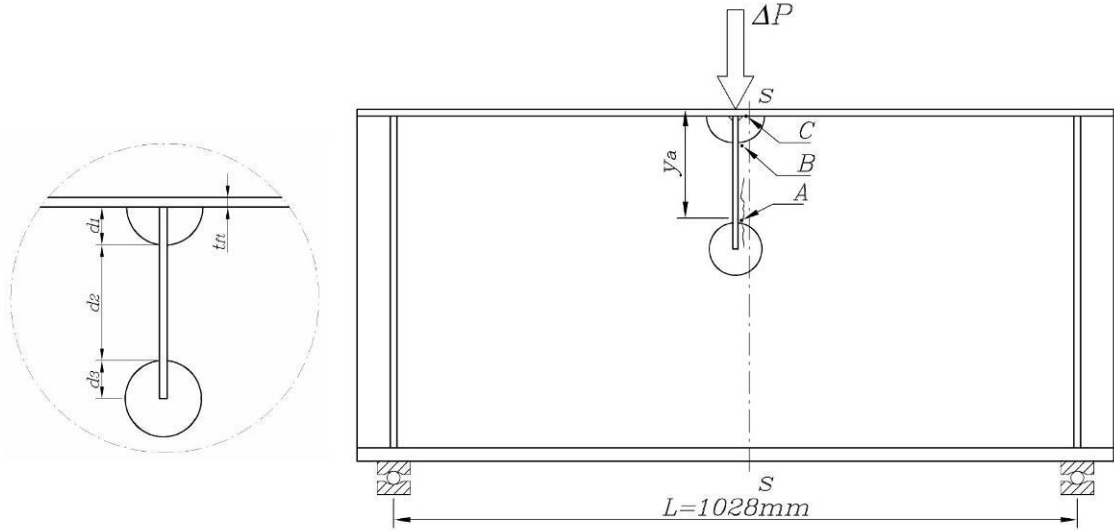
$$y_{CG} := \frac{(b_{ft} \cdot t_{ft} \cdot y_{ft} + h_{lw} \cdot t_w \cdot y_w + b_{fb} \cdot t_{fb} \cdot y_{fb})}{A_{\text{beam}}} \quad y_{CG} = 245.42 \cdot \text{mm}$$

$$I_1 := \frac{1}{12} b_{ft} \cdot t_{ft}^3 + b_{ft} \cdot t_{ft} \cdot (y_{CG} - y_{ft})^2 \quad I_1 = 2.948 \times 10^8 \cdot \text{mm}^4$$

$$I_2 := \frac{1}{12} t_w \cdot h_{lw}^3 + h_{lw} \cdot t_w \cdot (y_{CG} - y_w)^2 \quad I_2 = 1.052 \times 10^8 \cdot \text{mm}^4$$

$$I_3 := \frac{1}{12} b_{fb} \cdot t_{fb}^3 + b_{fb} \cdot t_{fb} \cdot (y_{CG} - y_{fb})^2 \quad I_3 = 3.168 \times 10^8 \cdot \text{mm}^4$$

$$I := I_1 + I_2 + I_3 \quad I = 7.169 \times 10^8 \cdot \text{mm}^4$$



$$d_1 := 40\text{mm} \quad d_2 := 120\text{mm} \quad d_3 := 40\text{mm}$$

$$y_A := d_1 + d_2 + t_{ft} \quad y_A = 170 \cdot \text{mm} \quad (\text{Location of the cracking point 'A' in section S-S})$$

$$y_B := d_1 + t_{ft} \quad y_B = 50 \text{ mm} \quad (\text{Location of the cracking point 'B' in section S-S})$$

$$y_C := t_{ft} \quad y_C = 10 \text{ mm} \quad (\text{Location of the cracking point 'C' in section S-S})$$

$$A_{\text{net.s}} := A_{\text{beam}} - (d_1 + 2 \cdot d_3) \cdot t_w \quad A_{\text{net.s}} = 1.31 \times 10^4 \cdot \text{mm}^2$$

$$y_{\text{CG.red}} := \frac{\left[b_{ft} \cdot t_{ft} \cdot y_{ft} + h_{1w} \cdot t_w \cdot y_w - d_1 \cdot t_w \cdot \left(t_{ft} + \frac{d_1}{2} \right) - 2 \cdot d_3 \cdot t_w (t_{ft} + d_1 + d_2 + d_3) + b_{fb} \cdot t_{fb} \cdot y_{fb} \right]}{A_{\text{net.s}}}$$

$$y_{\text{CG.red}} = 254.16 \cdot \text{mm}$$

$$I_{1.ss} := \frac{1}{12} b_{ft} \cdot t_{ft}^3 + b_{ft} \cdot t_{ft} \cdot (y_{\text{CG.red}} - y_{ft})^2 \quad I_{1.ss} = 3.167 \times 10^8 \cdot \text{mm}^4$$

$$I_{2.ss} := \frac{1}{12} t_w \cdot h_{1w}^3 + h_{1w} \cdot t_w \cdot (y_{\text{CG.red}} - y_w)^2 \quad I_{2.ss} = 1.043 \times 10^8 \cdot \text{mm}^4$$

$$I_{3.ss} := \frac{1}{12} b_{fb} \cdot t_{fb}^3 + b_{fb} \cdot t_{fb} \cdot (y_{\text{CG.red}} - y_{fb})^2 \quad I_{3.ss} = 2.97 \times 10^8 \cdot \text{mm}^4$$

$$I_{4.ss} := - \left[\frac{1}{12} t_w \cdot d_1^3 + d_1 \cdot t_w \cdot \left(t_{ft} + \frac{d_1}{2} - y_{\text{CG.red}} \right)^2 \right] \quad I_{4.ss} = -2.015 \times 10^7 \cdot \text{mm}^4$$

$$I_{5.ss} := - \left[\frac{1}{12} t_w \cdot (2d_3)^3 + 2d_3 \cdot t_w \cdot (t_{ft} + d_1 + d_2 + d_3 - y_{CG.red})^2 \right] \quad I_{5.ss} = -1.987 \times 10^6 \cdot \text{mm}^4$$

$$I_{net.s} := I_{1.ss} + I_{2.ss} + I_{3.ss} + I_{4.ss} + I_{5.ss} \quad I_{net.s} = 6.958 \times 10^8 \cdot \text{mm}^4$$

$$W_{net.s.A} := \frac{I_{net.s}}{y_{CG.red} - y_A} \quad W_{net.s.A} = 8.268 \times 10^6 \cdot \text{mm}^3$$

$$W_{net.s.B} := \frac{I_{net.s}}{y_{CG.red} - y_B} \quad W_{net.s.B} = 3.408 \times 10^6 \cdot \text{mm}^3$$

$$W_{net.s.C} := \frac{I_{net.s}}{y_{CG.red} - y_C} \quad W_{net.s.C} = 2.85 \times 10^6 \cdot \text{mm}^3$$

$$A_{w.net.s} := (h_{1w} - d_1 - 2 \cdot d_3) \cdot t_w \quad A_{w.net.s} = 3.8 \times 10^3 \cdot \text{mm}^2$$

Shear force and moment in the section s-s:

$$\Delta P := \begin{pmatrix} 200 \\ 400 \end{pmatrix} \text{kN} \quad L_{beam} := 1028 \text{mm} \quad \Delta V_s := \frac{\Delta P}{2} \quad \Delta V_s = \begin{pmatrix} 100 \\ 200 \end{pmatrix} \cdot \text{kN}$$

$$\Delta M_s := \Delta P \cdot \frac{L_{beam}}{4} \quad \Delta M_s = \begin{pmatrix} 51.4 \\ 102.8 \end{pmatrix} \cdot \text{kN} \cdot \text{m}$$

Fatigue classes for the assessment points in section s-s:

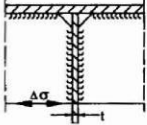
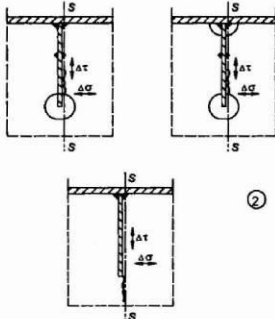
Point	Fatigue Class	Reference in Ch.9 of EC3
A	56	Detail 2 - Table 8.9
B	56	Detail 2 - Table 8.9
C	56	Detail 1 - Table 8.4

Calculation of fatigue damage in point 'A':

$$\Delta\sigma_A := \frac{\Delta M_s}{W_{net.s.A}} \quad \Delta\sigma_A = \left(\frac{6.217}{12.434} \right) \cdot \text{MPa} \quad \Delta\tau_A := \frac{\Delta V_s}{A_{w.net.s}} \quad \Delta\tau_A = \left(\frac{26.316}{52.632} \right) \cdot \text{MPa}$$

$$\Delta\sigma_{eq.A} := \frac{1}{2} \left(\Delta\sigma_A + \sqrt{\Delta\sigma_A^2 + 4 \cdot \Delta\tau_A^2} \right) \quad (\text{See table below}) \quad \Delta\sigma_{eq.A} = \left(\frac{29.607}{59.214} \right) \cdot \text{MPa}$$

Table 8.9: Orthotropic decks – open stringers

Detail category	Constructional detail		Description	Requirements
80	$t \leq 12\text{mm}$		1) Connection of longitudinal stringer to cross girder.	1) Assessment based on the direct stress range $\Delta\sigma$ in the stringer.
71	$t > 12\text{mm}$			
56			2) Connection of continuous longitudinal stringer to cross girder. $\Delta\sigma = \frac{\Delta M_s}{W_{net,s}}$ $\Delta\tau = \frac{\Delta V_s}{A_{w,net,s}}$ Check also stress range between stringers as defined in EN 1993-2.	2) Assessment based on combining the shear stress range $\Delta\tau$ and direct stress range $\Delta\sigma$ in the web of the cross girder, as an equivalent stress range: $\Delta\sigma_{eq} = \frac{1}{2} \left(\Delta\sigma + \sqrt{\Delta\sigma^2 + 4\Delta\tau^2} \right)$

The total damage is not allowed to be above 100% ($D \leq 1,0$).

Partial factors for are set to unity to calculate the real fatigue life without safety margin:

$$\gamma_{Mf} := 1.00 \quad \gamma_{Ff} := 1.0$$

Detail category 56:

$$\Delta\sigma_{C.A} := 56\text{MPa} \quad \Delta\sigma_{D.A} := \left(\frac{2}{5} \right)^{\frac{1}{3}} \cdot \Delta\sigma_{C.A} = 41.261 \cdot \text{MPa} \quad \Delta\sigma_{L.A} := \left(\frac{5}{100} \right)^{\frac{1}{5}} \cdot \Delta\sigma_{D.A} = 22.664 \cdot \text{MPa}$$

Number of cycles to failure:

$$i := 0..1$$

$$N_{A_i} := \begin{cases} \infty & \text{if } \gamma_{Ff} \cdot \Delta\sigma_{eq.A_i} < \frac{\Delta\sigma_{L.A}}{\gamma_{Mf}} \\ 5 \cdot 10^6 \cdot \left(\frac{\frac{\Delta\sigma_{D.A}}{\gamma_{Mf}}}{\gamma_{Ff} \cdot \Delta\sigma_{eq.A_i}} \right)^3 & \text{if } \gamma_{Ff} \cdot \Delta\sigma_{eq.A_i} \geq \frac{\Delta\sigma_{D.A}}{\gamma_{Mf}} \\ 5 \cdot 10^6 \cdot \left(\frac{\frac{\Delta\sigma_{D.A}}{\gamma_{Mf}}}{\gamma_{Ff} \cdot \Delta\sigma_{eq.A_i}} \right)^5 & \text{otherwise} \end{cases}$$

$$N_A = \begin{pmatrix} 2.628 \times 10^7 \\ 1.692 \times 10^6 \end{pmatrix}$$

$$n := \begin{pmatrix} 5 \cdot 10^6 \\ 380000 \end{pmatrix}$$

$$\Delta D_A := \overrightarrow{\left(\frac{n}{N_A} \right)} \quad \Delta D_A = \begin{pmatrix} 0.19 \\ 0.225 \end{pmatrix} \quad D_A := \sum \Delta D_A \quad D_A = 0.415$$

Calculation of fatigue damage in point 'B':

$$\Delta \sigma_B := \frac{\Delta M_s}{W_{\text{net.s.B}}} \quad \Delta \sigma_B = \begin{pmatrix} 15.081 \\ 30.163 \end{pmatrix} \cdot \text{MPa} \quad \Delta \tau_B := \frac{\Delta V_s}{A_{\text{w.net.s}}} \quad \Delta \tau_B = \begin{pmatrix} 26.316 \\ 52.632 \end{pmatrix} \cdot \text{MPa}$$

$$\Delta \sigma_{\text{eq.B}} := \frac{1}{2} \left(\Delta \sigma_B + \sqrt{\Delta \sigma_B^2 + 4 \cdot \Delta \tau_B^2} \right) \quad \Delta \sigma_{\text{eq.B}} = \begin{pmatrix} 34.916 \\ 69.831 \end{pmatrix} \cdot \text{MPa}$$

Detail category 56:

$$\Delta \sigma_{\text{C.B}} := 56 \text{ MPa} \quad \Delta \sigma_{\text{D.B}} := \left(\frac{2}{5} \right)^{\frac{1}{3}} \cdot \Delta \sigma_{\text{C.B}} = 41.261 \cdot \text{MPa} \quad \Delta \sigma_{\text{L.B}} := \left(\frac{5}{100} \right)^{\frac{1}{5}} \cdot \Delta \sigma_{\text{D.B}} = 22.664 \cdot \text{MPa}$$

Number of cycles to failure:

$$i := 0..1$$

$$N_{B_i} := \begin{cases} \infty & \text{if } \gamma_{\text{Ff}} \cdot \Delta \sigma_{\text{eq.B}_i} < \frac{\Delta \sigma_{\text{L.B}}}{\gamma_{\text{Mf}}} \\ 5 \cdot 10^6 \cdot \left(\frac{\frac{\Delta \sigma_{\text{D.B}}}{\gamma_{\text{Mf}}}}{\gamma_{\text{Ff}} \cdot \Delta \sigma_{\text{eq.B}_i}} \right)^3 & \text{if } \gamma_{\text{Ff}} \cdot \Delta \sigma_{\text{eq.B}_i} \geq \frac{\Delta \sigma_{\text{D.B}}}{\gamma_{\text{Mf}}} \\ 5 \cdot 10^6 \cdot \left(\frac{\frac{\Delta \sigma_{\text{D.B}}}{\gamma_{\text{Mf}}}}{\gamma_{\text{Ff}} \cdot \Delta \sigma_{\text{eq.B}_i}} \right)^5 & \text{otherwise} \end{cases} \quad N_B = \begin{pmatrix} 1.152 \times 10^7 \\ 1.031 \times 10^6 \end{pmatrix}$$

$$n := \begin{pmatrix} 5 \cdot 10^6 \\ 380000 \end{pmatrix}$$

$$\Delta D_B := \overrightarrow{\left(\frac{n}{N_B} \right)} \quad \Delta D_B = \begin{pmatrix} 0.434 \\ 0.368 \end{pmatrix}$$

$$D_B := \sum \Delta D_B \quad D_B = 0.802$$

Calculation of fatigue damage in point 'C':

Only direct stress acts on the detail:

$$\Delta\sigma_C := \frac{\Delta M_s}{W_{\text{net.s.C}}} \quad \Delta\sigma_C = \left(\frac{18.036}{36.073} \right) \cdot \text{MPa}$$

Detail category 80:

$$\Delta\sigma_{C.C} := 56 \text{MPa} \quad \Delta\sigma_{D.C} := \left(\frac{2}{5} \right)^{\frac{1}{3}} \cdot \Delta\sigma_{C.C} = 41.261 \cdot \text{MPa} \quad \Delta\sigma_{L.C} := \left(\frac{5}{100} \right)^{\frac{1}{5}} \cdot \Delta\sigma_{D.C} = 22.664 \cdot \text{MPa}$$

Number of cycles to failure:

$$i := 0..1$$

$$N_{C_i} := \begin{cases} \infty & \text{if } \gamma_{Ff} \Delta\sigma_{C_i} < \frac{\Delta\sigma_{L.C}}{\gamma_{Mf}} \\ 5 \cdot 10^6 \cdot \left(\frac{\frac{\Delta\sigma_{D.C}}{\gamma_{Mf}}}{\gamma_{Ff} \Delta\sigma_{C_i}} \right)^3 & \text{if } \gamma_{Ff} \Delta\sigma_{C_i} \geq \frac{\Delta\sigma_{D.C}}{\gamma_{Mf}} \\ 5 \cdot 10^6 \cdot \left(\frac{\frac{\Delta\sigma_{D.C}}{\gamma_{Mf}}}{\gamma_{Ff} \Delta\sigma_{C_i}} \right)^5 & \text{otherwise} \end{cases} \quad N_C = \left(\frac{1 \times 10^{307}}{9.79 \times 10^6} \right)$$

$$n := \left(\frac{5 \cdot 10^6}{380000} \right)$$

$$\Delta D_C := \left(\frac{n}{N_C} \right) \quad \Delta D_C = \begin{pmatrix} 0 \\ 0.039 \end{pmatrix}$$

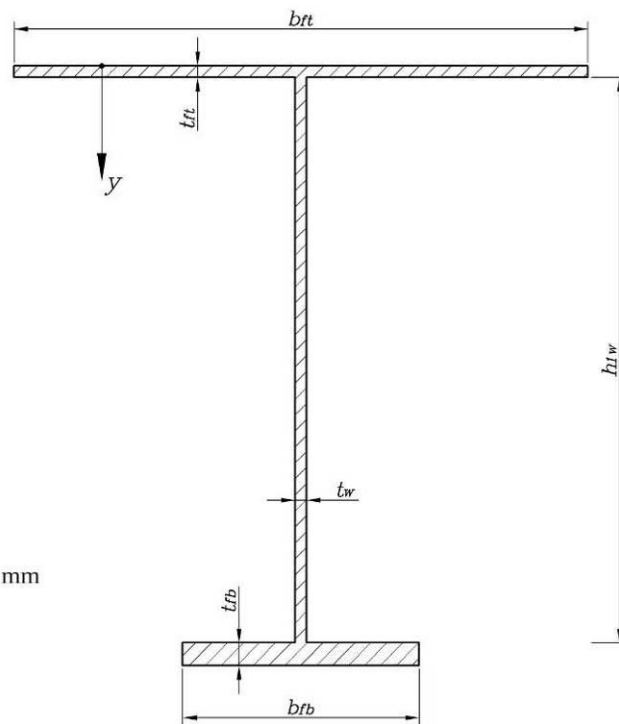
$$D_C := \sum \Delta D_C \quad D_C = 0.039$$

9 Appendix B: Verification of the finite element models

Calculation of stresses and beam deflection for verification of the FE models

Cross section dimensions:

$$\begin{aligned} b_{ft} &:= 510\text{mm} & t_{ft} &:= 10\text{mm} \\ b_{fb} &:= 210\text{mm} & t_{fb} &:= 20\text{mm} \\ h_{lw} &:= 500\text{mm} & t_w &:= 10\text{mm} \\ h_{tot} &:= h_{lw} + t_{ft} + t_{fb} & h_{tot} &= 530\text{mm} \end{aligned}$$



$$\begin{aligned} y_{ft} &:= \frac{t_{ft}}{2} & y_w &:= \frac{h_{lw}}{2} + t_{ft} & y_{fb} &:= t_{ft} + h_{lw} + \frac{t_{fb}}{2} \\ y_{ft} &= 5\text{mm} & y_w &= 260\text{mm} & y_{fb} &= 520\text{mm} \end{aligned}$$

Cross section properties:

$$\begin{aligned} A_{beam} &:= b_{ft} \cdot t_{ft} + h_{lw} \cdot t_w + b_{fb} \cdot t_{fb} & A_{beam} &= 1.43 \times 10^4 \cdot \text{mm}^2 \\ y_{CG} &:= \frac{(b_{ft} \cdot t_{ft} \cdot y_{ft} + h_{lw} \cdot t_w \cdot y_w + b_{fb} \cdot t_{fb} \cdot y_{fb})}{A_{beam}} & y_{CG} &= 245.42\text{mm} \\ I_1 &:= \frac{1}{12} b_{ft} \cdot t_{ft}^3 + b_{ft} \cdot t_{ft} \cdot (y_{CG} - y_{ft})^2 & I_1 &= 2.948 \times 10^8 \cdot \text{mm}^4 \\ I_2 &:= \frac{1}{12} t_w \cdot h_{lw}^3 + h_{lw} \cdot t_w \cdot (y_{CG} - y_w)^2 & I_2 &= 1.052 \times 10^8 \cdot \text{mm}^4 \end{aligned}$$

$$I_3 := \frac{1}{12} b_{fb} \cdot t_{fb}^3 + b_{fb} \cdot t_{fb} \cdot (y_{CG} - y_{fb})^2 \quad I_3 = 3.168 \times 10^8 \cdot \text{mm}^4$$

$$I_{beam} := I_1 + I_2 + I_3 \quad I_{beam} = 7.169 \times 10^8 \cdot \text{mm}^4$$

$$c_{bot} := h_{tot} - y_{CG}$$

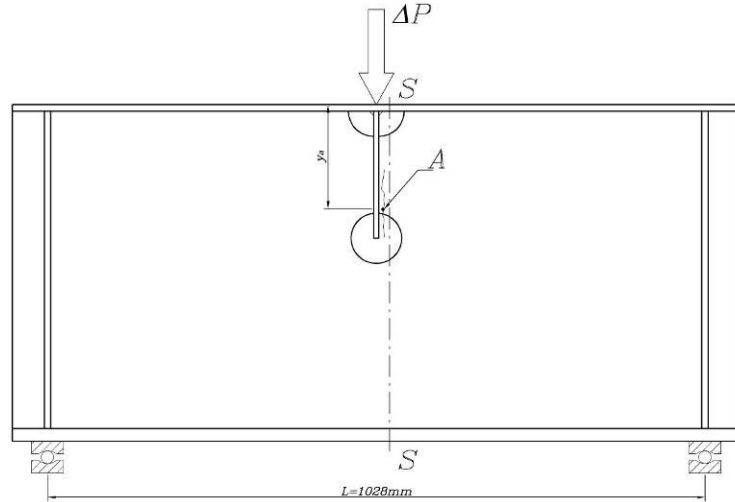
$$c_{bot} = 284.58 \cdot \text{mm}$$

$$W_{xx} := \frac{I_{beam}}{c_{bot}}$$

$$W_{xx} = 2.519 \times 10^6 \cdot \text{mm}^3$$

$$A_{web} := h_{1w} \cdot t_w$$

$$A_{web} = 5 \times 10^3 \cdot \text{mm}^2$$



Shear force and moment in the section s-s:

$$\Delta P := \begin{pmatrix} 200 \\ 400 \end{pmatrix} \text{kN} \quad L_{beam} := 1028 \text{mm} \quad \Delta V_s := \frac{\Delta P}{2} \quad \Delta V_s = \begin{pmatrix} 100 \\ 200 \end{pmatrix} \cdot \text{kN}$$

$$\Delta M_s := \Delta P \cdot \frac{L_{beam}}{4} \quad \Delta M_s = \begin{pmatrix} 51.4 \\ 102.8 \end{pmatrix} \cdot \text{kN} \cdot \text{m}$$

Maximum bending stress in the bottom flange in section s-s:

$$\Delta \sigma := \frac{\Delta M_s}{W_{xx}} \quad \Delta \sigma = \begin{pmatrix} 20.405 \\ 40.81 \end{pmatrix} \cdot \text{MPa}$$

Maximum nominal bending stress in the Deck plate in section s-s:

$$\Delta \sigma_{deck} := \frac{\Delta M_s}{\left(\frac{I_{beam}}{y_{CG}} \right)} \quad \Delta \sigma_{deck} = \begin{pmatrix} 17.597 \\ 35.194 \end{pmatrix} \text{MPa}$$

Deflection at the mid-span:

$$E_{\text{steel}} := 210 \text{ GPa} \quad \nu_{\text{steel}} := 0.3 \quad G_{\text{steel}} := \frac{E_{\text{steel}}}{2 \cdot (1 + \nu_{\text{steel}})} \quad G_{\text{steel}} = 80.769 \cdot \text{GPa}$$

$$\delta_{\text{s.flexure}} := \frac{(\Delta P \cdot L_{\text{beam}}^3)}{48 \cdot E_{\text{steel}} \cdot I_{\text{beam}}} \quad \delta_{\text{s.flexure}} = \begin{pmatrix} 0.03 \\ 0.06 \end{pmatrix} \cdot \text{mm}$$

$$k := \frac{A_{\text{web}}}{A_{\text{beam}}} \quad k = 0.35$$

$$\delta_{\text{s.shear}} := \frac{(\Delta P \cdot L_{\text{beam}})}{4 \cdot k \cdot A_{\text{beam}} \cdot G_{\text{steel}}} \quad \delta_{\text{s.shear}} = \begin{pmatrix} 0.127 \\ 0.255 \end{pmatrix} \cdot \text{mm}$$

$$\delta_{\text{s}} := \delta_{\text{s.flexure}} + \delta_{\text{s.shear}} \quad \delta_{\text{s}} = \begin{pmatrix} 0.157 \\ 0.315 \end{pmatrix} \cdot \text{mm}$$

10 Appendix C: HS-Fatigue program source code

A Program for fatigue calculations based on hot spot (structural stress) method

Author: Farshid Zamiri A.

Date: 2009-04-18

Version: 1.0

Contents

- [Initialization](#)
- [Read the data from Excel file](#)
- [Hot spot stress evaluation](#)
- [Plot the extrapolated results and write the image files](#)
- [Consolidate results](#)
- [end of file](#)

Initialization

```
clear all
close all
HSPoints=['wb';'wt';'fl']; % Naming convention of points in which
hotspot stresses are investigated. the program can not determine it
by itself
graphpoints=200; % Max. number of points in a graph
stresscomponents=['s11';'spr']; % Names of stress components used
```

Read the data from Excel file

```
filename='Extrapolation.xls';

[typ, desc]=xlsfinfo(filename);
[dummy,numsheets]=size(desc);
HS.SSE=cell2struct(desc,{'name'},1);
for i=1:numsheets
    HS.SSE(i).name=lower(HS.SSE(i).name); % Change the series names
to lower case
    s=xlsread(filename,HS.SSE(i).name);
    HS.SSE(i).xraw=s(:,1);
    co=s(:,3);
    co=co(~isnan(co));
    HS.SSE(i).lfac=co(end);
    co(end)=[];
    HS.SSE(i).control=co;
    HS.SSE(i).yraw=s(:,2)*HS.SSE(i).lfac; % multiply the stress to
load factor
    if HS.SSE(i).yraw(1)<0 % Make HSS positive, if it is negative,
        HS.SSE(i).yraw=-HS.SSE(i).yraw;
    end
    [x,m]=unique(HS.SSE(i).xraw);
    s=HS.SSE(i).yraw(m);
    if size(m,1)~=size(HS.SSE(i).xraw,1)
        fprintf ('Warning: Found repetitive row in the data sheet %s
\n', HS.SSE(i).name);
        fprintf ('check the excel worksheet for possible mistakes
\n');
```

```

end
[xs,ys]=smooth(HS.SSE(i).xraw,HS.SSE(i).yraw,graphpoints);
HS.SSE(i).xspline=xs;
HS.SSE(i).yspline=ys;
end

```

Hot spot stress evaluation

```

for i=1:numsheets
    [geostr]=sse(HS.SSE(i).control,HS.SSE(i).xraw,HS.SSE(i).yraw);
    HS.SSE(i).geostress=geostr;
end

```

Plot the extrapolated results and write the image files

```

close all
for i=1:numsheets
    figure(i)
    hold on
    grid on
    x=HS.SSE(i).xspline;
    y=HS.SSE(i).yspline;
    xext=HS.SSE(i).geostress(1,:);
    yext=HS.SSE(i).geostress(2,:);
    [xs,ys]=smooth(xext,yext,graphpoints/4);
    plot(x,y,'-','linewidth',1)
    plot(xs,ys,'-','linewidth',2)
    plot(xext,yext,'o','linewidth',1)
    switch length(xext)
        case 3
            exmet='Lin';
        case 4
            exmet='Qua';
        otherwise
            exmet='';
    end
    outfile=[exmet,'-',HS.SSE(i).name];
    title(outfile)
    print(i, '-djpeg','-r300',outfile);
end

```

Consolidate results

```

numpoints=size(HSPoints,1);
numstrcomp=size(stresscomponents,1);
startfignum=30;
ltypes=[ 'b- ' ;
         'b--';
         'r- ' ;
         'r--';
         'b: ' ;
         'r: '];
lmarks=[ 'o'; 's'; '^'; 'd'; '*'; '+'];

for j=1:numpoints
    for k=1:numstrcomp
        graph=(k-1)*numpoints+j;
        figure(startfignum+graph)
        hold on
        grid on
        figname=[HSPoints(j,:) '- ' stresscomponents(k,:)];
        title(figname)
        counter=0;
    end
end

```

```

        legtxt={};
        for i=1:numsheets
            cond1=~isempty(strfind(HS.SSE(i).name,HSPoints(j,:)));

cond2=~isempty(strfind(HS.SSE(i).name, stresscomponents(k,:)));
            if cond1 && cond2
                counter=counter+1;
                x=HS.SSE(i).xspline;
                y=HS.SSE(i).yspline;
                xext=HS.SSE(i).geostress(1,:);
                yext=HS.SSE(i).geostress(2,:);
%                 [xs,ys]=smooth(xext,yext,graphpoints/4);
                plot (x,y,ltypes(counter,:), 'linewidth',1)
%                 plot (xs,ys,ltypes(counter,:), 'linewidth',2)
                plot
                (xext,yext,[ltypes(counter,:),lmarks(counter,:)], 'linewidth',2)
                legtxt=[legtxt;{HS.SSE(i).name};{['extrapolated
',HS.SSE(i).name,'
\sigma_h_s=',num2str(HS.SSE(i).geostress(2,1),'%4.0f')]}}];
            end
        end
        axis auto
        legend(legtxt)
        print(startfignum+graph, '-djpeg', '-r300', ['summary-'
figname]);
    end
end

```

end of file

Published with MATLAB® 7.3

```

function [geostress]=sse(control,X,S)
% Calculates structural hot spot stress.
% Syntax:    [geostress]=sse(control,X,S)
% Input:
%   control: a vector containing plate thickness and extrapolation
%             points locations.
%             Plate thickness is used in type 'a' hot spot evaluation.
%             A zero plate thickness means a type 'b' hot spot is being
%             evaluated. two extrapolation points means linear
%             extrapolation and three e.p. points means quadratic e.p.).
%   X,S: data series containing stress (S) profile.
%
% Output:
%   geostress: a two column matrix defining X and S data points of the
%   extrapolation (suitable for subsequent plotting).
%
% Reference: IIW Fatigue Recommendations XIII-1965-03/XV-1127-03
% Update - January 2003-pp. 28~30

```

```

geostress=[];
t=control(1);
switch length(control)
    case 3 % linear extrapolation
        switch t
            case 0 % Type 'b' hot spot
                x1=control(2);
                x2=control(3);
            otherwise % Type 'a' hot spot
                x1=control(2)*t;
                x2=control(3)*t;
        end
        sigma1=interp1q(X,S,x1);
        sigma2=interp1q(X,S,x2);
        sigma1s=(x2/(x2-x1))*sigma1+(1-x2/(x2-x1))*sigma2;
        geostress=[0 x1 x2; sigma1s sigma1 sigma2];

    case 4 % Quadratic extrapolation
        switch t
            case 0 % Type 'b' hot spot
                x1=control(2);
                x2=control(3);
                x3=control(4);
            otherwise % Type 'a' hot spot
                x1=control(2)*t;
                x2=control(3)*t;
                x3=control(4)*t;
        end
        sigma1=interp1q(X,S,x1);
        sigma2=interp1q(X,S,x2);
        sigma3=interp1q(X,S,x3);
        M=[x1^2 x1 1; x2^2 x2 1; x3^2 x3 1];
        N=[sigma1;sigma2;sigma3];
        C=M\N;
        sigma1s=polyval(C,0);
        geostress=[0 x1 x2 x3; sigma1s sigma1 sigma2 sigma3];
    end
end
if isempty(geostress)
    geostress=-1;
end

```

```
end
```

```
function [xs,ys]=smooth(x,y,n)
% Creates an 'smoothed' curve out of data points
% (uses spline command)
% Syntax: [xs,ys]=smooth(x,y,n)
% Input:
%     - x,y : data points (vectors), x should be in ascending order
%     - n    : number of points on the smoothed curve (should be
%              sufficiently large)
%
%Output:
%     -xs,ys : points on the smoothed curve

xmin=x(1);
xmax=x(end);
xs=linspace(xmin,xmax,n);
ys = spline(x,y,xs);
```

11 Appendix D: Study of different techniques for modelling of simple and notched joints

In this appendix the effect of different modelling techniques on the computed structural hot spot stress values for two edge details is investigated. The results from solid element models are generally considered to be more accurate. The question here is to see whether the results from shell element models are in agreement with the solid element models or not.

The first detail is a fillet-welded simple cruciform joint shown in Figure 11.1. The material properties and modelling assumptions are generally similar to the main model described in Section 4.1. The loading and boundary conditions are shown in Figure 11.2. The detail has been modelled in two ways: (a) with solid elements, and (b) with shell elements (Figure 11.3). As the figure shows, the weld was not modelled in the shell element model. Both FE models were made based on the IIW recommendations for fine-mesh models. Figure 11.4 shows the deformed shape of the joint modelled with solid elements.

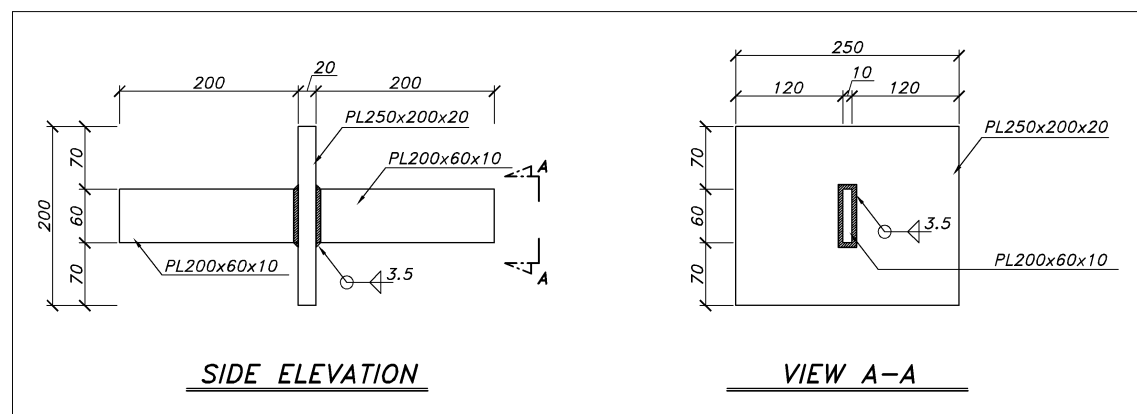


Figure 11.1 Geometry and dimensions of the simple edge detail.

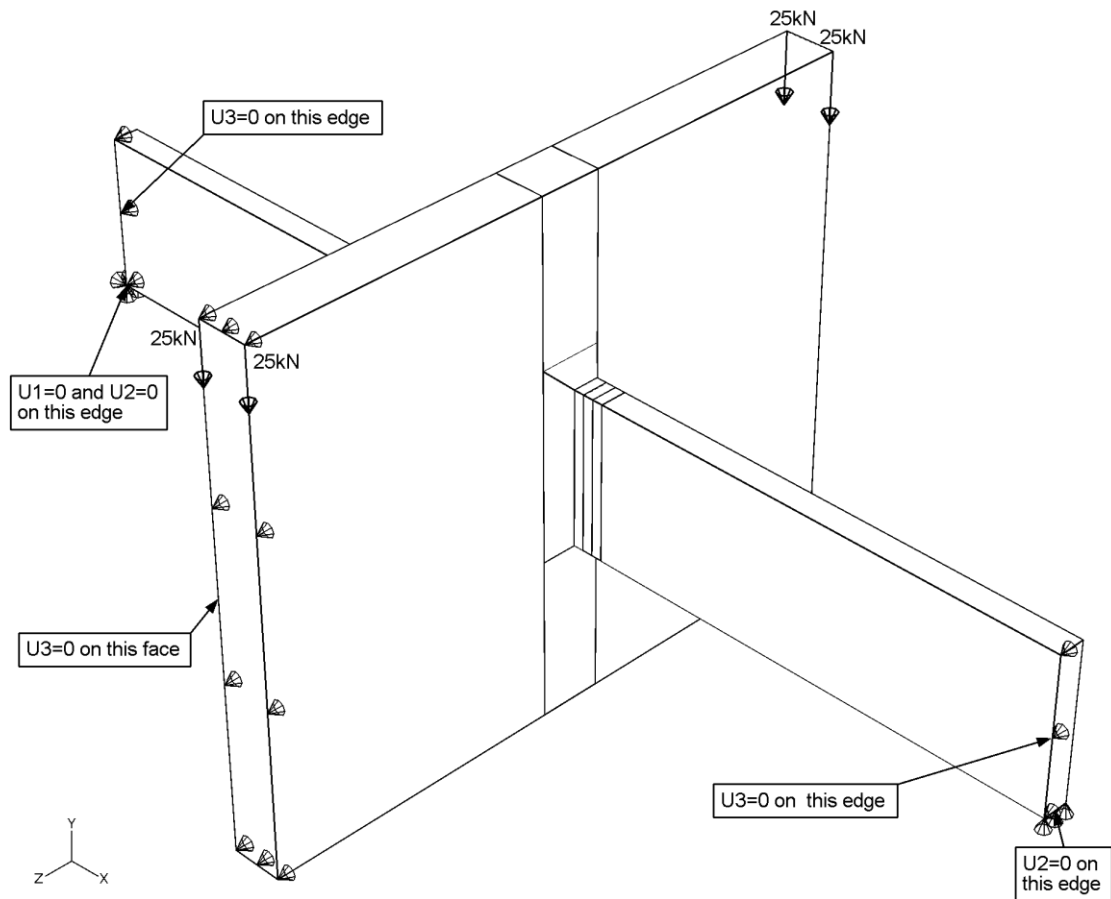


Figure 11.2 Loading and boundary conditions for the FE models of simple edge detail.

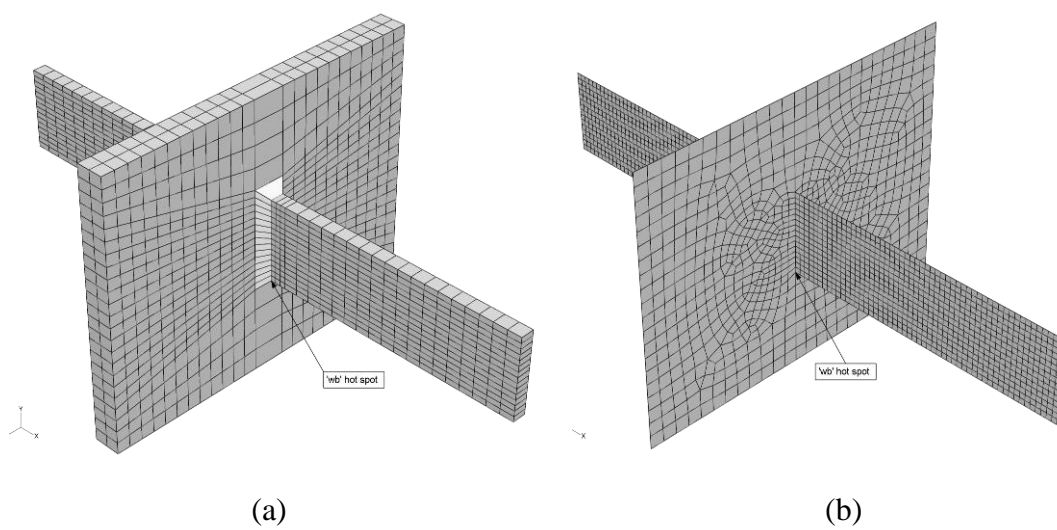


Figure 11.3 Finite element models of the joint; (a) Solid elements, (b) shell elements.

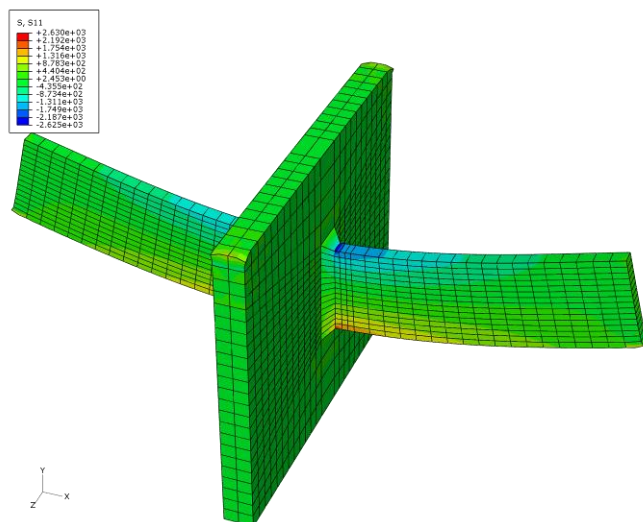


Figure 11.4 Deformed shape of the joint (solid element model).

The stress profiles in the 'wb' hot spot region are presented in Figure 11.6. The stress component perpendicular to the weld (S11) was selected to evaluate the hot spot stress. Table 11.1 shows the evaluated hot spot stresses for the two models. In this case, the SHSS value evaluated from shell element model is in good agreement with the result from solid element model.

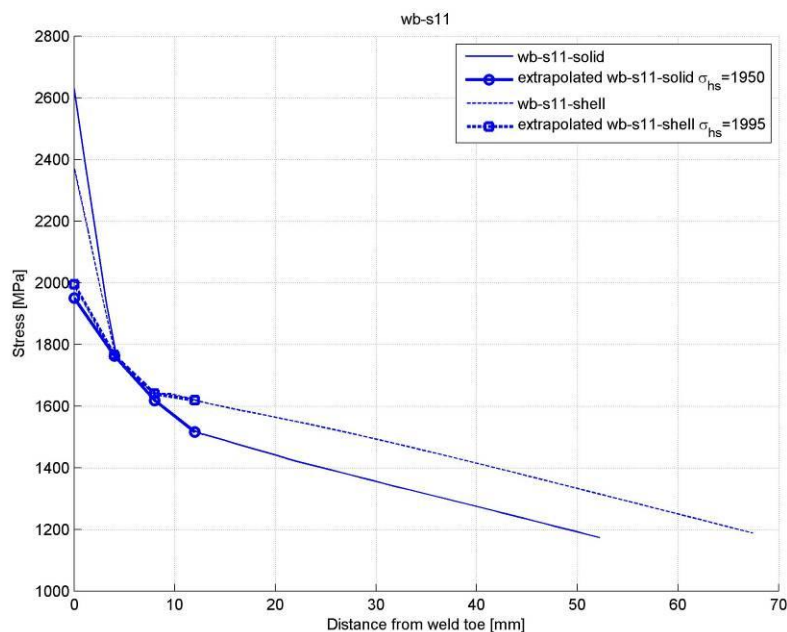


Figure 11.5 S11 (stress component perpendicular to the weld toe) profiles in the 'wb' hot spot region for two models.

Table 11.1 Computed hot spot stresses at the 'wb' hot spot for two models

	Shell element model	Solid element model	Ratio of shell element results to solid element
Hot spot stress based on σ_{11} [MPa]	1995	1950	1.02

The second studied case was similar to the first edge detail, but made with notched plates to incorporate an extra geometric feature into the detail. The geometry and dimensions of the joint can be seen in Figure 11.6. The length of the weld line was 60 mm, similar to the previous studied case. The loading and boundary conditions were also kept similar to the first studied case. In this case, the difference between SHSS values from shell and solid element models (BR04-OP and SH04-OP models, see Table 11.2) was considerable. The SHSS value from the SH04-OP model was too much underestimated (see Table 11.4). So, the SW04-OP model was made which incorporated the geometry of the weld into the shell element model by means of oblique shell elements. The thickness of these oblique shell elements was considered to be equal to the weld throat thickness, according to recommendations by Eriksson et al. (2003). The results were within the acceptable agreement range with the results from the solid element model, see Table 11.4. The stress profiles for these models are presented in Figure 11.7. The figure obviously shows that the shell element model (SH04-OP) fails to capture the stress gradient in the weld toe region. It should be noted that the fall in the stress values at the weld toe ($x=0$) in the stress profiles is because of the stress averaging in that location. This does not affect the hot spot results.

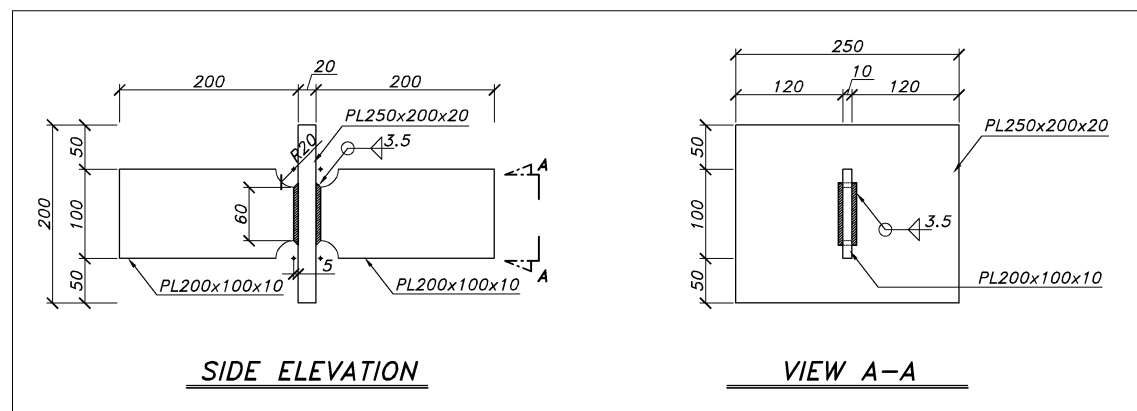
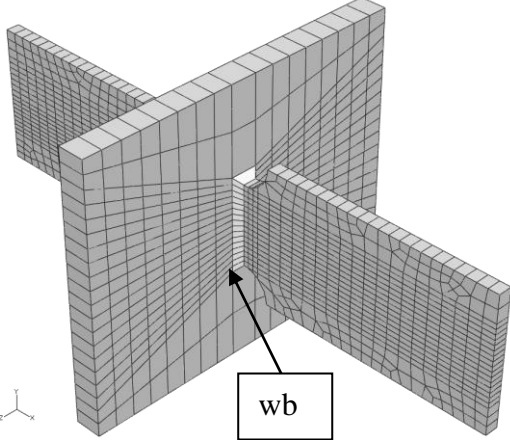
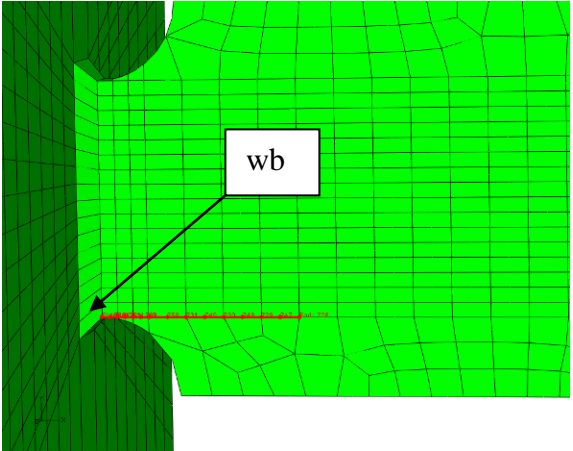
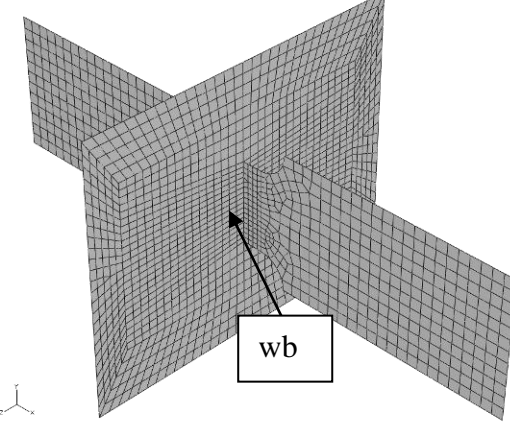
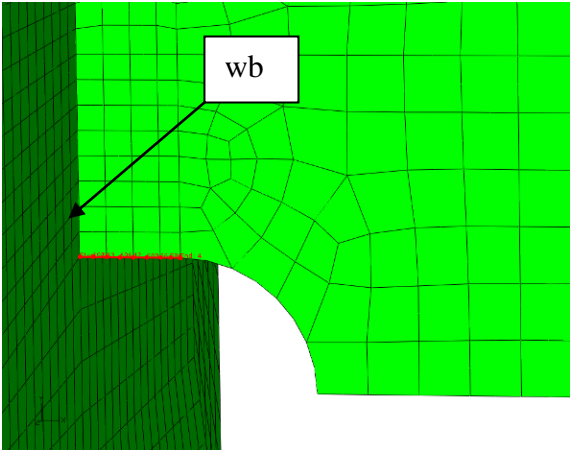
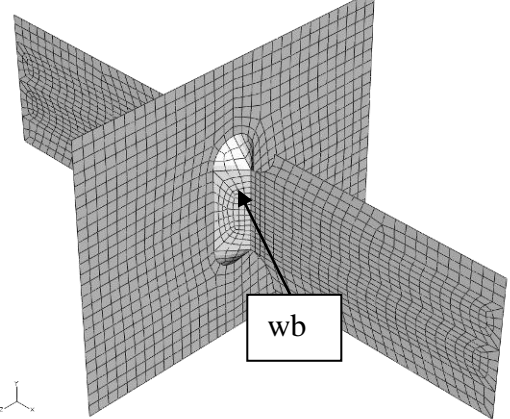
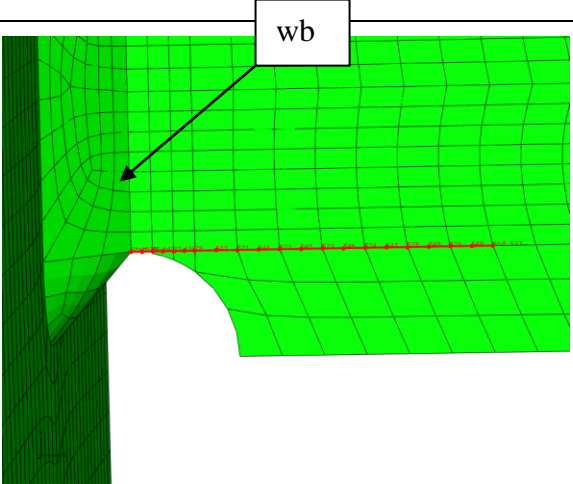


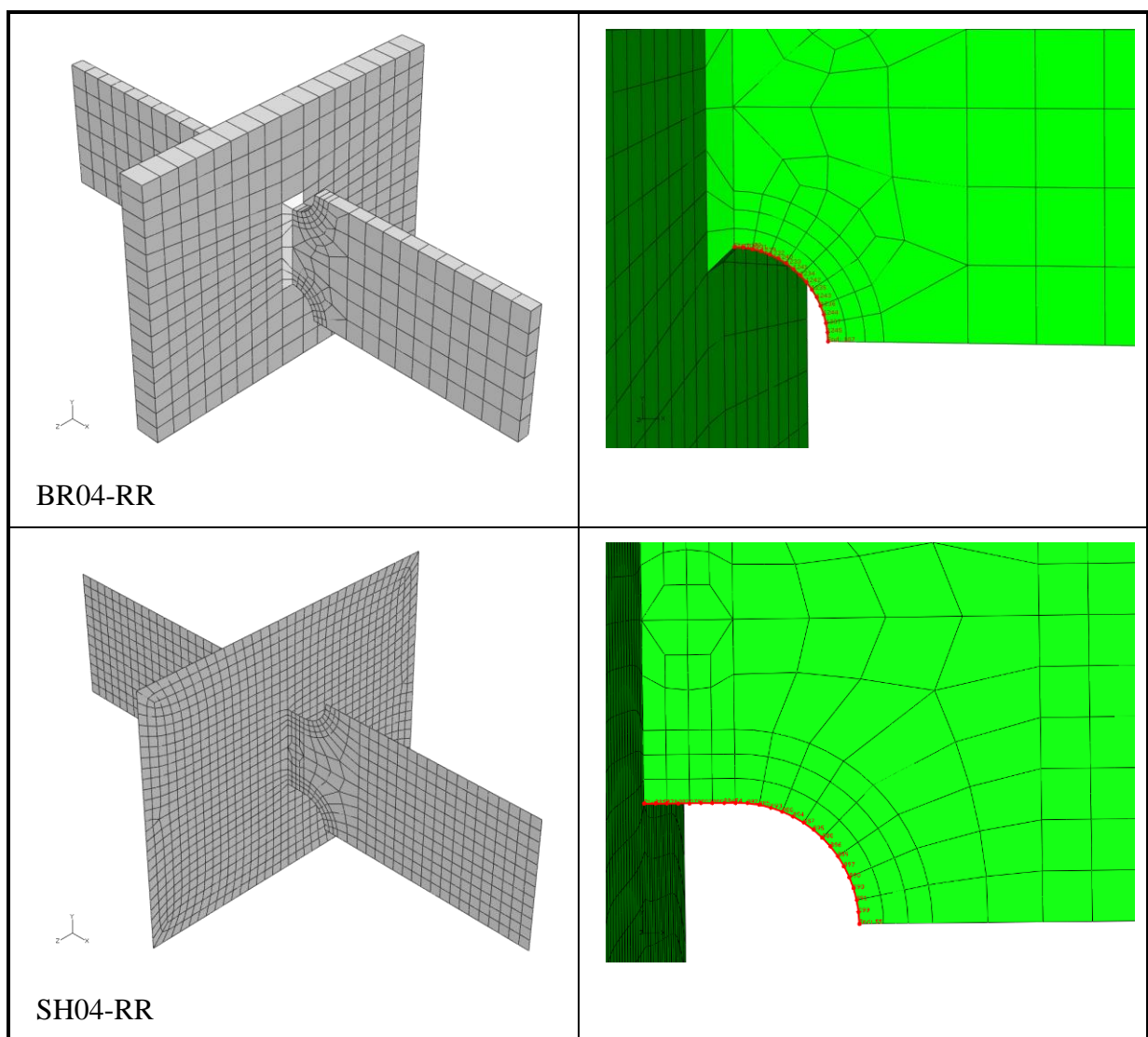
Figure 11.6 Geometry and dimensions of the notched edge detail.

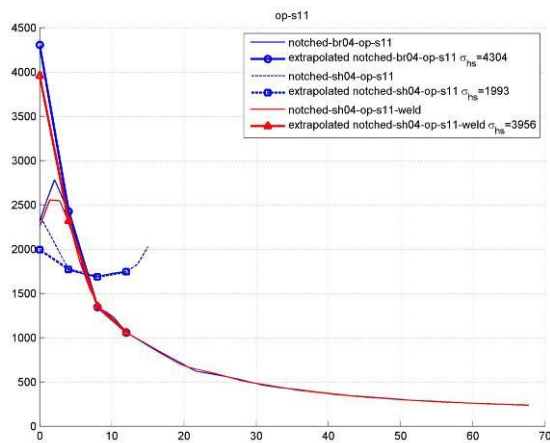
Table 11.2 Different FE models made for evaluation of SHSS in notched edge detail with stress profile measured on an orthogonal path.

 <p>BR04-OP</p>	
 <p>SH04-OP</p>	
 <p>SW04-OP</p>	

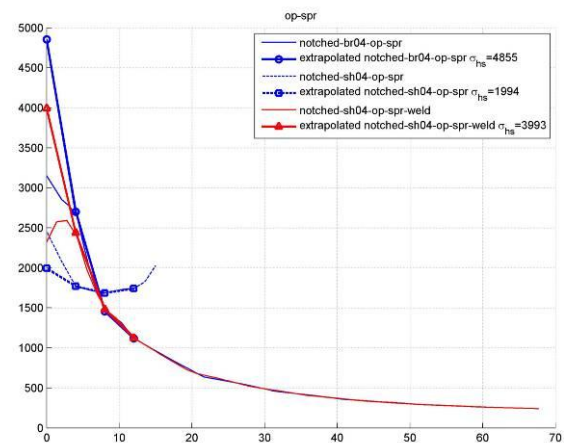
For all of the described models, the stress profile was measured on a straight path orthogonal to the weld line. Another alternative, which was inspired by the definition of type 'b' hot spot, was to take the curved line on the plate edge as the path to extract the stresses. This was the basis to construct two more models BR04-RR and SH04-RR which can be seen in Table 11.3. In these models the FE mesh is modified such that stress profile can be extracted on a curved path along the plate edge. However, the stress profiles along this curved path do not seem to be reasonable since the curvature of the quadratic extrapolation curve is in wrong direction (it is downward), see Figure 11.8. Also, the evaluated SHSS values for the curved path (Table 11.4) are comparable to the values from the un-notched joint (compare with Table 11.1). For example, compare SHSS value evaluated based on σ_{11} in the BR04-RR model (2027 MPa) with similar SHSS value from the un-notched detail (1950 MPa). This does not seem acceptable, because the presence of the notch in the detail should cause a higher structural hot spot stress value.

Table 11.3 FE models made for evaluation of SHSS in notched edge detail with stress profile measured on a curved path along the plate edge.



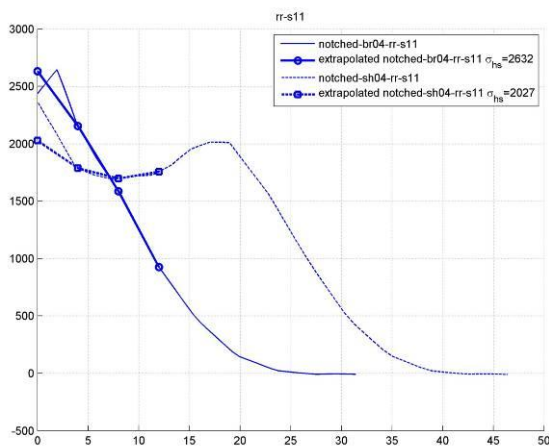


(a)

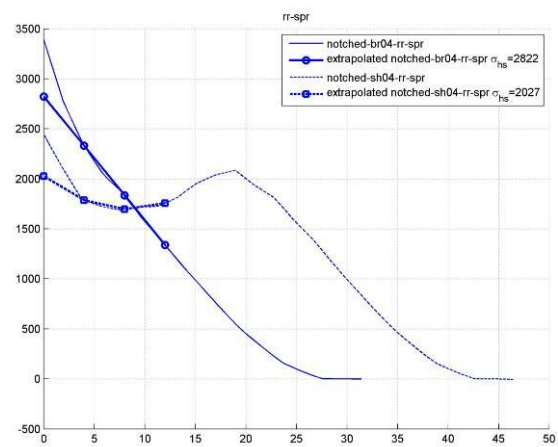


(b)

Figure 11.7 Stress profiles along the orthogonal path (a) stress component perpendicular to the weld toe, (b) principal stress.



(a)



(b)

Figure 11.8 Stress profiles along the curved path (a) stress component perpendicular to the weld toe, (b) principal stress.

Table 11.4 Computed hot spot stresses at the 'wb' hot spot for two models

Profile	Model	Element type	Hot spot stress [MPa]		Ratio of shell element results to solid element	
			based on σ_{11}	based on $\sigma_{\text{principal}}$	based on σ_{11}	based on $\sigma_{\text{principal}}$
Curved path (RR)	SH04-RR	Shell	2632	2027	1.30	0.72
	BR04-RR	Solid	2027	2822	1.00	1.00
Orthogonal path (OP)	SH04-OP	Shell	1993	1994	0.46	0.41
	SW04-OP	Shell w/ weld	3956	3993	0.92	0.82
	BR04-OP	Solid	4304	4855	1.00	1.00

In conclusion, the shell element models result in questionable SHSS values for edge details (i.e. type 'b' hot spots) when a geometric feature at the weld toe region exists. To attain better results, it is essential to include the weld geometry and stiffness into the model. Moreover, it seems more reasonable to use the straight path perpendicular to the weld toe, if the surface stress extrapolation technique (SSE) is used¹⁵. It is also interesting to study other SHSS evaluation methods in such cases. That is, through thickness stress linearization at the weld toe (TTWT) and Dong (2001) method.

¹⁵ This was also confirmed by some of the researchers in the field during personal conversations.